

AD-A212 849

## DOCUMENTATION PAGE

Form Approved  
OMB No. 0704-0188

1a. REPORT SECURITY CLASSIFICATION Unclassified			1b. RESTRICTIVE MARKINGS		
2a. SECURITY CLASSIFICATION AUTHORITY			3. DISTRIBUTION/AVAILABILITY OF REPORT Distribution unlimited, approved for public release.		
2b. DECLASSIFICATION/DOWNGRADING SCHEDULE			4. PERFORMING ORGANIZATION REPORT NUMBER(S)		
5. MONITORING ORGANIZATION REPORT NUMBER(S) AFOSR-TR-89-1242			6a. NAME OF PERFORMING ORGANIZATION Meteorology Research Center Control Data Corporation		
6b. OFFICE SYMBOL (If applicable)			7a. NAME OF MONITORING ORGANIZATION AFOSR/NC		
6c. ADDRESS (City, State, and ZIP Code) 2800 East Old Shakopee Road Minneapolis, MN 55420			7b. ADDRESS (City, State, and ZIP Code) Building 410 Bolling AFB, DC 20332-6448		
8a. NAME OF FUNDING/SPONSORING ORGANIZATION AFOSR			8b. OFFICE SYMBOL (If applicable)		
9. PROCUREMENT INSTRUMENT IDENTIFICATION NUMBER Contract No. F49620-86-C-0027			10. SOURCE OF FUNDING NUMBERS		
8c. ADDRESS (City, State, and ZIP Code) Building 410 Bolling AFB, D.C. 20332			PROGRAM ELEMENT NO. 61102F	PROJECT NO. 2310	TASK NO. A1
11. TITLE (Include Security Classification) The Interaction and Variation of Waves and Turbulence from MST Radar Data					
12. PERSONAL AUTHOR(S) M.R. Peterson					
13a. TYPE OF REPORT Final		13b. TIME COVERED FROM 86/2/1 TO 89/7/31		14. DATE OF REPORT (Year, Month, Day) 89/8/31	
15. PAGE COUNT 12					
16. SUPPLEMENTARY NOTATION					
17. COSATI CODES			18. SUBJECT TERMS (Continue on reverse if necessary and identify by block number)		
FIELD	GROUP	SUB-GROUP	MST Radar Gravity Waves Vertical Velocity Turbulence		
19. ABSTRACT (Continue on reverse if necessary and identify by block number) This report summarizes research results on the interactions of gravity waves, small-scale turbulence, and the background weather conditions obtained using data from clear-air Doppler profilers (also called MST radars), and from aircraft and balloons. The major results from these studies are as follows: (1) it was found from analysis of a set of aircraft data taken near the tropopause and from MST radar taken in Alaska and Colorado that there is enhanced mesoscale variability over mountains compared to over plains or oceans. These observational results were compared with predictions from the theory of stratified turbulence and the theory of Doppler-shifted gravity waves, and it was found that neither theory predicts all of the observed features. (2) Modeling of the refractivity turbulence structure constant ( $C_n^2$ ) showed that small-scale shears of the horizontal wind are about twice as large over the mountainous regions of Colorado compared to over the plains of Illinois, presumably due to terrain differences. (3) It was found that gravity wave activity is enhanced near fronts, jet streams, and convective elements. (4) The Flatland MST radar was					
20. DISTRIBUTION/AVAILABILITY OF ABSTRACT <input checked="" type="checkbox"/> UNCLASSIFIED/UNLIMITED <input checked="" type="checkbox"/> SAME AS RPT <input type="checkbox"/> DTIC USERS			21. ABSTRACT SECURITY CLASSIFICATION Unclassified		
22a. NAME OF RESPONSIBLE INDIVIDUAL Lt Col James G. Stovie			22b. TELEPHONE (Include Area Code) (202) 767-4960		22c. OFFICE SYMBOL AFOSR/NC

Block 19 (continued)

used to monitor tropopause folding events under a variety of background conditions and a preliminary climatology of the occurrence of folds was developed. (5)The spectrum of vertical motions at Flatland was analyzed and was found to closely match predictions for a spectrum of Doppler-shifted gravity waves. (6)Temporal mean vertical velocities measured by the radar reflect the large-scale flow when weather systems are changing slowly enough that the radar sample is representative of a large area. (7)Finally, it was found that the sampling strategy for vertical motions must be carefully designed to accommodate the frequency spectrum.

# COMPLETED PROJECT SUMMARY

TITLE: The Interaction and Variation of Waves and  
Turbulence from MST Radar Data

PRINCIPAL INVESTIGATOR: Miriam R. Peterson  
Meteorology Research Center  
Control Data Corporation  
P. O. Box 1249  
Minneapolis, MN 55440

INCLUSIVE DATES: 1 Feb 1986 - 31 July 1989

CONTRACT NUMBER: F49620-86-C-0027

COSTS AND FY SOURCE: \$71055, FY86; \$109144, FY87;  
\$114344, FY88; \$38768, FY89

SENIOR RESEARCH  
PERSONNEL: Dr. Gregory D. Nastrom

## PUBLICATIONS:

Spectrum of atmospheric vertical displacements and spectrum of conservative passive additives due to quasi-horizontal atmospheric motions. Gage, K.S. and G.D. Nastrom, J. Geophys. Res., 91, 13211-13216 (1986).

VHF radar measurements of the vertical momentum flux. Nastrom, G.D., and J.L. Green, Preprint volume, 23rd Conference on Radar Meteorology, Snowmass, CO, Sept 22-26 (1986).

The effects of terrain on the mesoscale spectrum of atmospheric motions. Nastrom, G.D., D.C. Fritts, and K.S. Gage, XIX General Assembly of IUGG, Vancouver, Aug. 9-22 (1987).

Dependence of the frequency spectrum observed with ST radars on background wind speed. Gage, K.S., and G.D. Nastrom, AMS Sixth Conference on Atmos. and Ocean. Waves and Stability, Seattle, August 25-28 (1987).

An investigation of terrain effects on the mesoscale spectrum of atmospheric motions. Nastrom, G.D., D.C. Fritts, and K.S. Gage, J. Atmos. Sci., 44, 3087-3096 (1987).

Further discussion of the dynamical processes that contribute to the spectrum of mesoscale atmospheric motions. Gage, K.S. and G.D. Nastrom, Preprint volume, Eighth

Conference on Turbulence and Diffusion, Amer. Meteor. Soc. (1988).

Tropopause folding and the variability of the tropopause height as seen by the Flatland VHF radar. Nastrom, G.D., J.L. Green, M.R. Peterson, and K.S. Gage, presented at Fourth Workshop on MST Radars, Kyoto, Nov 29-Dec 2, 1988. Handbook for MAP, to appear (1989).

Utilization of a single clear-air Doppler radar beam to measure vertical divergence. Clark, W.L., G.D. Nastrom, K.S. Gage, J.L. Green, R.G. Strauch and J.M. Warnock, Preprint volume, Symposium on Lower Tropospheric Profiling: Needs and Technologies, Amer. Meteor. Soc., Boulder (1988).

Measurement of vertical velocity using clear-air Doppler radars. Van Zandt, T.E., J.L. Green, G.D. Nastrom, K.S. Gage, W.L. Clark, and J.M. Warnock, Preprint volume, Symposium on Lower Tropospheric Profiling: Needs and Technologies, Amer. Meteor. Soc., Boulder; and at COSPAR, 1988, Helsinki, as Poster 6.P.11 (1988).

Measurement of large-scale vertical velocity using clear-air Doppler radars. Nastrom, G.D., J.L. Green, T.E. VanZandt, K.S. Gage, and W.L. Clark, presented at the Fourth Workshop on MST Radars, Kyoto, Nov 29-Dec 2, 1988. Handbook for MAP, to appear (1989).

A simple model for the enhanced frequency spectrum of vertical velocity based on tilting of atmospheric layers by lee waves. Gage, K.S., and G.D. Nastrom, Spring Meeting of the American Geophysical Union, Baltimore (1988).

A simple model for the enhanced frequency spectrum of vertical velocity based on tilting of atmospheric layers by lee waves. Gage, K.S., and G.D. Nastrom, presented at the Fourth Workshop on MST Radars, Kyoto, Nov 29-Dec 2, 1988. Handbook for MAP, to appear (1989).

The effects of sampling strategy on the estimates of mean vertical velocity. Nastrom, G.D., K.S. Gage, and W.L. Ecklund, presented at the Fourth Workshop on MST Radars, Kyoto, Nov 29-Dec 2, 1988. Handbook for MAP, to appear (1989).

Comparison among clear-air radar, thermosonde and optical measurements and model estimates of  $C_n^2$  made in very flat terrain over Illinois. Warnock, J.M., R.R. Beland, J.H. Brown, W.L. Clark, F.D. Eaton, L.D. Favier, K.S. Gage, J.L. Green, W.H. Hatch, J.R. Hines, E.A. Murphy, G.D. Nastrom, W. A. Peterson, and T.E. VanZandt, presented at the Fourth Workshop on MST Radars, Kyoto, Nov 29-Dec 2, 1988. Handbook for MAP, to appear (1989).

AIR FORCE OFFICE OF SCIENTIFIC RESEARCH (AFOSR)  
 (AFOSR-TR-89-1242)  
 This report is the property of AFOSR and is  
 loaned to you. It and its contents are not to be  
 distributed outside your organization.  
 Chief, Technical Information Division

Panel report on "The structure and dynamics of the free atmosphere as observed by VHF/UHF radar by K. S. Gage". Hooke, W.H., D. Atlas, F. Einaudi, D.C. Fritts, T. Gal-Chen, E.E. Gossard, C.O. Hines, J. Koerner, M. Larsen, C.H. Liu, G.D. Nastrom, W. McGovern, J. Riley, M.A. Shapiro, S. Smith, T.E. VanZandt, S. Williams, and E. Zipser, Radar in Meteorology, D. Atlas, ed., Amer. Meteor. Soc., to appear (1989).

Tropopause folding and the variability of the tropopause height as seen by the Flatland VHF radar. Nastrom, G.D., J.L. Green, M.R. Peterson, and K.S. Gage, J. Appl. Meteor., in press (1989).

Sources of gravity waves as seen in the vertical velocity measured by the Flatland VHF radar. Nastrom, G.D., M.R. Peterson, J.L. Green, K.S. Gage, and T.E. VanZandt, Preprint volume, 24th Conference on Radar Meteorology, Am. Meteor. Soc., Tallahassee, March 27-31 (1989).

Comparisons of refractivity turbulence estimates from the Flatland VHF radar with other measurement techniques. Green, J., R.R. Beland, J.H. Brown, W.L. Clark, F.D. Eaton, L.D. Favier, K.S. Gage, W.H. Hatch, J.R. Hines, E.A. Murphy, G.D. Nastrom, W.A. Peterson, T.E. VanZandt, and J.M. Warnock, Preprint volume, 24th Conference on Radar Meteorology, Am. Meteor. Soc., Tallahassee, March 27-31 (1989).

The spectrum of vertical velocity from Flatland radar observations. VanZandt, T.E., G.D. Nastrom, J.L. Green, and K.S. Gage, Preprint volume, 24th Conference on Radar Meteorology, Am. Meteor. Soc., Tallahassee, March 27-31 (1989).

Sources of gravity waves as seen in the vertical velocity measured by the Flatland VHF radar. Nastrom, G.D., M.R. Peterson, J.L. Green, and K.S. Gage, J. Appl. Meteor., in revision (1989).

Interpretation of the frequency spectra of horizontal winds over rough terrain as seen by clear-air Doppler radars and aircraft. Nastrom, G.D., and K.S. Gage, 7th AMS Conference on Atmos. and Ocean. Waves and Stability, San Francisco, April 10-14 (1989).

A simple model for the enhanced frequency spectrum of vertical velocity based on tilting of atmospheric layers by lee waves. Gage, K.S., and G.D. Nastrom, Radio Sci., in revision (1989).

The effects of sampling strategy on the estimates of mean vertical velocity. Nastrom, G.D., K.S. Gage, and W.L. Ecklund, Radio Sci., in revision (1989).

For	<input checked="" type="checkbox"/>
	<input type="checkbox"/>
	<input type="checkbox"/>

Atv Codes

and/or  
Special

Dist

A-1

Enhanced frequency spectra of winds at the mesoscale based on radar wind profiler observations. Nastrom, G.D., and K.S. Gage, Radio Sci., in revision (1989).

Measurement of large-scale vertical velocity using clear-air Doppler radars. Nastrom, G.D., M.R. Peterson, J.L. Green, T.E. VanZandt, K.S. Gage, and W.L. Clark, Mon. Wea. Rev., in preparation (1989).

#### ABSTRACT OF OBJECTIVES AND ACCOMPLISHMENTS:

This study was aimed at understanding the mesoscale motions of the atmosphere, their interactions with other scales of flow, and applications of MST radars to meteorological problems. The primary observational data source was vertical and horizontal wind measurements from MST radars, also called clear-air Doppler profilers, plus some analyses of balloon and aircraft data. Investigations included (1) case studies of the interactions between motions of various scales, including study of the influence of underlying terrain on the interactions of meso- and larger-scale processes, (2) study of the frequency spectra of vertical and horizontal winds as a function of background weather conditions such as stability and wind speed, and (3) interpretation of the observed mesoscale variations in the framework of current theories of gravity waves and stratified turbulence.

It was concluded from analyses of aircraft data of wind and temperature that the observed scalar spectra are reasonably consistent with a simple model in which fluctuations are produced by quasi two-dimensional motions acting in a plane inclined slightly to isentropic surfaces and to the isopleths of constant mixing ratios of trace species. It was also found that the variances are up to six times larger over mountainous terrain than over oceans or plains. The results showed only partial agreement with predictions from the theories of stratified turbulence and of a spectrum of gravity waves (see paper C.2), indicating that further study was needed to understand the physics of the motions involved. MST data from Colorado and Alaska were used to examine the response of mesoscale horizontal motions to changes in weather conditions. It was found that there is an enhancement of amplitude at high frequencies, with magnitude of about a factor of four relative to values extrapolated from the low frequency spectra, regardless of season, altitude, or weather conditions, and which likely represents high frequency gravity waves launched by flow over rough terrain. Comparisons of the results from Colorado with theoretical predictions, including the effects of Doppler-shifting, again showed that the observed spectra

do not follow either the wave or turbulence models closely in all respects.

The refractivity turbulence structure constant,  $C_n^2$ , was measured with several methods and instruments, and comparisons among the results obtained during night hours showed good agreement. During the daylight hours the thermosonde results were consistently larger than those from other techniques. An important result of this study was that the MST radar data at Flatland, in Illinois, could be modeled using the same model parameters developed from radar data collected in Colorado, except that the distribution of wind shears had to be reduced about a factor of two, suggesting that fine structure wind shear is smaller over the plains than over mountains, and, consequently, that eddy dissipation rates are smaller there.

Several results were obtained using the Flatland MST radar: (1) there is enhanced gravity wave activity around fronts, jet streams, and convective areas. (2) The radar data can be used to study tropopause folding events. In addition to case studies, a preliminary climatology of folding events was developed. (3) The spectrum of vertical motions at Flatland was found to closely match that predicted for a spectrum of gravity waves under the effects of Doppler shifting by the horizontal winds. (4) Finally, it was found that the radar measurements of vertical velocity reflect the large-scale motions when storms are not changing rapidly and conditions are statistically stationary. It was also found that care must be used to ensure that adequate temporal sampling is made when deriving time averages of vertical velocity; this is due to the relatively large energy of vertical motions at high frequencies.

THE INTERACTION AND VARIATION OF WAVES AND  
TURBULENCE FROM MST RADAR DATA

Final Technical Report  
Contract Number F49620-86-C-0027  
1 Feb 1986 - 31 July 1989

Miriam R. Peterson  
Control Data Corporation, Minneapolis, MN 55440

A. RESEARCH OBJECTIVES (STATEMENT OF WORK):

1. Study the joint space and time variability of small-scale turbulence, gravity wave activity, and background flow using data from the Colorado Profiler Network and from the Sunset VHF radar.
2. Draw conclusions regarding the influence of the underlying terrain on the interactions of the processes occurring at different scales.
3. Study the variations of vertical velocity and small-scale turbulence during summer to define the diurnal variations and determine the influence of background stability on gravity wave activity.
4. Compare the frequency spectra of horizontal and vertical winds during different seasons, times of day, locations, altitudes, and background weather conditions to draw conclusions regarding the interpretation of the mesoscale wind spectra in terms of gravity waves, quasi two-dimensional turbulence or a mix of processes.

B. STATUS OF THE RESEARCH EFFORT:

Data from the Platteville MST radar in the Colorado Profiler Network were used to study changes in the spectrum of horizontal winds as a function of mean wind speed, altitude, season, and stability. It was found that the high frequency portion of the spectrum is enhanced relative to an extrapolation of the low frequency regime. This high frequency enhancement is likely due to gravity waves launched by flow over rough terrain. This was reported in the papers listed below as C.13 and D.11.

Spectra of winds and temperatures from aircraft were sorted according to underlying terrain, and it was found that there is a significant enhancement of the variance over mountainous regions. This was reported in papers C.2 and D.2.

The small-scale eddies that lead to radar reflections at VHF are linked to the eddy dissipation rate and to the radar refractivity turbulence structure constant,  $C_n^2$ . Measurements of  $C_n^2$  had been made in the past at Sunset and at Denver, and had been used to calibrate a theoretical model of  $C_n^2$  as a function of large-scale winds and stability. This model was applied to VHF radar data from the Flatland radar in Illinois and it was found that the distribution of wind shears had to be reduced by about a factor of two from the values used in Colorado. This indicates the fine structure wind shear over the plains is smaller than over the mountains for the same large-scale wind structure, and implies that eddy dissipation rates are also smaller. This was reported in papers C.7 and D.9.

Further, an effort was made to obtain estimates of the vertical flux of horizontal momentum using data from the Sunset radar in the so-called five-beam configuration. Unfortunately, the data were spaced in time such that motions with time scales less than about 40 minutes were not resolved. From our own work and that of others it has become clear that a significant amount of the gravity wave energy is at periods less than an hour or so, especially over the mountains (see paper C.13), which makes results based on coarse time resolution of limited value. Further, since Sunset is near the continental divide, conditions change rapidly and a statistically stationary period is difficult to define. As a result of these limitations, it was decided to delay expanding our initial analysis, reported in paper D.1, until a more appropriate data set becomes available.

Simultaneous measurements of horizontal and vertical velocity at Platteville were spectrally analyzed and the results compared with predictions from the model of Doppler-shifted gravity waves presented by Fritts and VanZandt (J. Geophys. Res., 92:9723-9732, 1987). Large discrepancies were noted, but as Platteville is near the mountains they could be due to another process such as mountain wave effects. This was reported in paper D.3 and expanded upon in paper D.4

Analyses of aircraft data were contrasted with predictions from the theory of stratified turbulence (reported in paper C.1) and it was found that the scalar spectra are reasonably consistent with a simple model in which fluctuations are produced by quasi two-dimensional motions acting in a plane inclined slightly to isentropic surfaces and to the isopleths of constant mixing ratios of trace species. Similar concepts of tilting of atmospheric layers were used to derive a simple model for the enhanced frequency spectrum of vertical velocities and are reported in papers C.5, C.11, and D.7.

Vertical velocity measurements from the Flatland VHF radar in Illinois were spectrally analyzed and the results compared with the theory of Doppler-shifted gravity waves as presented by Fritts and VanZandt. Excellent agreement was found, on a statistical basis, suggesting that over the plains the vertical velocity fluctuations are primarily due to propagating gravity waves. This was reported in papers C.14 and D.10.

The Flatland radar data were also used to study the correlation between periods of increased gravity wave activity and the background weather conditions. As reported in papers C.10 and D.8, there is evidence that every weather system, such as a front or jet streak passage, produces enhanced gravity wave activity (as detected by the radar) and that every instance of enhanced gravity wave activity detected by the radar could be traced to a nearby weather system.

On a larger scale, the Flatland radar was used to monitor variations in tropopause height during several cases when tropopause folds developed, as determined from analyses of isentropic potential vorticity. This work, reported in papers C.3 and C.9, demonstrates the usefulness of MST radars for monitoring the tropopause and its folds which are believed to play a key role in stratosphere-troposphere exchange processes.

Other large-scale processes considered during this study were the divergence and vertical velocity. These studies were reported in papers C.4, C.15, D.5, and D.6. They were proof-of-concept efforts intended to show the feasibility of this analysis approach, and demonstrated the great versatility of MST radar data in application to many meteorological analysis and forecasting problems. The data are relatively new to meteorologists, and care must be taken to interpret them properly (as discussed in papers C.6 and C.12). Other applications of the data to broad problems were discussed in a major review session, reported in paper C.8.

#### C. PUBLICATIONS:

1. Spectrum of atmospheric vertical displacements and spectrum of conservative passive additives due to quasi-horizontal atmospheric motions. Gage, K.S. and G.D. Nastrom, J. Geophys. Res., 91, 13211-13216 (1986).
2. An investigation of terrain effects on the mesoscale spectrum of atmospheric motions. Nastrom, G.D., D.C. Fritts, and K.S. Gage, J. Atmos. Sci., 44, 3087-3096 (1987).

3. Tropopause folding and the variability of the tropopause height as seen by the Flatland VHF radar. Nastrom, G.D., J.L. Green, M.R. Peterson, and K.S. Gage, presented at Fourth Workshop on MST Radars, Kyoto, Nov 29-Dec 2, 1988. Handbook for MAP, to appear (1989).
4. Measurement of large-scale vertical velocity using clear-air Doppler radars. Nastrom, G.D., J.L. Green, T.E. VanZandt, K.S. Gage, and W.L. Clark, presented at the Fourth Workshop on MST Radars, Kyoto, Nov 29-Dec 2, 1988. Handbook for MAP, to appear (1989).
5. A simple model for the enhanced frequency spectrum of vertical velocity based on tilting of atmospheric layers by lee waves. Gage, K.S., and G.D. Nastrom, presented at the Fourth Workshop on MST Radars, Kyoto, Nov 29-Dec 2, 1988. Handbook for MAP, to appear (1989).
6. The effects of sampling strategy on the estimates of mean vertical velocity. Nastrom, G.D., K.S. Gage, and W.L. Ecklund, Presented at the Fourth Workshop on MST Radars, Kyoto, Nov 29-Dec 2, 1988. Handbook for MAP, to appear (1989).
7. Comparison among clear-air radar, thermosonde and optical measurements and model estimates of  $C_n^2$  made in very flat terrain over Illinois. Warnock, J.M., R.R. Beland, J.H. Brown, W.L. Clark, F.D. Eaton, L.D. Favier, K.S. Gage, J.L. Green, W.H. Hatch, J.R. Hines, E.A. Murphy, G.D. Nastrom, W. A. Peterson, and T.E. VanZandt, presented at the Fourth Workshop on MST Radars, Kyoto, Nov 29-Dec 2, 1988. Handbook for MAP, to appear (1989).
8. Panel report on "The structure and dynamics of the free atmosphere as observed by VHF/UHF radar by K. S. Gage". Hooke, W.H., D. Atlas, F. Einaudi, D.C. Fritts, T. Gal-Chen, E.E. Gossard, C.O. Hines, J. Koerner, M. Larsen, C.H. Liu, G.D. Nastrom, W. McGovern, J. Riley, M.A. Shapiro, S. Smith, T.E. VanZandt, S. Williams, and E. Zipser, Radar in Meteorology, D. Atlas, ed., Amer. Meteor. Soc., to appear (1989).
9. Tropopause folding and the variability of the tropopause height as seen by the Flatland VHF radar. Nastrom, G.D., J.L. Green, M.R. Peterson, and K.S. Gage, J. Appl. Meteor., in press (1989).
10. Sources of gravity waves as seen in the vertical velocity measured by the Flatland VHF radar. Nastrom, G.D., M.R. Peterson, J.L. Green, and K.S. Gage, J. Appl. Meteor., in revision (1989).
11. A simple model for the enhanced frequency spectrum of vertical velocity based on tilting of atmospheric layers by

lee waves. Gage, K.S., and G.D. Nastrom, Radio Sci., in revision (1989).

12. The effects of sampling strategy on the estimates of mean vertical velocity. Nastrom, G.D., K.S. Gage, and W.L. Ecklund, Radio Sci., in revision (1989).

13. Enhanced frequency spectra of winds at the mesoscale based on radar wind profiler observations. Nastrom, G.D., and K.S. Gage, Radio Sci., in revision (1989).

14. The spectrum of vertical velocity from Flatland radar observations. VanZandt, T.E., G.D. Nastrom, J.L. Green, and K.S. Gage, J. Geophysical Res., in preparation (1989).

15. Measurement of large-scale vertical velocity using clear-air Doppler radars. Nastrom, G.D., M.R. Peterson, J.L. Green, T.E. VanZandt, K.S. Gage, and W.L. Clark, Mon. Wea. Rev., in preparation (1989).

#### D. CONFERENCE PAPERS:

1. VHF radar measurements of the vertical momentum flux. Nastrom, G.D., and J.L. Green, Preprint volume, 23rd Conference on Radar Meteorology, Snowmass, CO, Sept 22-26 (1986).

2. The effects of terrain on the mesoscale spectrum of atmospheric motions. Nastrom, G.D., D.C. Fritts, and K.S. Gage, XIX General Assembly of IUGG, Vancouver, Aug. 9-22 (1987), and at AMS Sixth Conference on Atmos. and Ocean. Waves and Stability, Seattle, August 25-28 (1987).

3. Dependence of the frequency spectrum observed with ST radars on background wind speed. Gage, K.S., and G.D. Nastrom, AMS Sixth Conference on Atmos. and Ocean. Waves and Stability, Seattle, August 25-28 (1987).

4. Further discussion of the dynamical processes that contribute to the spectrum of mesoscale atmospheric motions. Gage, K.S. and G.D. Nastrom, Preprint volume, Eighth Conference on Turbulence and Diffusion, Amer. Meteor. Soc. (1988).

5. Utilization of a single clear-air Doppler radar beam to measure vertical divergence. Clark, W.L., G.D. Nastrom, K.S. Gage, J.L. Green, R.G. Strauch and J.M. Warnock, Preprint volume, Symposium on Lower Tropospheric Profiling: Needs and Technologies, Amer. Meteor. Soc., Boulder (1988).

6. Measurement of vertical velocity using clear-air Doppler radars. VanZandt, T.E., J.L. Green, G.D. Nastrom, K.S. Gage, W.L. Clark, and J.M. Warnock, Preprint volume,

Symposium on Lower Tropospheric Profiling: Needs and Technologies, Amer. Meteor. Soc., Boulder; and at COSPAR, 1988, Helsinki, as Poster 6.P.11 (1988).

7. A simple model for the enhanced frequency spectrum of vertical velocity based on tilting of atmospheric layers by lee waves. Gage, K.S., and G.D. Nastrom, Spring Meeting of the American Geophysical Union, Baltimore (1988).

8. Sources of gravity waves as seen in the vertical velocity measured by the Flatland VHF radar. Nastrom, G.D., M.R. Peterson, J.L. Green, K.S. Gage, and T.E. VanZandt, Preprint volume, 24th Conference on Radar Meteorology, Am. Meteor. Soc., Tallahassee, March 27-31 (1989).

9. Comparisons of refractivity turbulence estimates from the Flatland VHF radar with other measurement techniques. Green, J., R.R. Beland, J.H. Brown, W.L. Clark, F.D. Eaton, L.D. Favier, K.S. Gage, W.H. Hatch, J.R. Hines, E.A. Murphy, G.D. Nastrom, W.A. Peterson, T.E. VanZandt, and J.M. Warnock, Preprint volume, 24th Conference on Radar Meteorology, Am. Meteor. Soc., Tallahassee, March 27-31 (1989).

10. The spectrum of vertical velocity from Flatland radar observations. VanZandt, T.E., G.D. Nastrom, J.L. Green, and K.S. Gage, Preprint volume, 24th Conference on Radar Meteorology, Am. Meteor. Soc., Tallahassee, March 27-31 (1989).

11. Interpretation of the frequency spectra of horizontal winds over rough terrain as seen by clear-air Doppler radars and aircraft. Nastrom, G.D., and K.S. Gage, 7th AMS Conference on Atmos. and Ocean. Waves and Stability, San Francisco, April 10-14 (1989).

Also, 7 papers (numbers 3,4,5,6,7,11,12 of Section C) were presented at the Fourth Workshop on MST Radars, Kyoto, Nov 29-Dec 2 (1988).

#### E. OTHER INTERACTIONS:

As reflected by the coauthors of the papers listed above, much of this work was done in collaboration with other scientists. Joint studies with NOAA's Aeronomy Laboratory and several university groups were made, with contact provided during personal visits, seminars or workshops, and at conferences attended as reflected in the conference papers listed.

In December, 1987, Dr. G.D. Nastrom participated in the 8th Annual EOSAEL/TWI Conference (Las Cruces, NM). The joint studies of refractivity turbulence involving groups

from the Air Force Geophysics Laboratory, the Army Atmospheric Sciences Laboratory, and the Flatland MST radar were an outgrowth of discussions at this conference.

Finally, peer reviews rendered on journal papers and on proposals for new work represent an interaction with the scientific community in a broad sense. During the period of this contract Dr. Nastrom provided reviews on 22 papers for the Journal of Atmospheric Sciences, Journal of Atmospheric and Terrestrial Physics, Geophysical Research Letters, Journal of Geophysical Research, Radio Science, and Journal of Climate and Applied Meteorology. Also, reviews were given for 8 proposals to the Air Force Office of Scientific Research and the National Science Foundation.

# Spectrum of Atmospheric Vertical Displacements and Spectrum of Conservative Scalar Passive Additives Due to Quasi-Horizontal Atmospheric Motions

K. S. GAGE

*Aeronomy Laboratory, National Oceanic and Atmospheric Administration Environmental Research Laboratories,  
Boulder, Colorado*

G. D. NASTROM

*Meteorology Research, Control Data Corporation, Minneapolis, Minnesota*

This paper is concerned with the relationship between the spectrum of vertical displacements associated with the mesoscale spectrum of quasi-horizontal motions in the atmosphere and the mesoscale spectra of scalar passive additives. This work is based on observations of mesoscale atmospheric wave number spectra of wind, temperature, and certain trace species sampled in the altitude range 9–14 km by commercial aircraft during the Global Atmospheric Sampling Program (GASP). The principal result is that the scalar spectra are reasonably consistent with a simple model in which scalar fluctuations are produced by quasi two-dimensional motions acting in a plane inclined slightly to isentropic surfaces and to the isopleths of constant mixing ratio of trace species.

## 1. INTRODUCTION

Following the work of *Reed and German* [1965] and many others, it has been widely recognized that much of the large-scale vertical transport in the atmosphere is due to quasi-horizontal motions that transport mass to great distances along sloping isentropic surfaces. Large-scale motions in the atmosphere are quasi-horizontal and are much more effective in diffusing mass in the horizontal than in the vertical direction. Yet since this diffusion takes place along sloping surfaces, there is a nonnegligible vertical component of mass transport. The diffusivity along the mixing surfaces so greatly exceeds the diffusivity normal to the surfaces of constant concentration that even a very small slope of the mixing surfaces is enough to produce a major contribution to vertical transport.

In this paper we are concerned primarily with the mesoscale contribution to the process of vertical transport due to the spectrum of nearly horizontal motions that has been studied using wind and temperature data collected during routine commercial airline flights during the Global Atmospheric Sampling Program (GASP) [*Nastrom et al.*, 1984; *Nastrom and Gage*, 1985]. The interpretation of these mesoscale spectra offered by *Gage and Nastrom* [1986] points toward the existence of a mesoscale spectrum of quasi two-dimensional turbulence which should contribute very effectively to horizontal diffusivity. Analysis of the temperature spectra suggests that they are also the result of quasi two-dimensional turbulence acting on the background temperature gradient. The quasi two-dimensional turbulence acting on a background gradient of the mixing ratio of a passive scalar quantity should, in a similar way, lead to a mesoscale spectrum of scalar fluctuations.

In this paper we develop a physical model linking the observed GASP spectra of wind, temperature, and trace species.

In a companion paper by *Nastrom et al.* [this issue] we consider the consistency of the observed spectra with the physical model proposed here.

## 2. OBSERVED SPECTRA OF ATMOSPHERIC MOTIONS AND TEMPERATURE FROM THE GASP DATA SET

A detailed climatology of mesoscale horizontal wave number spectra of wind at tropopause altitude has been presented by *Nastrom et al.* [1984] and *Nastrom and Gage* [1985]. These spectra were deduced from an analysis of data from over 6900 routine commercial airline flights which comprised GASP. The wind spectra are shown in summary form in Figure 1. The spectra show two regimes of distinctly different slope. The mesoscale regime extends from about 500 km or so on the large-scale end down to a few kilometers. Here the slope is  $-5/3$ , as expected for quasi two-dimensional stratified turbulence [*Gage*, 1979; *Lilly*, 1983]. At large scales the spectra steepen toward the  $-3$  slope expected for the enstrophy-cascading range of quasi two-dimensional turbulence, which is usually referred to as geostrophic turbulence [*Charney*, 1971]. A schematic representation of these two inertial ranges shown in Figure 2 [*Larsen et al.*, 1982] fits the GASP spectra quite well.

The wave number spectrum of potential temperature obtained from analysis of the GASP data is shown in summary form in Figure 1 and for the longest flights in Figure 3. It is obvious at first glance that the temperature spectrum is basically the same shape as the velocity spectra. Note that this result differs from model calculations of quasi two-dimensional turbulence, which predicts the slope of a passive scalar quantity to be  $-1$  in the enstrophy-cascading range and  $+1/3$  in the energy-cascading range [*Lesieur and Herring*, 1985]. Reasons for this will be discussed in section 4.

Evidently, the magnitude and shape of the potential temperature spectrum are determined by the same dynamics that govern the velocity spectra. Indeed, as discussed by *Gage and Nastrom* [1986], the potential temperature spectrum appears to be in equilibrium with the velocity spectra, as evidenced by

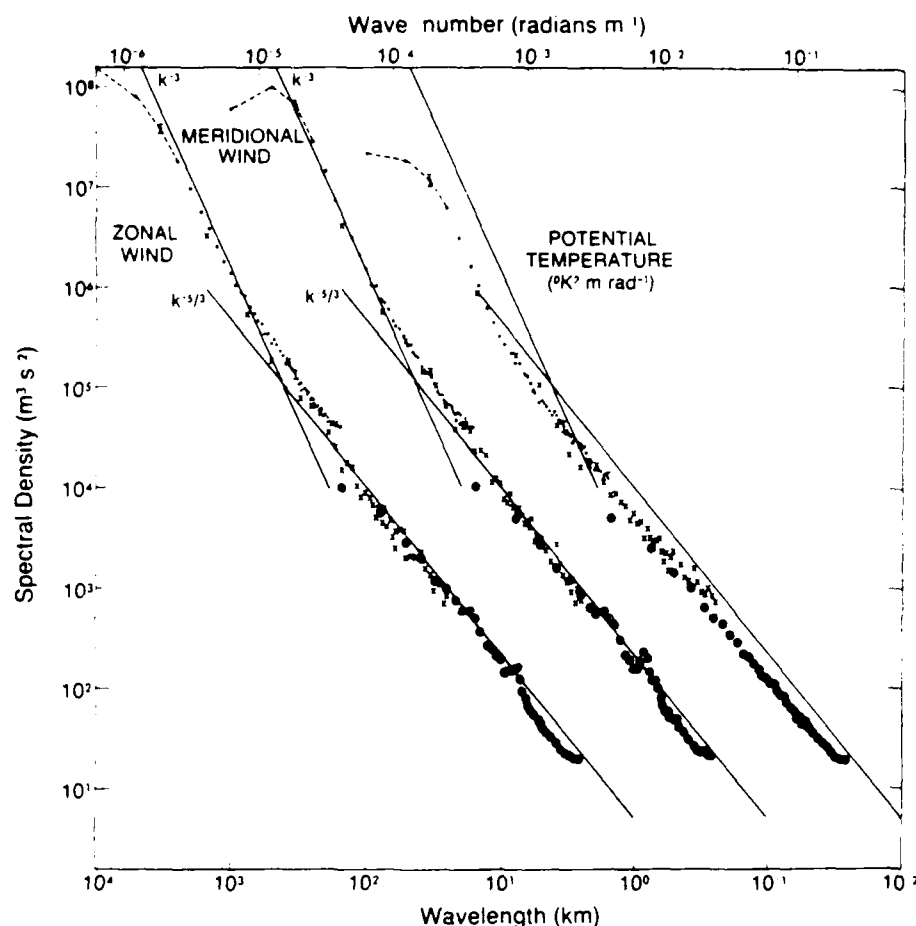


Fig. 1 Summary comparison of GASP wave number spectra of potential temperature and zonal and meridional velocity composed from three groups of flight segments of different lengths. The three types of symbols show results from each group. Straight lines indicate slopes of  $-3$  and  $-5/3$ . The meridional wind spectra are shifted one decade to the right, and the potential temperature spectra are shifted two decades to the right [after Nastrom and Gage, 1985].

the relationship of the potential energy spectrum to the kinetic energy spectrum. As anticipated by Charney [1971] for geostrophic turbulence, the spectral energy is partitioned approximately equally among the two components of kinetic energy and potential energy. This result is reproduced in Figure 4. The potential temperature spectrum is related to the potential energy spectrum by

$$\Phi_{\theta\theta} = \frac{2N^2\theta^2}{g^2} \Phi_{PF} \quad (1)$$

where  $N$  is the Brunt-Vaisala frequency and  $g$  is gravitational acceleration. Since  $N^2$  is larger in the stratosphere than in the troposphere, the amplitude of the potential temperature spectrum is larger in the stratosphere than the troposphere. These relationships appear to hold throughout the atmospheric mesoscale as well as in the geostrophic regime.

Note that the equipartitioning referred to above is evidently intrinsic to the quasi-horizontal motions themselves. This does not imply an equipartitioning between the quasi-horizontal motions and wave motions, as discussed by Gage and Nastrom [1986]. In this context the low Froude number regime of stratified turbulence [Riley *et al.*, 1981; Lilly, 1983] implies a regime of decoupled modes of internal waves and quasi-horizontal motions. Indeed, if the stratification is sufficiently stable, the kinetic energy associated with the quasi-horizontal

mode of motion can be expected to dominate the kinetic and potential energy associated with the internal wave mode.

In section 3 we consider the consequences of a spectrum of quasi-horizontal eddies flowing along sloping "mixing sur-

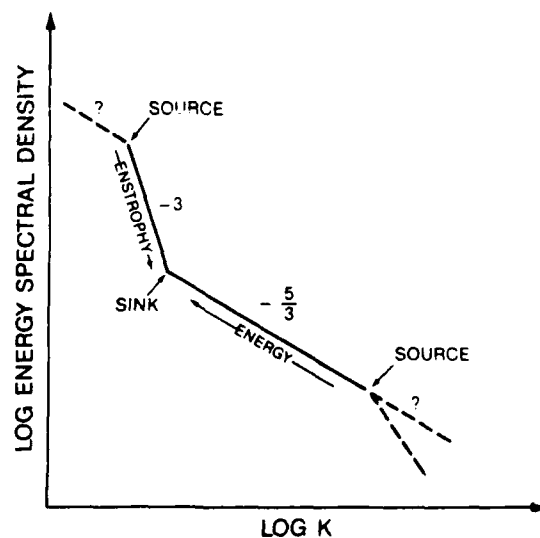


Fig. 2 Schematic representation of spectral ranges in quasi two-dimensional turbulence [after Larsen *et al.*, 1982]

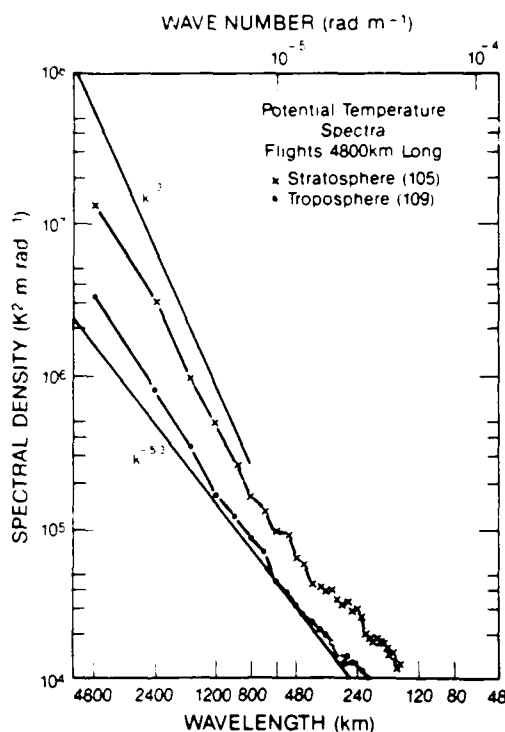


Fig. 3. Potential temperature spectra from flights at least 4800 km long. Stratospheric and tropospheric spectra are plotted separately. The number of cases averaged in each group is given in parentheses [after Gage and Nastrom, 1986].

faces," as anticipated in the analysis of Reed and German [1965]. Specifically, we shall consider what happens when these "mixing surfaces" are inclined relative to isentropic surfaces or isopleths of constant mixing ratio of trace species such as ozone.

### 3. SPECTRUM OF VERTICAL DISPLACEMENT DEDUCED FROM THE GASP TEMPERATURE SPECTRUM

Fluctuations in any conservative passive scalar quantity will be produced whenever there is a component of motion parallel to the gradient of the scalar quantity. In the atmosphere, and especially in the stratosphere, gradients of conservative passive scalar quantities usually are very much larger in the vertical than in the horizontal directions. This is just another way of saying the atmosphere is horizontally stratified, and to first order, gradients of potential temperature, ozone, etc., are in the vertical direction. The exception being in the vicinity of fronts, strong convection, etc.

For the purposes of this paper we shall define "vertical displacements" relative to isentropic surfaces. Thus quasi-horizontal motions which are coincident with isentropic surfaces would not produce "vertical displacements" even if the isentropic surfaces were inclined to the horizontal. Our concern is rather with the small displacements taking place orthogonal to the isentropic surfaces or isopleths of constant mixing ratio. From this perspective the vertical displacement spectrum  $\Phi_{zz}$  is the projection of the quasi-horizontal displacement spectrum in the mixing surface  $\Phi_{xz}$  in the direction normal to the isentropic surface. Thus the vertical displacement spectrum is given by

$$\Phi_{zz} = (\sin \delta)^2 \Phi_{xz} \quad (2)$$

where  $\delta$  is the angle that the isentropic surface makes with the mixing surface.

With vertical displacement defined in this way the vertical displacement spectrum can be deduced from the potential temperature spectrum, provided the background potential temperature gradient is known. If the background potential temperature gradient is constant, the relationship between the potential temperature spectrum and the vertical displacement

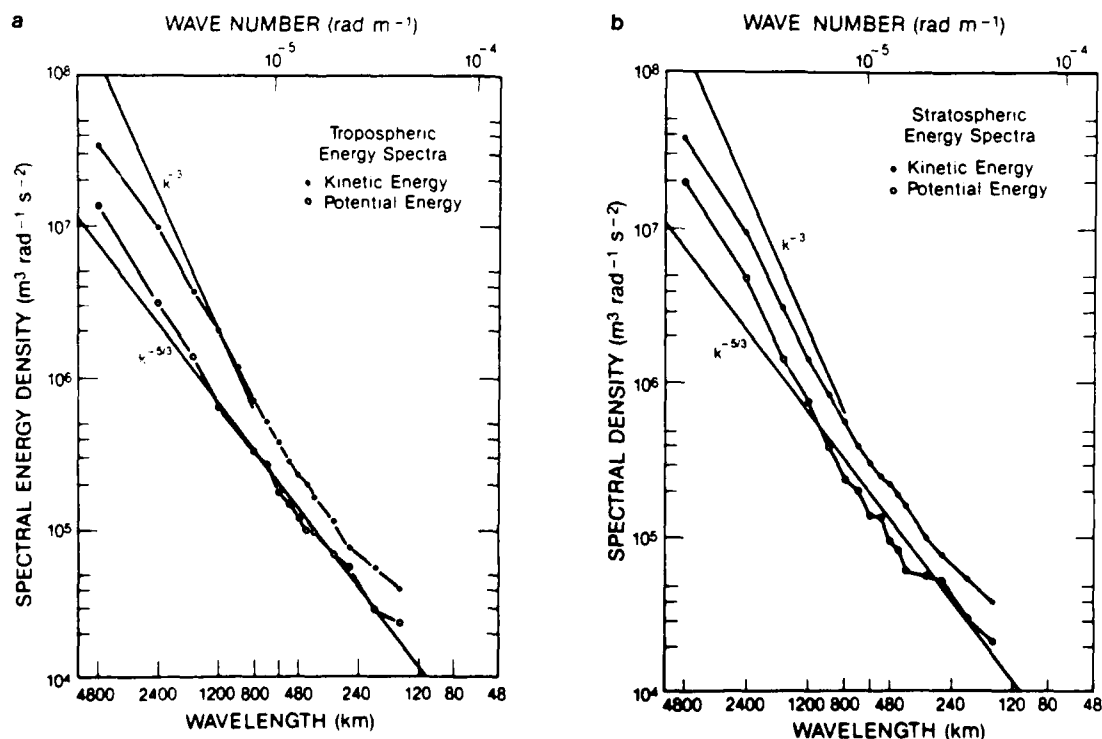


Fig. 4. Kinetic and potential energy spectra from flights at least 4800 km long: (a) tropospheric energy and (b) stratospheric energy spectra [after Gage and Nastrom, 1986].

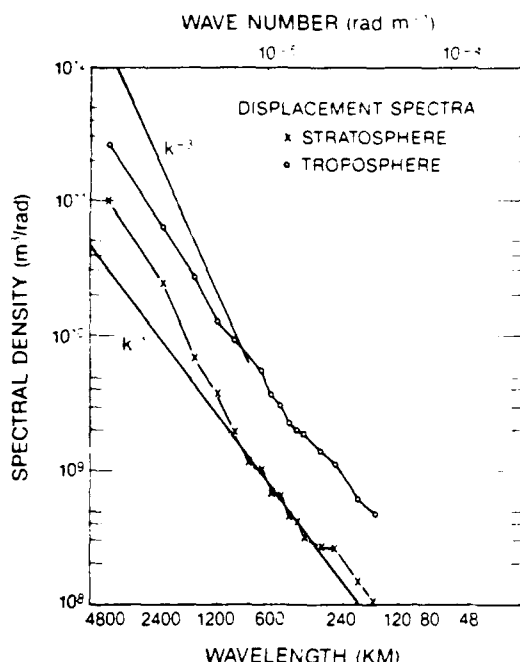


Fig. 5. Vertical displacement spectra in the troposphere and stratosphere, deduced from the potential temperature spectrum and assumed background gradients of potential temperature.

spectrum, as defined above, is given by

$$\Phi_{zz} = \frac{\Phi_{\theta\theta}}{(\partial\theta/\partial z)^2} = \frac{2\Phi_{PE}}{N^2} \quad (3)$$

where we have made use of (1). The vertical displacement spectrum defined in this way is easily deduced from either the potential temperature spectrum of Figure 3 or the potential energy spectrum of Figure 4. The result is shown in Figure 5. Note that the magnitude of the displacement spectrum is reduced in the stratosphere relative to the troposphere. Evidently, stable stratification causes stratospheric motions to deviate less from isentropic surfaces than tropospheric motions.

Consider now any conservative passive scalar quantity  $\chi$  that has isopleths of constant mixing ratio coincident with isentropic surfaces. It would then follow that

$$\Phi_{zz} = \Phi_{\chi\chi} \left( \frac{\partial\chi}{\partial z} \right)^2 \quad (4)$$

provided the gradient of  $\chi$  is constant within the region where  $\chi$  is measured. Under these circumstances we would anticipate

$$\Phi_{zz} = \Phi_{\theta\theta} \frac{(\partial\chi/\partial z)^2}{(\partial\theta/\partial z)^2} \quad (5)$$

and this relationship can be used to check for consistency between passive scalar spectra and potential temperature spectra. The results of this calculation are given by Nastrom *et al.* [this issue] and show reasonable agreement among spectral amplitudes.

More generally, we expect that the slopes of isopleths of constant mixing ratio will not coincide with isentropic surfaces. In this event the vertical displacements defined relative to the isopleths of constant mixing ratio will differ from the displacements relative to the isentropic surfaces so that

$$\Phi_{zz}' = \Phi_{zz} \left( \frac{\sin \delta'}{\sin \delta} \right)^2 \quad (6)$$

where  $\delta$  represents the angle of the isopleths of constant mixing ratio relative to the mixing surfaces. Then the fluctuations of conservative passive scalar quantity will satisfy

$$\Phi_{zz} = \Phi_{zz}' \left( \frac{\partial\chi}{\partial z} \right)^2 \quad (7)$$

The ratio of slopes  $\sin \delta' / \sin \delta$  can be evaluated as follows. The variance of each spectrum can be obtained by integrating across the wave number spectrum

$$\Delta^2 = \int \Phi_{zz} dk$$

$$(\Delta')^2 = \int \Phi_{zz}' dk \quad (8)$$

$$\sigma_{zz}^2 = \int \Phi_{zz} dk$$

and

$$\sigma_{zz'}^2 = \int \Phi_{zz}' dk$$

From (3) we find

$$\Delta = \frac{\sigma_{zz'}}{\partial\theta/\partial z} \quad (9)$$

from (7) we find

$$\Delta' = \frac{\sigma_{zz'}}{\partial\chi/\partial z} \quad (10)$$

and from (6) we find

$$\frac{(\Delta')^2}{(\Delta)^2} = \left( \frac{\sin \delta'}{\sin \delta} \right)^2 \quad (11)$$

From these relationships we deduce

$$\Phi_{zz} = \Phi_{zz}' \left( \frac{\Delta'}{\Delta} \right)^2 \left( \frac{\partial\chi}{\partial z} \right)^2 \quad (12)$$

The quantities  $\Delta$  and  $\Delta'$  are analogous to Ehrlh's [Ehrlh *et al.*, 1983] equivalent vertical displacement.

#### 4. DISCUSSION

In this paper we have developed a simple model relating the spectrum of conservative passive scalars to the spectrum of vertical displacements of quasi-horizontal motions. The model provides a straightforward interpretation of the spectra of temperature and trace species observed during GASP.

For the development presented here we have focused on the mesoscale atmospheric motions and assumed the background mean concentrations and associated isopleths of constant mixing ratio to be given. In reality, of course, isentropic surfaces and mixing ratio isopleths must evolve out of the large-scale dynamics, as described by Mahiman *et al.* [1984] and by Mahlman [1985]. According to this picture, the slopes of constant mixing ratios of trace species are determined by a balance between the meridional circulation, which tends to increase their slope, and the quasi-horizontal eddy motions, which tend to decrease their slope. Radiation has the effect of changing the potential temperature of parcels which are otherwise assumed to remain on isentropic surfaces. Chemical reactions can alter this picture for reactive species and these species can have slopes differing from nonreactive species.

The dynamical model developed here attributes the fluctuations of scalar quantities solely to the vertical displacements experienced by parcels of fluid in quasi-horizontal motion. The motion field in the presence of a mean gradient of the conservative scalar quantity is from this perspective responsible for the observed scalar fluctuations. This picture of passive scalar transport implies a spectrum of scalar fluctuations closely tied to the spectrum of fluid motions. There is no reason why a spectrum of scalar fluctuations determined in this way should bear any particular relationship to the scalar spectrum predicted from turbulence model simulations [Lesieur and Herring, 1985]. The latter spectra are produced when scalar variance in an otherwise homogeneous fluid is added to the turbulence model at specified wave numbers. The scalar quantity then participates in the turbulence cascades of the model, and a scalar spectrum is produced. For example, when scalar variance is added at small wave numbers to a turbulence model that simulates the enstrophy cascade of geostrophic turbulence, a scalar variance spectrum with spectral slope  $-1$  is produced. These model simulations are unlikely to simulate the spectra observed in GASP, since they do not account for the gradients in mean scalar concentration.

Throughout this work we have assumed that the motions represented by the GASP velocity spectra are quasi-horizontal and turbulence-like. Dewan [1979] and VanZandt [1982] suggested that such spectra could be due to internal waves familiar to oceanographers as the Garrett-Munk spectrum [Garrett and Munk, 1972, 1975; Olbers, 1983], and the two hypotheses are contrasted next.

Our main reasons for asserting that the GASP spectra are not internal wave spectra are given in detail by Gage and Nastrom [1986]. The principal problem with the Dewan-VanZandt hypothesis can be stated very succinctly: There is too much energy in the spectrum of horizontal atmospheric motions compared to the spectrum of atmospheric vertical motions to be consistent with the idea that both spectra are manifestations of a common spectrum of internal waves. The background vertical velocity spectrum in the atmosphere does appear to have a striking resemblance to the Garrett-Munk spectrum in the ocean, but the horizontal wind spectral amplitude consistent with this is very much smaller than the amplitudes observed. A preliminary climatology of vertical velocity spectra taken at various geographical locations by vertically looking clear-air Doppler radar under light-wind conditions shows a flat spectrum of fairly universal amplitude with a sharp cutoff at frequencies higher than the Brunt-Vaisala frequency [Ecklund et al., 1986]. They show that the variance of this spectrum is

$$\overline{w^2} = \int_{f_i}^{f_N} \Phi_{ww}(f) = \frac{A_{ww}}{\tau_B} \approx 1.0-2.0 \times 10^{-2} \text{ m}^2 \text{ s}^{-2} \quad (13)$$

where the frequency spectrum of vertical motions is approximated by

$$\Phi_{ww} = A_{ww} \quad f_i \leq f \leq f_N$$

Otherwise,

$$\Phi_{ww} = 0$$

where  $f_i (\equiv 1/\tau_i)$  is the inertial frequency and  $f_N (\equiv 1/\tau_B)$  is the buoyancy frequency  $N/2\pi$ . The variance of horizontal velocity for a spectrum of internal waves can be estimated as

$$\overline{u^2} = \int_{f_i}^{f_N} \Phi_{uu}(f) = A_{uu} \tau_i \quad (14)$$

where the frequency spectrum of zonal horizontal motions is approximated by

$$\Phi_{uu} = A_{uu} f^{-2} \quad f_i \leq f \leq f_N$$

Otherwise,

$$\Phi_{uu} = 0$$

The constants  $A_{ww}$  and  $A_{uu}$  can be related by the polarization relation in the form

$$\frac{E_H}{E_w} = \frac{2\Phi_{uw}}{\Phi_{ww}} = \frac{N^2 - \omega^2}{\omega^2} \quad (15)$$

where  $\omega = 2\pi f$ ,  $E_w = \frac{1}{2}\Phi_{ww}$ ,  $E_H = \frac{1}{2}(\Phi_{uu} + \Phi_{ii})$ , and we have assumed  $\Phi_{uw} = \Phi_{iu}$ . The value of  $\omega$  for which  $\Phi_{uw} = \Phi_{ww}$  gives the desired relationship between  $A_{uu}$  and  $A_{ww}$ , namely,

$$\frac{A_{uu}}{A_{ww}} = \frac{1}{3\tau_B^2} \quad (16)$$

The ratio of variances of horizontal and vertical motions is then found to be

$$\frac{\overline{u^2}}{\overline{w^2}} = \frac{A_{uu}}{A_{ww}} \tau_i \tau_B = \frac{1}{3} \frac{\tau_i}{\tau_B}$$

If we take  $\tau_B = 10$  min,  $\overline{w^2} = 2.0 \times 10^{-2} \text{ m}^2 \text{ s}^{-2}$ , and  $\tau_i = 18$  hours, corresponding to approximately 42° latitude, we find that  $\overline{u^2} \approx 0.72 \text{ m}^2 \text{ s}^{-2}$ . This variance associated with the internal wave spectrum is about an order of magnitude less than the variance contained in the mesoscale spectrum of quasi-horizontal eddies considered in this paper and evident in the GASP spectra [cf., Gage and Nastrom, 1985, 1986].

## 5. CONCLUSIONS

In this paper we have developed a simple physical model to relate the spectra of conservative passive scalar tracers to the spectra of vertical displacements associated with quasi-horizontal atmospheric motions. The vertical displacement spectra were deduced from the GASP spectra of potential temperature. The consistency between the spectral shape and amplitude of observed GASP spectra with this simple model supports the hypothesis that mesoscale quasi-horizontal motions play an important role in vertical as well as horizontal transport for the atmospheric mesoscale much as they do in large-scale planetary wave motions. The existence of an entire spectrum of quasi two-dimensional motions has important implications for the horizontal and vertical transport of trace species in the atmosphere. At the very least, local mixing by this process should complement the large-scale transport associated with planetary waves and geostrophic turbulence.

*Acknowledgment.* One of us (G.D.N.) was partially supported by the Air Force Office of Scientific Research.

## REFERENCES

- Charney, J. G., Geostrophic turbulence, *J. Atmos. Sci.*, 28, 1087-1095, 1971.
- Dewan, E. M., Stratospheric spectra resembling turbulence, *Science*, 204, 832-835, 1979.
- Ecklund, W. L., K. S. Gage, G. D. Nastrom, and B. B. Balsley, A preliminary climatology of the atmospheric vertical velocity spectrum observed by clear-air radar, *J. Clim. Appl. Meteorol.*, 25, 885-892, 1986.
- Ehhalt, D. H., E. P. Roth, and U. Schmidt, On the temporal variance of stratospheric trace gas concentrations, *J. Atmos. Chem.*, 1, 27-51, 1983.
- Gage, K. S., Evidence for a  $k^{-5/3}$  law inertial range in mesoscale two-dimensional turbulence, *J. Atmos. Sci.*, 36, 1950-1954, 1979.

- Gage, K. S., and G. D. Nastrom, On the spectrum of atmospheric velocity fluctuations seen by ST MST radar and their interpretation, *Radio Sci.*, 20, 1339-1347, 1985.
- Gage, K. S., and G. D. Nastrom, Theoretical interpretation of atmospheric wavenumber spectra of wind and temperature observed by commercial aircraft during GASP, *J. Atmos. Sci.*, 43, 729-740, 1986.
- Garrett, C., and W. Munk, Space-time scales of internal waves, *Geophys. Astrophys. Fluid Dyn.*, 2, 225-264, 1972.
- Garrett, C., and W. Munk, Space-time scales of internal waves: A progress report, *J. Geophys. Res.*, 80, 291-297, 1975.
- Larsen, M. F., M. C. Kelley, and K. S. Gage, Turbulence spectra in the upper troposphere and lower stratosphere between 2 hours and 40 days, *J. Atmos. Sci.*, 39, 1035-1041, 1982.
- Lesieur, M., and J. Herring, Diffusion of a passive scalar in two-dimensional turbulence, *J. Fluid Mech.*, 161, 77-95, 1985.
- Lilly, D. K., Stratified turbulence and the mesoscale variability of the atmosphere, *J. Atmos. Sci.*, 40, 749-761, 1983.
- Mahlman, J. D., Mechanistic interpretation of stratospheric tracer transport, *Adv. Geophys.*, 28, 301-323, 1985.
- Mahlman, J. D., G. Andrews, H. V. Dutsch, D. L. Hartmann, T. Matsuno, and R. J. Murgatroyd, Transport of trace constituents in the stratosphere, in *Dynamics of the Middle Atmosphere*, edited by J. R. Holton and T. Matsuno, pp. 387-416, Terra Reidel, Tokyo, 1984.
- Nastrom, G. D., and K. S. Gage, A climatology of atmospheric wavenumber spectra observed by commercial aircraft, *J. Atmos. Sci.*, 42, 950-960, 1985.
- Nastrom, G. D., K. S. Gage, and W. H. Jasperson, Kinetic energy spectrum of large- and mesoscale atmospheric processes, *Nature*, 310, 36-38, 1984.
- Nastrom, G. D., W. H. Jasperson, and K. S. Gage, Horizontal spectra of atmospheric tracers measured during the Global Atmospheric Sampling Program, *J. Geophys. Res.*, this issue.
- Olbers, D. J., Models of the oceanic internal wave field, *Rev. Geophys.*, 21, 1567-1606, 1983.
- Reed, R. J., and K. E. German, A contribution to the problem of large-scale mixing, *Mon. Weather Rev.*, 93, 313-321, 1965.
- Riley, J. J., R. W. Metcalfe, and M. A. Weissman, Direct numerical simulations of homogeneous turbulence in density-stratified fluids, in *Proceedings of AIP Conference on Nonlinear Properties of Internal Waves*, edited by Bruce J. West, pp. 79-112, American Institute of Physics, New York, 1981.
- VanZandt, T. E., A universal spectrum of buoyancy waves in the atmosphere, *Geophys. Res. Lett.*, 9, 575-578, 1982.

K. S. Gage, Aeronomy Laboratory, National Oceanic and Atmospheric Administration, Environmental Research Laboratories, 325 Broadway, Boulder, CO 80303.

G. D. Nastrom, Meteorology Research, Control Data Corporation, Box 1249-B, Minneapolis, MN 55420.

(Received November 28, 1985,  
revised July 28, 1986,  
accepted July 29, 1986.)

# An Investigation of Terrain Effects on the Mesoscale Spectrum of Atmospheric Motions

G. D. NASTROM

*Meteorology Research, Control Data, Minneapolis, MN 55440*

D. C. FRITTS

*Geophysical Institute, University of Alaska, Fairbanks, AK 99775*

K. S. GAGE

*Aeronomy Laboratory, NOAA/ERL, Boulder, CO 80303*

(Manuscript received 3 February 1987, in final form 13 May 1987)

## ABSTRACT

Wind and temperature data collected on commercial aircraft during the Global Atmospheric Sampling Program (GASP) are used to investigate the effects of underlying terrain on mesoscale variability, and the observational results are interpreted within the theories of gravity wave motions and quasi-two-dimensional turbulence. The data show the variances are up to six times larger over mountainous terrain than over oceans or plains, with the most striking differences at horizontal scales from 4 to 80 km. Results were subdivided between the stratosphere and troposphere, and between high- and low-background wind speed cases, and show basically the same response to topography in all cases. The linear theory of gravity waves is found to predict correctly the scaling of wave amplitude with background stability in the case of low-background wind speeds, while the two-dimensional turbulence theory correctly predicts the shape of the variance spectrum and the observed amplitude scales with  $\epsilon$  as required by the theory. In other cases the theoretical predictions are less satisfactory. Some possible causes of the discrepancies and likely methods to resolve them are discussed.

## 1. Introduction

It has become increasingly apparent in recent years that mesoscale variations of the atmosphere have an important impact on a wide variety of meteorological problems. Part of this awareness comes from the use of improved measurement systems that permit us more adequately to sample mesoscale motions, and part of it comes from theoretical advances that highlight the relevance of the mesoscale in meteorological processes (e.g., Atkinson, 1981; Lilly and Gal-Chen, 1983). Despite this progress, many observational and theoretical problems remain. For example, the relationship of mesoscale variability near the tropopause with the underlying topography is of interest for several reasons. One prominent reason is that mountain drag plays a significant role in the general circulation of the atmosphere (White, 1949). Palmer et al. (1986) have recently pointed out the possible need to model more closely mountain wave drag in order to achieve more realistic simulations of the tropospheric and lower stratospheric circulation. Dedicated field programs such as ALPEX can help us to understand mountain drag (Davies and Phillips, 1985), and observations from less closely focused data collection efforts also can provide information on the coupling of mesoscale variance and underlying topography. In a study of the climatology

of the variance power spectrum of winds and temperatures at airline cruise altitudes based on data from the Global Atmospheric Sampling Program (GASP), Nastrom and Gage (1985, hereafter called NG) found, among other things, that the variance associated with motions for scales less than about 400 km is somewhat greater over land than over oceans. However, no details were given in that paper of the changes in the shape or amplitude of the spectrum as a function of topography, or of any dependence of the relationship on synoptic weather conditions. One purpose of the present paper is to describe more thoroughly the changes in the mesoscale spectra as functions of topography and background conditions by analysis of data from GASP.

The interpretation of observed mesoscale spectra has been approached from two fundamentally different theoretical bases in recent years: waves and turbulence. Waves are dispersive, with well-defined relationships between frequency and wavenumber and among the amplitudes of atmospheric variables, while turbulence is a strongly nonlinear process with strong coupling between different scales. There is no question that well-defined lee waves are sometimes present over mountainous terrain, and it seems likely that small-amplitude buoyancy waves are present to some extent under most atmospheric conditions (Ecklund et al., 1986). It has

been suggested that a background spectrum of gravity waves gives rise to the observed spectrum of mesoscale variability (Dewan, 1979; VanZandt, 1982). Recent studies of the vertical wavenumber ( $m$ ) spectrum of horizontal velocities show that the observed spectra appear consistent with the notion of a saturated gravity wave spectrum (Dewan and Good, 1986; Smith et al., 1985, 1987). On the other hand, certain aspects of the observed spectra also appear consistent with the concept of a spectrum of quasi-two-dimensional stratified turbulence as put forward by Gage (1979) and Lilly (1983). Aspects of agreement are the ratio of spectral amplitudes of vertical velocity and temperature to horizontal velocity and the apparent success of the Taylor hypothesis for transforming frequency and wavenumber spectra (Gage and Nastrom, 1985, 1986). The point is that two very different interpretations can be offered for the observed mesoscale variations. The second purpose of this paper is to examine and compare the implications of both theories in light of the present observational results.

The data and method of data analysis are described in section 2. Results of the analysis procedure are discussed in section 3. Sections 4 and 5 examine the interpretation of these results in the context of gravity wave and two-dimensional turbulence theory, respectively. Our conclusions are presented in section 6.

## 2. Data and method

All aircraft data used here are from the observations taken during GASP and are a subset of the data analyzed in NG. The data collection phase of GASP was during 1975–1979. Instruments for the measurement of trace gases such as ozone were placed aboard B747 aircraft operating in routine commercial service. These and other variables such as aircraft location, flight level, pressure, wind, and temperature data were automatically recorded on a cassette tape during flight above 6.1 km, and the full cassettes were returned to NASA for quality control and archiving. Tropopause pressures were interpolated in time and space from gridded NMC analyses to each GASP data location during archiving. On about 93 of the flights, the system was preset to record data at 4 s intervals (1 km intervals) at all times above 6.1 km altitude. Normally, on other flights, data were recorded at 5 min intervals (75 km intervals at 250 m s<sup>-1</sup> airspeed). However, when moderate or greater turbulence was encountered (defined as whenever the vertical accelerometer reading fell outside the range 0.8–1.2 g) the system recorded data at 4 s intervals from the beginning of the turbulence until 1 min after the last “limit” exceedence. A few of these episodes lasted for up to several minutes. Other details, including a map of the geographic distribution of GASP data, are given in NG and references therein. All GASP data are available from the National Climatic Center, Asheville, North Carolina.

One goal of this study is to examine mesoscale variability over regions of the globe with varying surface topography. As a first step toward that goal, we have limited attention to the three zones shown in Fig. 1 in the latitude belt from 30° to 50°N. Zone 1 is entirely over the Pacific Ocean, zone 2 includes the rough terrain of the western United States, and zone 3 lies mostly over the central plains. The Appalachian Mountains extend into the southeast corner of zone 3, but since nearly all GASP flights to the Eastern United States terminated in New York or Boston the flight paths rarely crossed the mountains.

The first step of this analysis was to search for a geographic bias in the frequency of occurrence of turbulence “limit” episodes and of the mean vertical accelerometer range (the range over the previous 4 s intervals was recorded with each observation). Most cases when the vertical accelerometer reading fell outside the range 0.8 to 1.2 g are within a 100 km or so of airports; this is perhaps not surprising as it is in the approach region that pilots have the least freedom to choose their flight path to avoid turbulence. Away from airports, there is no obvious difference in the frequency of “limit” episodes among the three zones. This result is likely an indication of the skill of aircrews in avoiding turbulence rather than evidence that turbulence levels are the same over oceans, plains and mountains, especially since research flights (e.g., Lilly et al., 1974) found more turbulence over rough terrain. We conclude that our data from commercial airliners are not useful for studying the frequency of turbulence occurrence.

Variance power spectra of mesoscale variations of wind and temperature were computed by the same methods used in NG. Briefly, data from the high-frequency recording (1 km data interval) flights were divided into segments. A segment was retained for analysis only if it fell entirely within a zone, did not cross

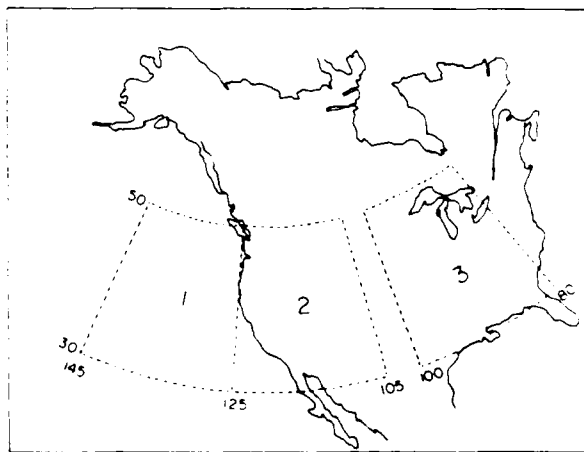


FIG. 1. Location of geographic zones.

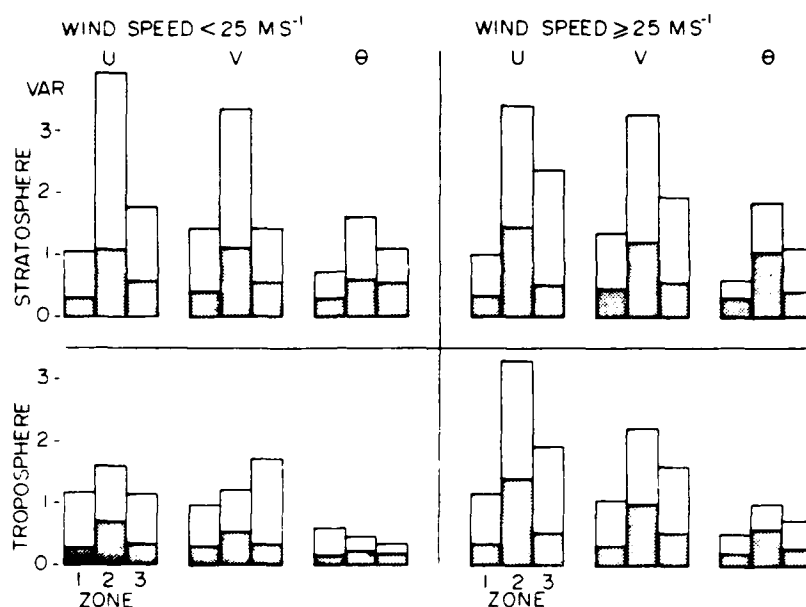


FIG. 2. Average variance ( $\text{m}^2 \text{s}^{-2}$  and  $\text{K}^2$ ) over segments 64 km long (shaded bar) and 256 km long (total bar), by geographic zone for each subdivision of the data.

the tropopause, the flight level did not vary more than 50 m, and data gaps were not longer than a prescribed limit. The analysis was made using segments 64 or 256 km long. On the 64 km (256 km) segments, the data were linearly interpolated to 1.25 km (2.58 km) intervals, with no interpolation allowed over gaps greater than 3.5 km (7.0 km). The mean and a linear trend were removed from the interpolated data, and the spectrum was estimated with a fast Fourier transform. The results were stratified by geographic zone, by troposphere and stratosphere, and according to whether the average wind speed along the segment was greater or less than  $25 \text{ m s}^{-1}$ .

### 3. Results

Before comparing the spectra among different data stratification groups, it is interesting to compare the total variance under the spectra to gain a first impression of topographic effects. Figure 2 shows the variance values in a bar graph format for zonal ( $u$ ) and meridional ( $v$ ) wind and potential temperature ( $\theta$ ) for each geographic zone and separated between troposphere and stratosphere and between low- and high-background wind speeds. The shaded portion of each bar represents the average variance on the 64 km segments, and the entire bar represents the average variance on 256 km segments. The number of values averaged in each case is listed in Table 1 along with the corresponding mean wind speed, and the average variances are listed in Table 2. Comparing zones within each data group, we note that for the 64 km segments (shaded), in every case the variance in zone 2 is largest,

and zone 1 smallest. For zonal wind, the ratio of zone 2 to zone 1 variance ranges from 4.3 in the stratosphere, high wind speed cases, to 2.5 in the troposphere, low wind speed cases. The pattern of ratios for  $v$  and  $\theta$  is similar. Further, the same pattern among zones is found for the variances on 256 km segments except in the troposphere, low wind cases, for  $v$  and  $\theta$ .

Comparison of variances in the same zones shows that for  $u$  and  $v$  from the 64 km segments for high wind speeds, there is little difference between the troposphere and stratosphere. This can be seen in Fig. 1, and also in Table 2. In fact, for  $u$  and  $v$  in zones 2 and 3, the only noticeable difference is between the tro-

TABLE 1. Number of spectra averaged by zone and data group.

Group	Tropospheric zone			Stratospheric zone		
	1	2	3	1	2	3
<i>a. Cases with mean wind speed less than <math>25 \text{ m s}^{-1}</math></i>						
64-km segments	136	130	71	49	78	120
256-km segments	30	25	18	12	18	25
1200-km segments	75	82	46	58	76	40
Mean wind speed ( $\text{m s}^{-1}$ )	14	18	19	20	18	18
<i>b. Cases with mean wind speed greater than <math>25 \text{ m s}^{-1}</math></i>						
64-km segments	132	162	127	42	149	166
256-km segments	29	35	31	9	35	37
1200-km segments	68	98	48	32	85	85
Mean wind speed ( $\text{m s}^{-1}$ )	37	40	44	36	36	37

TABLE 2. Average variance under the spectrum ( $m^2 s^{-2}$  and  $K^2$ ) by geographic zone.

Level	Component	Zone 1 (ocean)		Zone 2 (mountains)		Zone 3 (plains)	
		LW*	HW*	LW	HW	LW	HW
64-km segments							
Stratosphere	<i>u</i>	0.28	0.34	1.09	1.45	0.58	0.52
Troposphere	<i>u</i>	0.27	0.34	0.69	1.40	0.34	0.53
Stratosphere	<i>v</i>	0.40	0.46	1.11	1.20	0.55	0.56
Troposphere	<i>v</i>	0.30	0.32	0.54	1.00	0.33	0.52
Stratosphere	<i>θ</i>	0.29	0.31	0.60	1.05	0.55	0.41
Troposphere	<i>θ</i>	0.14	0.19	0.23	0.59	0.17	0.28
256-km segments							
Stratosphere	<i>u</i>	1.03	1.00	3.91	3.38	1.76	2.37
Troposphere	<i>u</i>	1.17	1.15	1.61	3.30	1.15	1.92
Stratosphere	<i>v</i>	1.42	1.37	3.34	3.25	1.41	1.93
Troposphere	<i>v</i>	0.97	1.07	1.22	2.22	1.71	1.60
Stratosphere	<i>θ</i>	0.73	0.60	1.60	1.86	1.10	1.11
Troposphere	<i>θ</i>	0.60	0.51	0.46	0.99	0.34	0.72

\* LW: Low wind speed cases

† HW: High wind speed cases

pospheric low wind speed cases, and the other three data groups. In zone 1, the differences among all four data groups are small. For temperature, the most striking differences among data groups are between the troposphere and stratosphere, with the stratospheric values a factor of 2.0 larger on the average. In all zones, the smallest temperature results are found in the tropospheric low wind speed cases. In zone 2, the result for temperature in the stratospheric high wind speed cases is much larger than that for other data groups. The comparisons for 256 km segment results show similar, but not identical, patterns to the 64 km results, but the small number of 256 km segments give reduced statistical significance.

There are sufficient segments of the 64 km results to check the statistical significance of the differences among the means, and to make other statistical analyses. For example, the frequency distributions of variances of zonal wind speed along segments from each geographic zone for the tropospheric high wind cases are compared in Fig. 3. The upper panel of Fig. 3 shows the curves in standard histogram format, while the lower panel shows them in cumulative probability coordinates. The curves appear approximately lognormal, consistent with the findings of NG. The Student's  $t$ -test indicates that the mean values for zone 1 and zone 3 are different from the mean for zone 2 at the 99 percent significance level, but that the means for zones 1 and 3 are not significantly different in this example. Results for other data groups are similar, and we conclude that there is significantly more variance at mesoscales over the mountains than over oceans or plains.

In order to assess the horizontal wavelength ( $\lambda$ ) dependence of the differences among variances, it is necessary to examine the spectra. Figures 4 and 5 show the spectra for  $u$  for low and high wind conditions, respectively. As these illustrate the main points, the

spectra of  $v$  and  $\theta$  are not shown. The coordinates along the ordinate apply to the upper three curves which are for the stratosphere, and the three tropospheric curves are shifted down one decade. Dashed lines, arbitrarily chosen with slope  $-5/3$  and offset by one decade, have been added to aid comparison. At wavelengths less than 64 km, the curves are based on analyses of the 64 km segment data. At longer wavelengths, they are based on the 256 km segments, with some fairing near 64 km. The zone number is entered several times along each curve. The plotted values are the averages over  $d$  samples, with  $d$  given in Table 1; no other smoothing has been applied. Error bars are entered at two wavelengths to illustrate the uncertainty of the means and extend  $2\sigma(d)^{-1/2}$  above and below the mean, where  $\sigma$  is the standard deviation.

Figure 4, for low wind conditions, shows that in the troposphere there are small differences among zones at  $\lambda < 4$  km and  $\lambda > 80$  km. At intermediate  $\lambda$ , the curve for zone 2, over the mountains, reflects significantly increased energy. Zone 1, over the ocean, has the lowest energy at intermediate  $\lambda$ . In the stratosphere, zone 1 has the lowest energy at all  $\lambda$  and zone 2 the highest energy at all  $\lambda > 4$  km. For high wind conditions (Fig. 5), the energy in zone 2 appears high, and in zone 1 is low, at all  $\lambda > 4$  km in both the troposphere and stratosphere. We have checked the continuation of these patterns to longer wavelengths using the 1200-km segment analyses based on normal recording-rate data used in NG. The number of segments is given in Table 1. These results (not shown) indicate the patterns seen at long  $\lambda$  in Figs. 4 and 5 persist to  $\lambda \sim 500$  km. At  $\lambda > 500$  km, the flow enters the enstrophy cascading regime associated with geostrophic turbulence following a  $k^{-3}$  spectral shape.

The variance and spectral analysis results presented here show there are significant differences in mesoscale

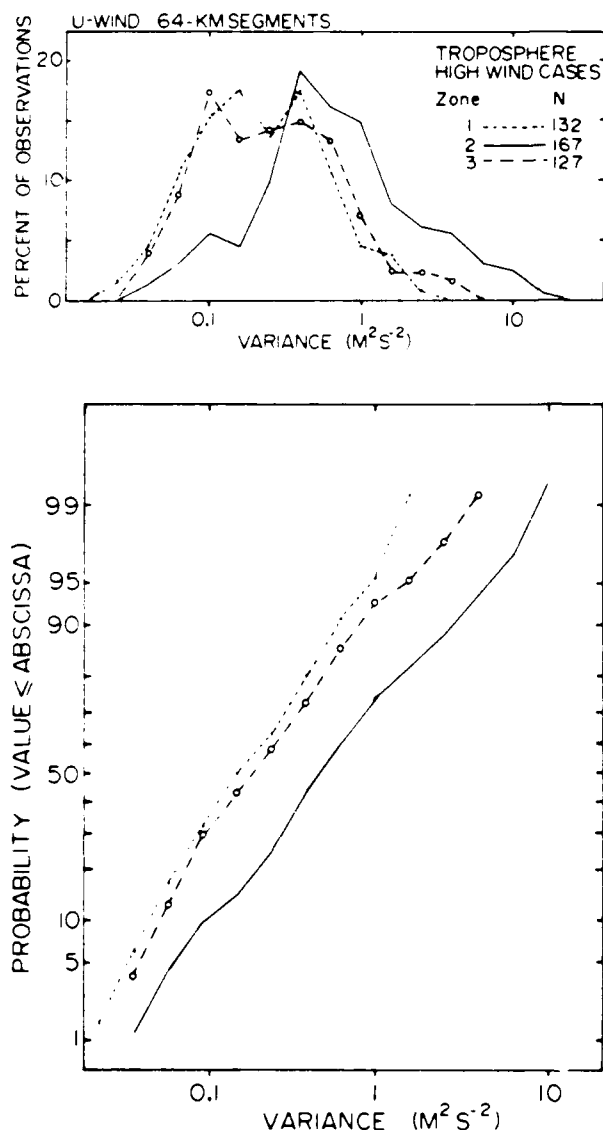


FIG. 3. Frequency distribution of variance of zonal wind speed along 64 km segments in three geographic zones. (a) Histogram format. (b) cumulative probability format.

variability related to surface topography. The differences range up to a factor of 6 in power, and are largest in the scale range  $10 < \lambda < 80$  km. A similar factor was noted by Lilly et al. (1974) between variances over ocean and mountains at scales less than 610 m. They interpreted their observations within the framework of three-dimensional turbulence theory. The present results are examined using the theories of internal gravity waves and quasi-two-dimensional stratified turbulence in the following sections.

#### 4. Internal gravity wave interpretation

We begin our discussion in this section by postulating that the motion and temperature spectra presented

previously are due to internal gravity waves and that these waves comprise a spectrum in which the amplitudes of the smallest vertical scales are limited by saturation processes (VanZandt, 1982; Dewan and Good, 1986; Smith et al., 1987). The effects of—and processes contributing to—gravity wave saturation have been reviewed by Fritts (1984) and Fritts and Rastogi (1985) and are now believed to contribute to the large-scale circulation and thermal structure throughout the atmosphere.

We assume a saturated vertical wavenumber spectrum of the form (Smith et al., 1987)

$$E(m) \sim \frac{1}{1 + (m/m_*)^3} \quad (1)$$

such that the maximum energy weighted by wavenumber ( $mE(m)$ ) occurs at a wavenumber  $m = m_*$ ,  $2\pi/\lambda$  where  $m_*$  is the characteristic vertical wavenumber. Typical values of  $2\pi/m_*$  inferred in the upper troposphere and lower stratosphere are  $\sim 2$ – $2.5$  km (Fritts and Chou, 1987; Fritts et al., 1987). We then assume

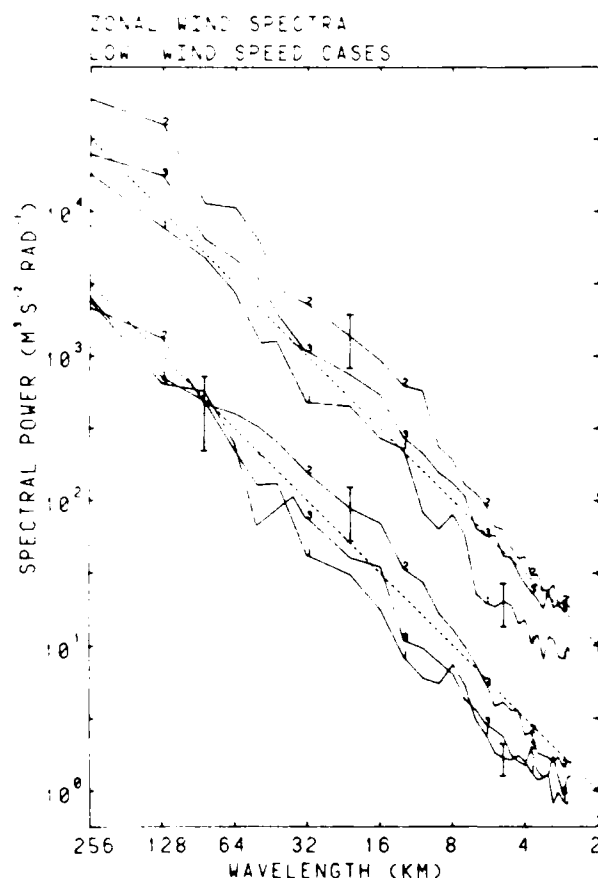


FIG. 4. Average spectra of zonal wind speed for cases of low-background winds. Geographic zone number is entered along each curve. Values on ordinate apply to stratospheric curves; tropospheric curves are shifted down one decade. (See text.)

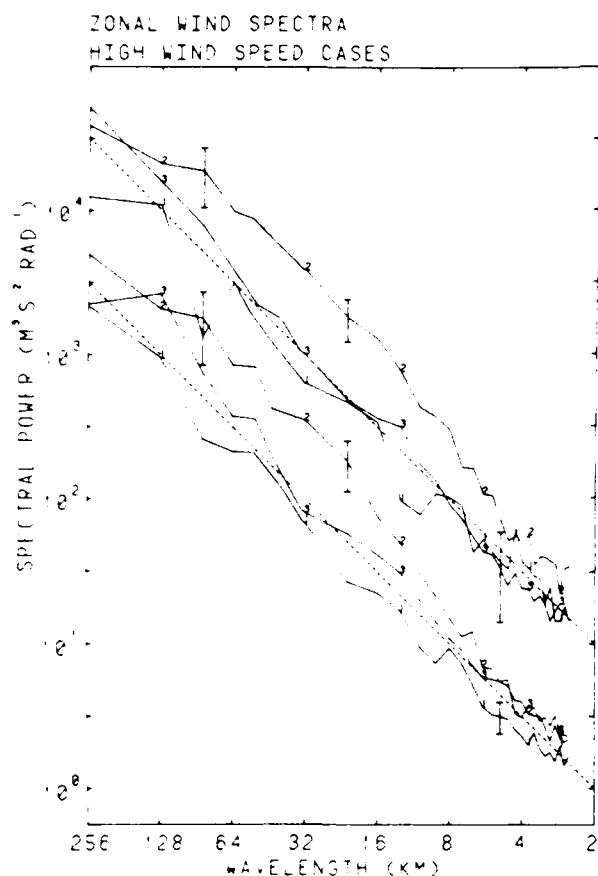


FIG. 5. As in Fig. 4, except for cases of high-background winds.

that this spectrum responds to increases in  $N$  following WKB scaling and relaxation to the new saturated amplitudes as anticipated by VanZandt and Fritts (1987). This causes the saturated spectrum to evolve as

$$m_* \sim N^{2/3}. \quad (2)$$

Thus a characteristic velocity, assuming hydrostatic two-dimensional wave motions, is

$$u' \sim (c - \bar{u}) = \frac{N}{m} = \frac{2^{1/3}N}{m_*} \sim N^{1/3}. \quad (3)$$

Consistent with (1), we have assumed here that the dominant vertical scale is near saturation amplitude. Also, from the linear thermodynamic equation,

$$\frac{T'}{T} \sim Nu', \quad (4)$$

implying that temperature fluctuations should be more sensitive than wind fluctuations to changes in stratification. Note that this saturation theory leads to a different dependence on  $N$  than the usual WKB scaling of the wave spectrum (i.e.,  $u' \sim N^{1/2}$ ).

Comparing these scalings with our observations, we

find the best agreement to occur for the average ratios of stratospheric to tropospheric wind variances under low wind conditions. These are 1.62 and 1.64 for the 64 km and 256 km segments, respectively, and compare very well with the value anticipated from (3) for a change in  $N$  of 2 ( $2^{2/3} = 1.59$ ). The ratios are somewhat smaller for high wind conditions (near 1.2), perhaps reflecting a tendency for higher wind speeds to allow for greater reflection or dissipation of wave energy near the tropopause, depending on the direction of wave propagation.

Like the velocity variances, the ratios of stratospheric to tropospheric temperature variances are most consistent with the foregoing scalings for low wind speeds. The 64 and 256 km segment averages are 2.67 and 2.45, with the largest individual values (from 2.61 to 3.48) occurring in zones 2 and 3 and the smallest values (1.22 and 2.07) in zone 1. These are approximately half of that expected ( $2^{2/3} = 6.36$ ), suggesting that another process, such as convection, rather than wave activity might have contributed appreciably to temperature variance in the troposphere.

We now consider the implications of the differences in wind and temperature variance in the three zones for the gravity wave spectrum and for wave propagation and effects in the lower and middle atmosphere. As noted in section 3, the variances, particularly for the 64 km data segments, exhibit statistically significant differences between zones. Variances are much larger, on average, in zone 2 than in zones 1 and 3, and those in zone 3 are somewhat larger than in zone 1. The zonal velocity spectra presented in Figs. 4 and 5 reveal a much more energetic motion field at horizontal scales from  $\sim 4$  to 80 km in zone 2, suggesting that these scales may be preferentially excited over rough terrain. The larger characteristic velocities imply a smaller value of  $m_*$  (and larger characteristic vertical wavelength) from (3) at a given horizontal scale, corresponding to wave motions with larger intrinsic frequencies. Thus, on the basis of the velocity variance data, we expect that the wave spectrum in zone 2, relative to that in zones 1 and 3, is composed of wave motions with larger vertical velocities, steeper propagation angles, and a greater potential for large vertical fluxes of energy and horizontal momentum,  $\overline{u'w'}$  and  $\overline{v'w'}$ .

To quantify these observations, we assume that the velocity variance is the best indication of the relative level of wave activity and note that a representative value in zone 2 is twice that in zone 1 or 3. Then a characteristic velocity or intrinsic frequency is also larger by  $\sim 1.4$  in zone 2. This causes the energy and momentum fluxes,

$$c_g E \sim \frac{\omega}{N} (c - \bar{u})^3 \quad (5)$$

and

$$\overline{u'w'} \sim \frac{\omega}{N} (c - \bar{u})^2 \quad (6)$$

to increase in zone 2 by  $\sim 4$  and 2.8, respectively, relative to those in zones 1 and 3, assuming that the wave spectrum in each zone has the same degree of anisotropy. If the majority of the enhanced wave activity in zone 2 can be attributed to topography; however, the potential momentum flux and applied drag in this region may be even larger due to a greater anisotropy of the wave field and because the greater variances in zone 2, if applicable to a smaller mountainous area, imply even greater enhancements of the energy and momentum fluxes in these regions.

These results are significant because they suggest that rough terrain may account for a disproportionately large fraction of the total momentum flux that affects the atmosphere at greater heights due to the larger wave amplitudes and intrinsic frequencies that arise in these regions. The results also support the suggestion by Palmer et al. (1986) that major topography might be responsible for the drag that is needed to achieve realistic mean winds in numerical simulations of the lower atmosphere. A related point is that due to the higher intrinsic frequencies and essentially vertical group velocities that appear to be associated with topographically generated waves, the drag and induced diffusion due to these wave motions should occur in the middle atmosphere primarily in those regions that overlie major topography.

The interpretation of the GASP data offered in this section was based on the assumption that the observed motion field is due primarily to internal gravity waves. This interpretation will be compared and contrasted with that offered in terms of quasi-two-dimensional turbulence in section 6.

### 5. Wave breaking, small-scale turbulence and mesoscale stratified turbulence

In section 4 it was assumed that the GASP spectra presented in section 3 were due solely to a spectrum of internal waves. In this section we consider the more general condition when the spectra are comprised of a combination of waves and turbulence. Specifically, we will consider what happens when enhanced wave activity over mountainous terrain leads to small-scale turbulence generation. Under these circumstances it is anticipated that some of the small-scale turbulent kinetic energy participates in an inverse cascade to larger scales as suggested by Gage (1979) and Lilly (1983) for quasi-two-dimensional stratified turbulence. According to this scenario a field of motion comprised of waves and turbulence can evolve into a field of quasi-horizontal eddy motions as wave energy radiates out of the fluid volume. The residual field of quasi-horizontal eddies is the vorticity-bearing mode of the motion field.

The possibility of a vorticity-bearing mode of quasi-horizontal motions in the atmospheric mesoscale follows directly from the RMW scaling of the equations of motion (Riley et al., 1981; Lilly, 1983). Briefly, at

low Froude numbers pertinent to the stably stratified atmosphere, the equations of motion decouple into a set of equations governing internal wave motions and a set of equations governing stratified turbulence. Stratified turbulence as described by Lilly (1983) is the vorticity-bearing mode of motion. The possibility that the vortical mode of motion exists in the ocean has been raised by Muller (1984) and Muller et al. (1986) as a way to account for departures from the Garrett-Munk internal wave spectrum observed during IWIN (Muller et al., 1978).

The basic idea of stratified turbulence has been discussed by Gage (1979) and Lilly (1983). Briefly, an inverse cascade is hypothesized to redistribute turbulent kinetic energy throughout the atmospheric mesoscale from a small-scale source. Lilly (1983) has described the source as upscale leakage from three-dimensional turbulence. He found that only a few percent of the energy present in three-dimensional turbulence is needed to account for the observed level of the mesoscale atmospheric horizontal velocity spectrum.

The range of horizontal scales pertinent to a transition between microscale three-dimensional turbulence and mesoscale stratified turbulence can be defined as follows. The smallest scale for this transition zone can be identified with the buoyancy length scale

$$L_B = 2\pi \frac{\epsilon^{1/2}}{N^{3/2}} \quad (7)$$

where  $\epsilon$  is the dissipation rate of turbulent kinetic energy and  $N$  the Brunt-Väisälä frequency. In the atmosphere, the buoyancy-length scale can vary from 10 m, or less, in very stable regions of the stratosphere to 300 m, or more, in turbulent regions of the troposphere.

For scales  $L < L_B$  the dynamics is fairly well described by the familiar Kolmogoroff turbulence theory. Consistent with this theory, the kinetic energy spectrum is described by

$$E(K) = A_1 \epsilon^{2/3} k^{-5/3}, \quad k > k_B \equiv \frac{2\pi}{L_B} \quad (8)$$

where  $k$  is horizontal wavenumber and  $A_1$  is a universal constant.

The energy source for the microscale turbulence in the stable atmosphere is thought to be breaking internal waves, although other sources are possible. Presumably, the energy content of stratified turbulence should be largest in regions of enhanced wave breaking.

The stratified turbulence has a spectrum of the form

$$E(K) = A_2 \left( \frac{dE}{dt} \right)^{2/3} k^{-5/3}, \quad k < k_u \quad (9)$$

where  $k_u$  is the largest wavenumber in the inertial range of stratified turbulence,  $dE/dt$  the rate of energy insertion into the inverse cascade and  $A_2$  the universal constant for stratified turbulence,  $A_2 \sim 9.4 A_1$  (Lilly, 1983). The scale of energy insertion  $k_i \equiv 2\pi/L_i$  is presumably

related to the vertical scale of wave breaking and is necessarily in the range

$$k_B > k_i > k_u. \quad (10)$$

The spectral forms given in Eqs. (8) and (9) both represent idealized equilibrium model spectra for inertial ranges in which the energy transfer up or down the spectrum is independent of wavenumber. At intermediate scales, i.e., those that occupy the range of wavenumber space adjacent to  $k_i$ , the energy cascade rate must be dependent on  $k$ .

Weinstock (1980) considered a spectral model in which the energy cascade rate is wavenumber dependent. He found a tendency for a spectral hump to form at length scales smaller than the source scale and for a gap to form at length scales associated with the source scale. At length scales larger than the scale of the source, there is thus a wavenumber domain of steepened (more negative) spectral slope. Similar issues have been discussed by Lilly (1983) in the context of an intermittent source of turbulent kinetic energy associated with convection. On the other hand, while Lilly's model shares some of the features of the Weinstock model, such as the inverse cascade, there is no clear connection between the Weinstock and Lilly models.

The physical mechanisms associated with wave breaking in the atmosphere have been discussed at length in the literature. (See, for example, Bretherton, 1969; Fritts and Rastogi, 1985; Dewan and Good, 1986.) Usually, wave breaking is treated as a manifestation of a local instability, such as convective overturning or Kelvin-Helmholtz instability. The turbulence that results from wave-breaking episodes is often referred to as wave-induced turbulence since it tends to occur when a local instability is produced in certain phases of an atmospheric wave. The consequence of wave breaking and turbulence generation on atmospheric spectra of stratified turbulence is presumably to create a transition region spanning a decade or so in wavenumber space at scales larger than the buoyancy-length scale. Presumably, the most intense wave-breaking episodes will be associated with instabilities on the largest vertical wave scales and with the largest turbulence production. Consequently, under conditions of enhanced wave-breaking activity we may anticipate, at least qualitatively, steepening of spectral slopes at larger scales, and an increased energy level of mesoscale spectra since  $dE/dt$  should be proportional to  $\epsilon$ .

An examination of the GASP spectra presented in Fig. 4 and Fig. 5 reveals the presence of enhanced spectral energy levels and steepened spectral slopes as previously discussed. To illustrate these features, Fig. 6 contains the GASP spectra over mountainous terrain under high wind conditions. In terms of the previous discussion, the vertical arrows indicate the spatial scale  $L_u = (2\pi/k_u)$  associated with the transition from a  $k^{-5/3}$  spectral slope at low wavenumber to a steepened

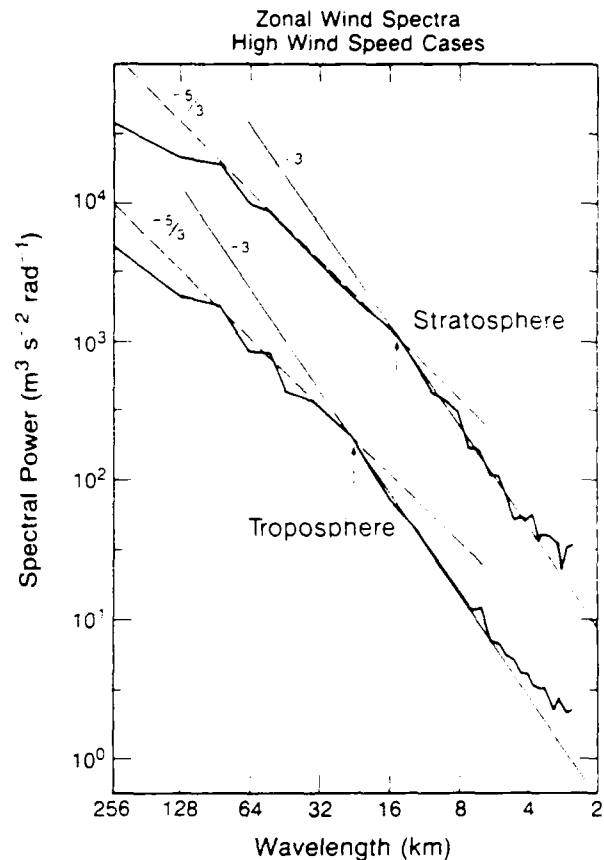


FIG. 6 As in Fig. 5, except only for geographic zone 2 and with spectral breaks noted.

spectral slope at high wavenumber. The scale of the source region lies to the right of the vertical arrows in Fig. 6 probably in the 1–3 km range and is not adequately resolved in the GASP spectra. In Fig. 6 the transition scale occurs at about 15 km in the stratosphere and about 23 km in the troposphere. In the  $k^{-5/3}$  region at larger scales the energy levels are about the same in the troposphere and stratosphere. These energy levels are more than half an order of magnitude larger than the more typical spectral amplitude evident in the GASP spectra (Nastrom et al., 1984; Nastrom and Gage, 1985) as shown in Fig. 7.

Under the assumptions made earlier in this section, regional differences in eddy dissipation rates appear to reflect regional differences in wave-breaking intensity. If the energy insertion rate  $dE/dt$  also reflects these regional differences, we would anticipate that the spectral amplitude in the  $k^{-5/3}$  range of the mesoscale spectrum would scale as  $\epsilon^{2/3}$ . At least in the stratosphere, eddy dissipation rates pertinent to the GASP data are probably about  $1 \text{ cm}^2 \text{ s}^{-3}$  over the mountainous region and  $0.1 \text{ cm}^2 \text{ s}^{-3}$  over the ocean (cf. Lilly et al., 1974). We anticipate, accordingly, about a factor of 5 increase of mesoscale spectral amplitude over the mountainous

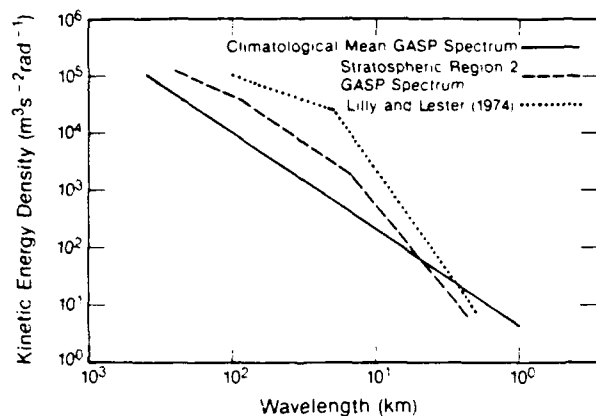


FIG. 7. Comparison of GASP zonal wind spectrum over mountainous terrain with the climatological mean GASP spectrum (Nastrom and Gage, 1985) and the spectrum of Lilly and Lester (1974).

terrain compared to mesoscale spectral amplitude over the oceans. The observed ratio, from Figs. 4 and 5, is about 3 or 4 on the average, and ranges up to 6. As might have been anticipated, these effects seem to be most pronounced with strong winds. Comparable climatological studies of turbulence intensity in the troposphere have yet to be made.

The higher amplitudes of GASP spectra over the plains compared to the ocean may be the result of eastward advection of decaying stratified turbulence or of the injection of turbulent energy by enhanced convective activity. Since stratified turbulence should be most persistent in the stratosphere, relatively high spectral levels may be anticipated in the stratosphere over the plains even under light wind conditions. Indeed, under such conditions stratospheric spectra are relatively energetic compared to the tropospheric spectra observed over the plains.

In comparing the results presented here with earlier work on mountain waves, it is important to recognize that the GASP flights avoid areas of intense wave activity and turbulence. Thus, spectra observed under very active conditions should be more energetic than the GASP spectra. The spectra reported by Lilly and Lester (1974) for example, under active conditions appear to be about an order of magnitude more intense than those reported here (Fig. 7). Lilly and Lester (1974) estimate the eddy dissipation rate to be about  $30 \text{ cm}^2 \text{ s}^{-3}$  for these distributed conditions. An order of magnitude increase of mesoscale spectral amplitude above the GASP spectral amplitude is consistent with the foregoing arguments.

In this section we have considered the consequences of an evolving field of motion comprised of waves and turbulence. We have found that many of the features of the GASP spectra reported in section 3 are consistent with the idea that these spectra have evolved from more active conditions in which the wave breaking and tur-

bulence generation leads to an inverse cascade and a persistent field of stratified turbulence. We have hypothesized that the dynamics of the disturbed flow over mountainous terrain may serve as a significant regional source for the GASP spectra reported in Nastrom and Gage (1985).

## 6. Conclusions

Wind and temperature measurements taken at airline cruise altitudes during GASP have been analyzed over three geographic regions: oceans, mountains, and plains. The results show that underlying terrain has a significant effect on the atmospheric variability at scales from about 4 to 80 km, with variances over mountains up to six times larger than those over oceans. The enhanced energy over mountains is found in both wind and temperature results and is persistent, being found in the troposphere and stratosphere during both low and high background wind speed conditions. At longer wavelengths, 80 to 500 km, the variances are also larger over mountains than in other regions in the stratosphere and, in most cases, in the troposphere.

These results complement past observational studies such as Lilly et al. (1974) and Pinus (1979). The GASP data are unique in that they are sufficiently copious to support comparisons of mean values for various background conditions, such as high and low-background wind speed and cover larger spatial scales than other datasets. Also, the large number of spectra available has permitted us to establish the lognormal distribution of variances regardless of underlying terrain. Finally, the capability to subdivide results has allowed some comparisons with predictions derived from the gravity wave and stratified turbulence theories of mesoscale variability.

The linear theory of gravity wave motions was used to predict the scaling of wave amplitude with background stability both for wind and temperature. Excellent agreement of the predicted scaling was found for the wind energy in the case of low-background wind speed. The comparison of the predicted scalings was less satisfactory for wind energy in the case of high-background wind speed, and for temperature for all background wind speeds. It was noted that other processes such as wave reflections, wave dissipation, convection, etc., which were not accounted for here may be important in reconciling the wave theory with the observations.

The theory of stratified turbulence was used to predict an excess of spectral energy over mountainous regions in the mesoscale  $k^{-5/3}$  region and a steepened spectral slope at higher wavenumbers. The observed spectral amplitudes in the mesoscale  $k^{-5/3}$  region vary among geographic regions approximately in accord with an  $\epsilon^{2/3}$  scaling. Also, the notion of advection of turbulence appears to be supported by the enhanced spectral amplitudes found downwind of the mountains

although no quantitative predictions were tested, and other source mechanisms, such as convection, are possible in such areas.

In summary, the theories of internal gravity waves and stratified turbulence each account for some, but not all, aspects of the observations as analyzed in this brief study. While there is no question that wave and turbulence processes both contribute to the observed mesoscale spectra, we have made only a small effort to synthesize the two theories. It appears that a more detailed investigation would have merit.

Resolution of the question of interpretation is of great practical significance as well as of theoretical interest. If the linear gravity wave theory can be correctly applied to the GASP data, results such as those given here could be extended to infer important quantities such as momentum and energy transfer. In addition to the linear theory, progress is being made in developing nonlinear wave theory (e.g., Fritts, 1984; Weinstock, 1985; Muller et al., 1986). The potential importance of the vortical mode and stratified turbulence has only recently been appreciated. Here, too, progress is being made (e.g., Metais and Herring, 1985; Herring and Metais, 1987). A major challenge for the future is to understand how each of these processes contributes to the observed mesoscale spectra and how they interact with one another.

*Acknowledgments.* Support for D.C.F. for this study was provided by the Division of Atmospheric Sciences of the National Science Foundation under Grant ATM8404017. Support for G.D.N. was provided by the Air Force Office of Scientific Research under Contract F49620-86-C-0027. Helpful comments by Dr. D. K. Lilly on an earlier draft are gladly acknowledged.

#### REFERENCES

- Atkinson, B. W., 1981: *Mesoscale Atmospheric Circulations*. Academic Press, chap. 1.
- Bretherton, F. P., 1969: Waves and turbulence in stably stratified fluids. *Radio Sci.*, **4**, 1279-1287.
- Davies, H. C., and P. D. Phillips, 1985: Mountain drag along the Gotthard section during ALPEX. *J. Atmos. Sci.*, **42**, 2093-2109.
- Dewan, E. M., 1979: Stratospheric wave spectra resembling turbulence. *Science*, **204**, 832-835.
- , and R. E. Good, 1986: Saturation and the universal spectrum for vertical profiles of horizontal scalar winds in the atmosphere. *J. Geophys. Res.*, **91**, 2742-2748.
- Ecklund, W. L., K. S. Gage, G. D. Nastrom and B. B. Balsley, 1986: A preliminary climatology of the spectrum of vertical velocity observed by clear-air doppler radar. *J. Climate Appl. Meteor.*, **25**, 885-892.
- Fritts, D. C., 1984: Gravity wave saturation in the middle atmosphere: A review of theory and observations. *Rev. Geophys. Space Phys.*, **22**, 275-308.
- , and P. K. Rastogi, 1985: Convective and dynamical instabilities due to gravity wave motions in the lower and middle atmosphere: theory and observations. *Radio Sci.*, **20**, 1247-1278.
- , and H.-G. Chou, 1987: An investigation of the vertical wavenumber and frequency spectra of gravity wave motions in the lower stratosphere. *J. Atmos. Sci.*, (in press).
- , T. Tsuda, T. Sato, S. Fukao and S. Kato, 1987: Observational evidence of a saturated gravity wave spectrum in the troposphere and lower stratosphere. *J. Atmos. Sci.*, (to be published).
- Gage, K. S., 1979: Evidence for  $k^{-5/3}$  law inertial range in mesoscale two-dimensional turbulence. *J. Atmos. Sci.*, **36**, 1950-1954.
- , and G. D. Nastrom, 1985: On the spectrum of atmospheric velocity fluctuations seen by MST/ST radar and their interpretation. *Radio Sci.*, **20**, 1339-1347.
- , and —, 1986: Theoretical interpretation of atmospheric wavenumber spectra of wind and temperature observed by commercial aircraft during GASP. *J. Atmos. Sci.*, **43**, 729-740.
- Herring, J. R., and O. Metais, 1987: Numerical Experiments in Forced Stably Stratified Turbulence, submitted to *J. Fluid Mech.*
- Lilly, D. K., 1983: Stratified turbulence and the mesoscale variability of the atmosphere. *J. Atmos. Sci.*, **40**, 749-761.
- , and T. Gal-Chen, 1983: *Mesoscale Meteorology—Theories, Observations, and Models*. D. Reidel, 781 pp.
- , and P. F. Lester, 1974: Waves and turbulence in the stratosphere. *J. Atmos. Sci.*, **31**, 800-811.
- , D. E. Waco and S. I. Adelfang, 1974: Stratospheric mixing estimated from high-altitude turbulence measurements. *J. Appl. Meteor.*, **13**, 488-493.
- Metais, O., and J. R. Herring, 1985: Numerical and theoretical results relating to mesoscale turbulence. *Preprints 7th Symposium on Turbulence and Diffusion*. Boulder: Amer. Meteor. Soc., 188-191.
- Muller, P., 1984: Small-scale vertical motions, in *Internal Gravity Waves and Small-Scale Turbulence*. Proc. Aha Huihiko Hawaiian Winter Workshop. P. Muller and R. Pujalet, Eds., Institute of Geophysics, Honolulu, HI., 249-261.
- , G. Holloway, F. Heney and N. Pomphrey, 1986: Nonlinear Interactions among internal gravity waves. *Rev. Geophys.*, **24**, 493.
- , D. J. Olbers and J. Willebrand, 1978: The IWEX spectrum. *J. Geophys. Res.*, **83**, 479-500.
- Nastrom, G. D., and K. S. Gage, 1985: A climatology of atmospheric wavenumber spectra of wind and temperature observed by commercial aircraft. *J. Atmos. Sci.*, **42**, 950-960.
- , K. S. Gage and W. H. Jasperson, 1984: Kinetic energy spectrum of large and mesoscale atmospheric processes. *Nature*, **310**, 36-38.
- Palmer, T. N., G. N. Shutts and R. Swinbank, 1986: Alleviation of a systematic westerly bias in general circulation and numerical weather prediction models through an orographic gravity wave drag parameterization. *Quart. J. Roy. Meteor. Soc.*, **112**, 1001-1040.
- Pinus, N. Z., 1979: Spectra of longitudinal and transverse fluctuations in wind speed at altitudes of 10-20 km. *Izv. Atmos. Ocean. Phys.*, **15**, 93-97.
- Riley, J. J., R. W. Metcalfe and M. A. Weissman, 1981: Direct numerical simulations of homogeneous turbulence in density-stratified fluids in *Nonlinear Properties of Internal Waves*, **76**, B. J. West, Ed. American Institute of Physics, 79-112.
- Smith, S. A., D. C. Fritts and T. E. VanZandt, 1985: Comparison of mesospheric wind spectra with a gravity wave model. *Radio Sci.*, **20**, 1331-1338.
- , —, and —, 1987: Evidence of a saturated spectrum of atmospheric gravity waves. *J. Atmos. Sci.*, **44**, 1404-1410.
- VanZandt, T. E., 1982: A universal spectrum of buoyancy waves in the atmosphere. *Geophys. Res. Lett.*, **9**, 575-578.
- , and D. Fritts, 1987: A theory of enhanced saturation of the gravity wave spectrum due to increases in atmospheric stability. *Pure Appl. Geophys.*, (submitted).
- Vinnichenko, N. K., 1966: Clear air turbulence at heights of 6-12 km. *Izv. Atmos. Ocean. Phys.*, **2**, 701-709.
- Weinstock, J., 1980: Theoretical gravity wave spectrum in the atmosphere: strong and weak wave interactions. *Radio Sci.*, **20**, 1295-1300.
- , 1985: A theory of gaps in the turbulence spectra of stably stratified shear flow. *J. Atmos. Sci.*, **37**, 1542-1549.
- White, R. M., 1949: The role of the mountains in the angular momentum balance of the atmosphere. *J. Meteor.*, **6**, 353-355.

## MEASUREMENT OF LARGE-SCALE VERTICAL VELOCITY USING CLEAR-AIR DOPPLER RADAR

G.D. Nastrom

Department of Earth Sciences, St. Cloud State University  
St. Cloud, MN 56301

J.L. Green, T.E. VanZandt, K. S. Gage, W.L. Clark  
NOAA Aeronomy Laboratory, R/E/AL3  
325 Broadway, Boulder, CO 80303

### 1. Introduction

Attempts to observe the vertical motion field at synoptic and larger scales with MST radars have been frustrated by the presence of geophysical "noise" in the data, consisting of contributions from small scales, which usually overwhelms any large-scale signal in the data. Two recent such studies are Nastrom, et al. (1985), and Larsen, et al. (1988), where more detailed discussion of the background and references to other work may be found. Briefly, all past studies were performed in regions where the noise produced by orographic effects could not usually be ignored, and the possibility existed that a station well-removed from such effects might be able to observe the large scale components in the wind field under more general conditions. Ongoing studies at the Flatland radar in central Illinois, USA, are testing this hypothesis, and an emerging result is that the vertical motion field is still dominated by scales smaller than synoptic even though orographic effects are evidently not present. This effect is clearly reflected in the power spectrum of observed vertical motions (Figure 1) as there is much more energy at periods less than an hour or so than at the longer periods commonly associated with synoptic-scale activity. While the high frequency variations in vertical velocity are apparently due to a field of propagating gravity waves which are Doppler shifted by the ambient horizontal wind field (VanZandt, et al., 1989), we expect that much of the energy at longer periods represents contributions from large-scale motion systems such as baroclinic storms. However, it is not obvious that temporal noise at a single station can in general be filtered to provide mean values consistent with a large spatial average (i.e., application of the Taylor hypothesis). Consequently, the observation of synoptic scale vertical motions, believed to be of the order of a few  $\text{cm s}^{-1}$ , may not be straightforward even at Flatland. The removal of orographic effects from the signal has simplified the problem to the extent that the nature of the other noise sources may now be more clearly identified. In this study we explore some preliminary aspects of these problems: first, we show that periods of enhanced variance of the vertical velocity during the interval studied are associated with the passage of

fronts at the surface, and identify a frontal signature that is sometimes present in the lower troposphere. Second, we illustrate the difficulties in verification of the Taylor hypothesis by comparing radar observed vertical motions with those deduced from the horizontal wind field derived from the twice daily NWS rawinsonde network, and discuss the problems associated with such a comparison.

## 2. Analysis

Time series of vertical velocity over Flatland during March 1987 are shown in Figure 2. As at other locations (e.g., Ecklund, et al., 1982), the presence of quiet and active periods is clearly visible, though the variance in all cases is less at Flatland than that at mountain sites (Green, et al., 1988). Along the bottom of Figure 2 letters have been entered to indicate when cold (c), warm (w), occluded (o), or quasi-stationary (qs) fronts passed or were in the vicinity of Flatland. Note that every active period is coupled with a front. While this coupling suggests the interesting notion that fronts are a source of gravity waves, it hinders the prospects for retrieving large-scale vertical motions from the Flatland data because the geophysical "noise" apparently increases just at those times when we hope to find a large-scale signal.

Next we will examine two cases in detail to illustrate two points: first, there is a frontal passage "signature" which is found in the vertical velocity time series in some cases; second, matching the signal at one station with a system which may be moving at an unsteady rate (as fronts and storms often move) and which may be decaying or developing at a rate which is only poorly defined by the 12-hourly radiosonde observation schedule is an extremely complex problem. Weather systems are fully three-dimensional phenomena which move and change with time. The Flatland radar provides a continuous record of the vertical motions over a single place. The morphology of the low-frequency signal in vertical velocity varies from case to case, depending upon the rate and consistency of the movement of the weather system and upon its rate of development or stage of maturity. In some cases the vertical velocity pattern seen by the radar is relatively clear and the synoptic feature easily discerned, while in other cases it is less well defined. We illustrate each of these points with specific examples.

First, we consider a relatively clear frontal passage signature. On 5 March a weak low was over western Illinois at 06 UTC with a warm front moving northward across the Flatland area. The front passed near 05 UTC based on surface observations at Champaign airport, although the National Weather Service analysis indicated it was weak and nearly dissipated by 12 UTC (Figure 3). The time series of vertical velocities display upward motion ahead of the surface frontal passage and downward motions behind it below 5 km, as seen in Figure 2 and as shown more clearly by the analysis of hourly mean velocities in Figure 4. This pattern was noticed by Larsen and Rottger (1982) in connection with the passage of a warm front, and we have seen it in other cases of

moving fronts. While it seems unlikely that the regions of upward and downward motion, located only about 4 hours (150 km if the front moved at  $10 \text{ m s}^{-1}$ ) apart, are due to the front itself as envisioned in the Norwegian frontal model, we suggest it is a typical frontal signature. Perhaps it is due to a gravity wave launched by the front and propagating along with it, similar to the events discussed by Gall, et al.(1988).

A front is in many respects a mesoscale feature, yet in order to compute vertical motions aloft from conventional data we must rely on the radiosonde network which reflects only larger scales. For example, around Flatland the triangle of radiosonde stations at Peoria, Salem and Dayton has an average leg-length of 379 km; which defines the smallest horizontal scale observable with this network over Flatland. The vertical motions computed using the continuity equation applied to the rawinsonde data over this triangle for 5/00 and 6/00 UTC; using Ekman pumping as a lower boundary condition following Nastrom, et al.(1985), are compared with radar time-averages in Figure 5. The radar data represent 6-hour averages and the error bars are the standard error of the mean. At 5/00 UTC the agreement appears satisfactory and at 6/00 UTC it appears excellent. However, the period centered at 6/00 UTC is depicted by plus-signs, and that centered at 6/03 UTC by triangles. The point of this case is that the rawinsonde based values are mean values over a very large area ( of course, the radiosonde data contain errors and noise which we have ignored here), and the radar time mean is for only one position inside the triangle, and that even though the radar is near the center of the triangle the time-mean and the space-mean do not necessarily match. This lack of agreement does not imply any error in either the radar data or the radiosonde data, but rather points to the frequent mismatch of the scales of motion they represent. In the next case we will use NMC data to further illustrate this notion of "shooting at a moving target".

On March 18th an occluded front approached Flatland from the southwest, as illustrated in Figure 6. The mean vertical motions during this period were upward as seen in Figure 2 and also in Figure 7. Green, et al.(1988), used proxy indicators of vertical motions, such as clouds and precipitation from surface reports and widespread echoes from storm surveillance radars, to corroborate the upward motions observed by the radar. Also, they noted that the 12-hour forecasts from the NMC model showed that a region of large vertical motion apparently passing Flatland during this period. Computation of diagnostic vertical motions specific to the Flatland location suitable for comparison with time-mean radar observations was outside the scope of their study.

We have computed vertical motions over Flatland based on the NMC gridded analyses using the kinematic method, the adiabatic method, and the adiabatic quasi-geostrophic omega-equation method. Details follow Nastrom, et al.(1985). The results for 18/12 UTC are compared with 9-hour averages from the radar in Figure 8. There is general agreement among all curves that the motion is upward at several  $\text{cm s}^{-1}$ , although at any height the comparison is not exact. We have included radar curves for two

overlapping time periods as the radar is representative of only a portion of one NMC grid square and the storm is moving in this square throughout the averaging period. The large difference between the radar means and the indirect values at lowest heights may reflect a difference in the scales each data type represents, or it may be due to limitations of the indirect methods, such as the neglect of latent heat release and the use of linear interpolation.

### 3. Conclusion

The Flatland radar experiment has provided copious data on the vertical motions over flat, mid-continental temperate latitude terrain, free from the effects of mountains. Preliminary studies of this data set have begun to shed light on the nature of the motion field in the absence of nearby sources of orographic effects. In particular, qualitative comparison of the time series of vertical motions with those times when surface fronts passed or were near Flatland indicates an association with active periods throughout the troposphere and sometimes into the stratosphere of large lateral extent. Further, the passage of fronts is often accompanied in the lower troposphere with a region of upward motion ahead of and downward motion behind the front, creating a signature of frontal passage.

Although these effects related to synoptic-scale features are easily observable, the observation of the large-scale vertical motion itself in the midst of larger amplitude signals due to small-scale motions is difficult. The absence of orographic noise in the signal has greatly facilitated the understanding of other aspects of the signal, such as the effect of doppler-shifted gravity waves, and this understanding may contribute to the eventual understanding of the large scale signal as well.

Verification of the Taylor hypothesis through comparison of temporal and spatial averages is also difficult. In particular, it has become clear that the velocity and rate of decay or development of a given system will determine the horizontal scale to which a temporal average at the radar site can be properly compared. Only in certain cases will this scale match that of the radiosonde network.

Each of these questions has important implications for the future application of MST radars. It appears that a very promising avenue for future progress is using multiple radars to assess spatial correlation features.

#### 4. References

Ecklund, W. L., K. S. Gage, B. B. Balsley, R. G. Strauch, and J. L. Green, 1982: Vertical wind variability observed by VHF radar in the lee of the Colorado Rockies. Mon. Wea. Rev., 110, 1451-1457.

Gall, R. L., R. T. Williams, T. L. Clark, 1988: Gravity waves generated during frontogenesis. J. Atmos. Sci., 45, 2204-2219.

Green, J. L., K. S. Gage, T. E. VanZandt, W. L. Clark, J. M. Warnock, and G. D. Nastrom, 1988: Observations of vertical velocity over Illinois by the Flatland radar. Geophys. Res. Lett., 15, 269-272.

Larsen, M. F., and J. Rottger, 1982: VHF and UHF Doppler radars as tools for synoptic research. Bull. Amer. Meteor. Soc., 63, 996-1008.

Larsen, M. F., J. Rottger, and T. S. Dennis, 1988: A comparison of operational analysis and VHF wind profiler vertical velocities. Mon. Wea. Rev., 48-59.

Nastrom, G. D., W. L. Ecklund, and K. S. Gage, 1985: On the direct measurement of large-scale vertical velocities using clear-air Doppler radars. Mon. Wea. Rev., 113, 708-718.

VanZandt, T. E., G. D. Nastrom, J. L. Green, and K. S. Gage, 1989: The spectrum of vertical velocity from Flatland radar observations, Preprint Vol., 24th Conf. on Radar Meteorology, Tallahassee, Amer. Meteor. Soc., Boston.

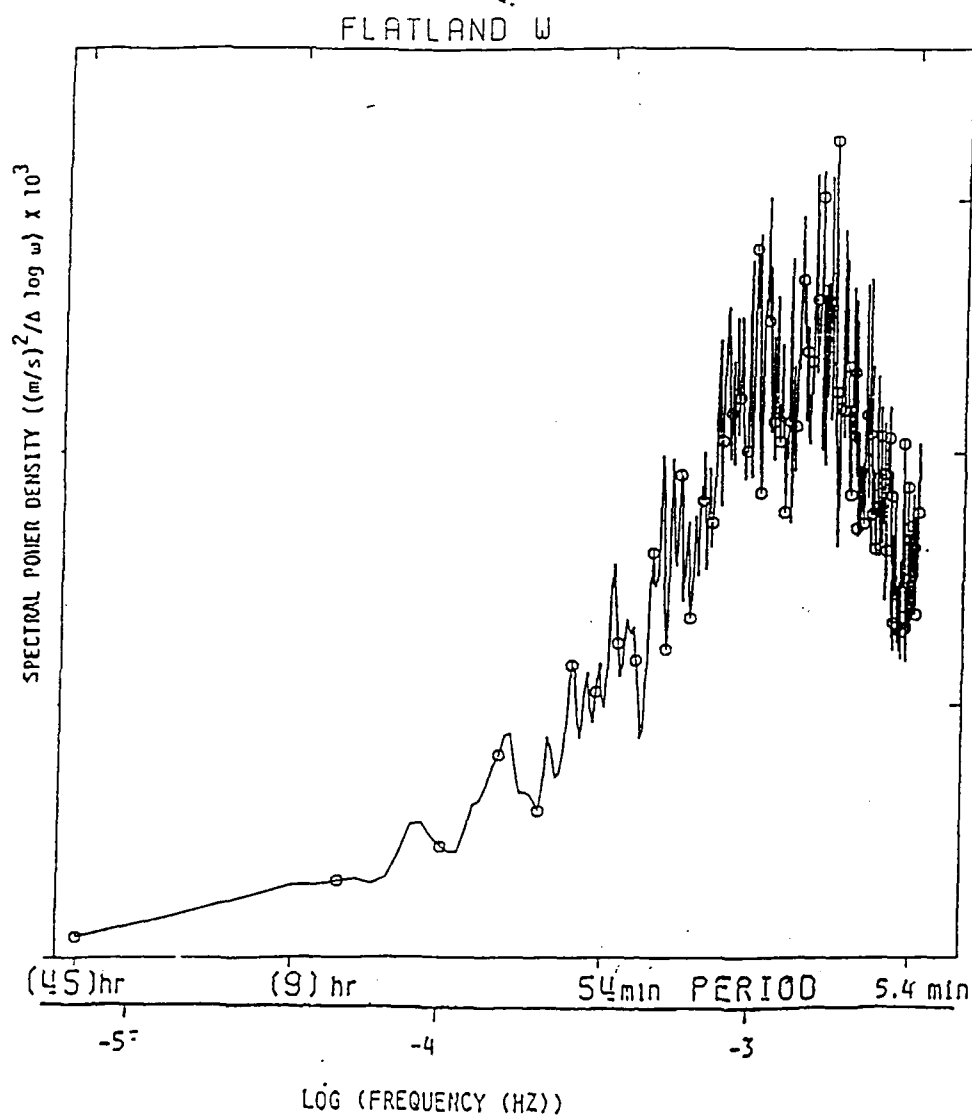


Figure 1. Average of 34 spectra of vertical velocity over 48-hour data periods at Flatland during March through September, 1987, in area preserving coordinates.

# FLATLAND RADAR VERTICAL VELOCITY

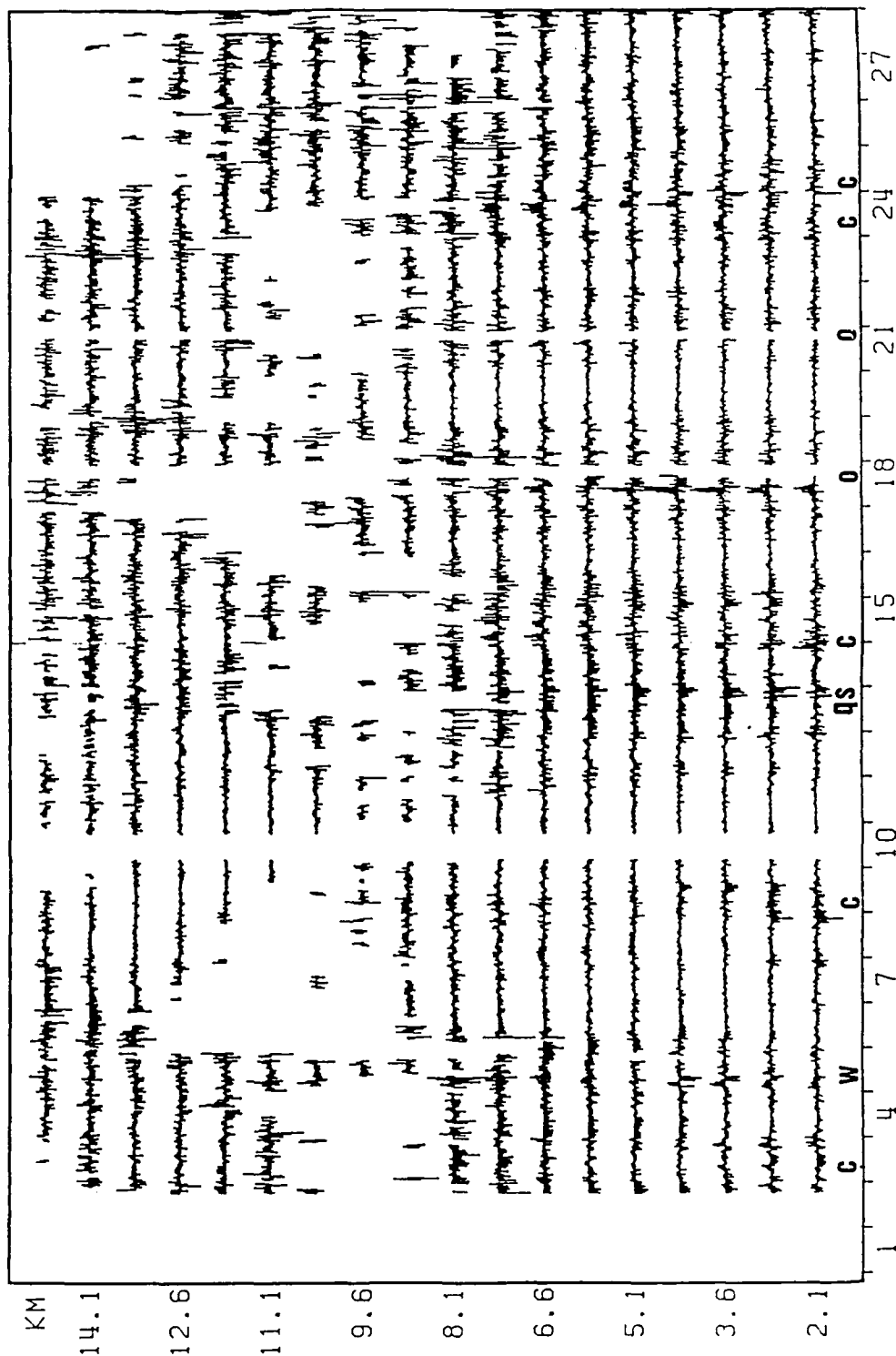


Figure 2. Time series of 15-minute average vertical motion over Flatland during March 1987. The letters along the bottom indicate times when fronts passed or were near Flatland.

1200 UT, MARCH 5, 1987

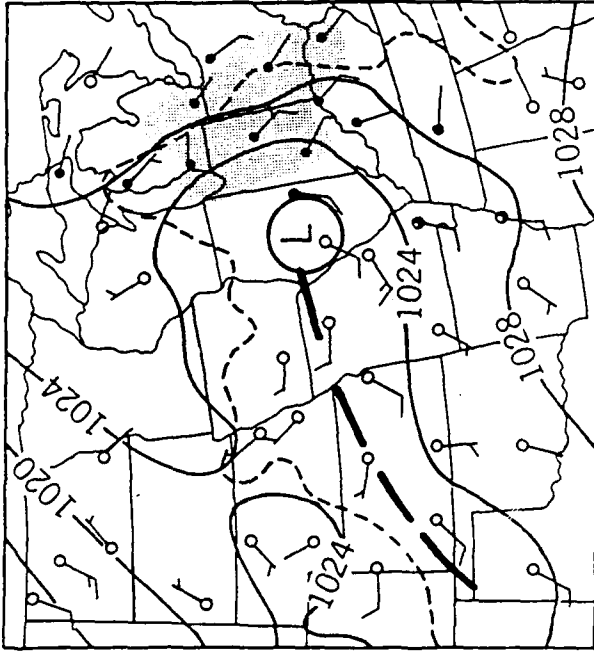
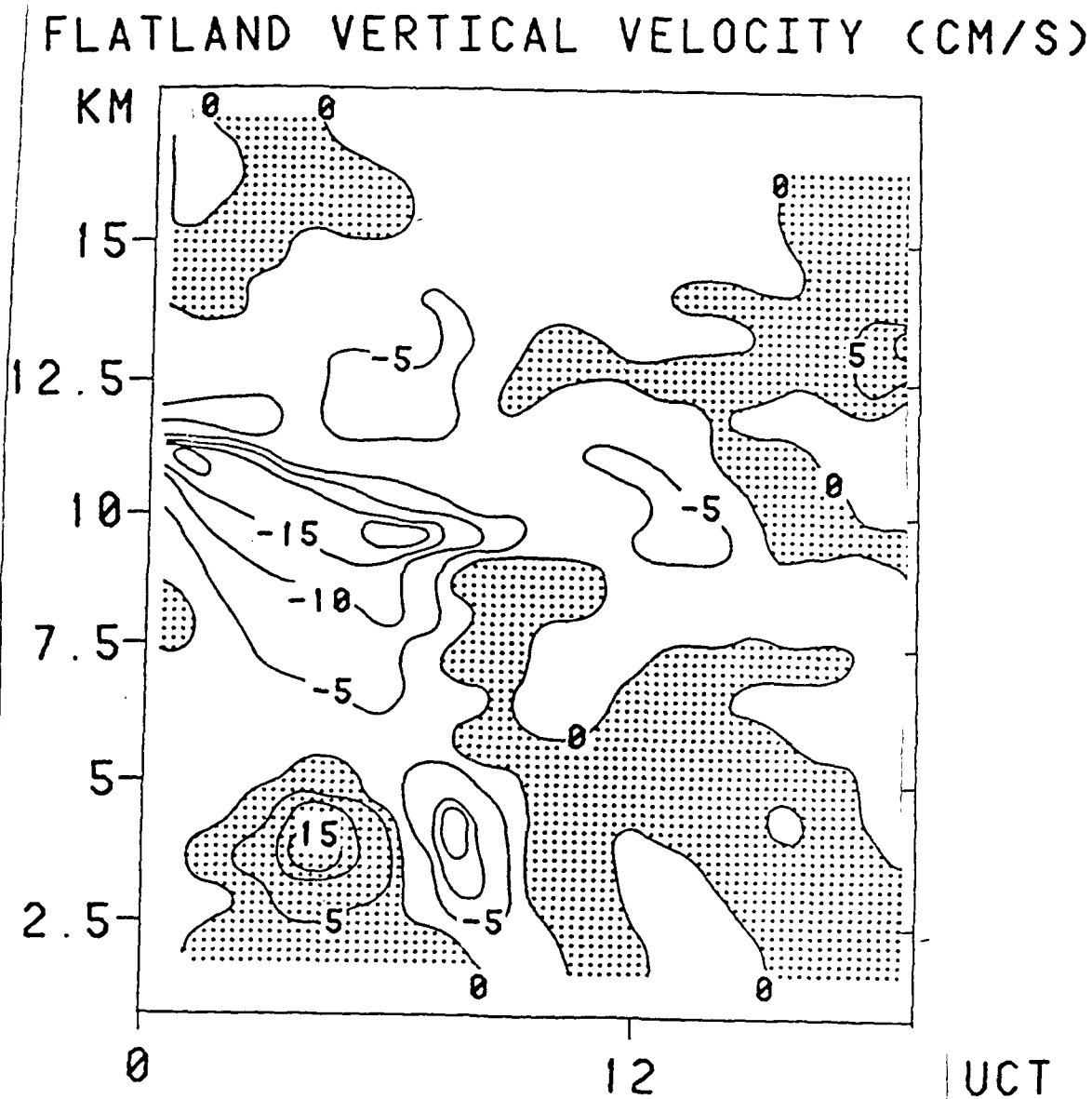


Figure 3. Synoptic weather map for 5 March 1987, 12 UTC.



5 MARCH 1987

Figure 4. Vertical motions over Flatland on 5 March 1987. Upward is positive.

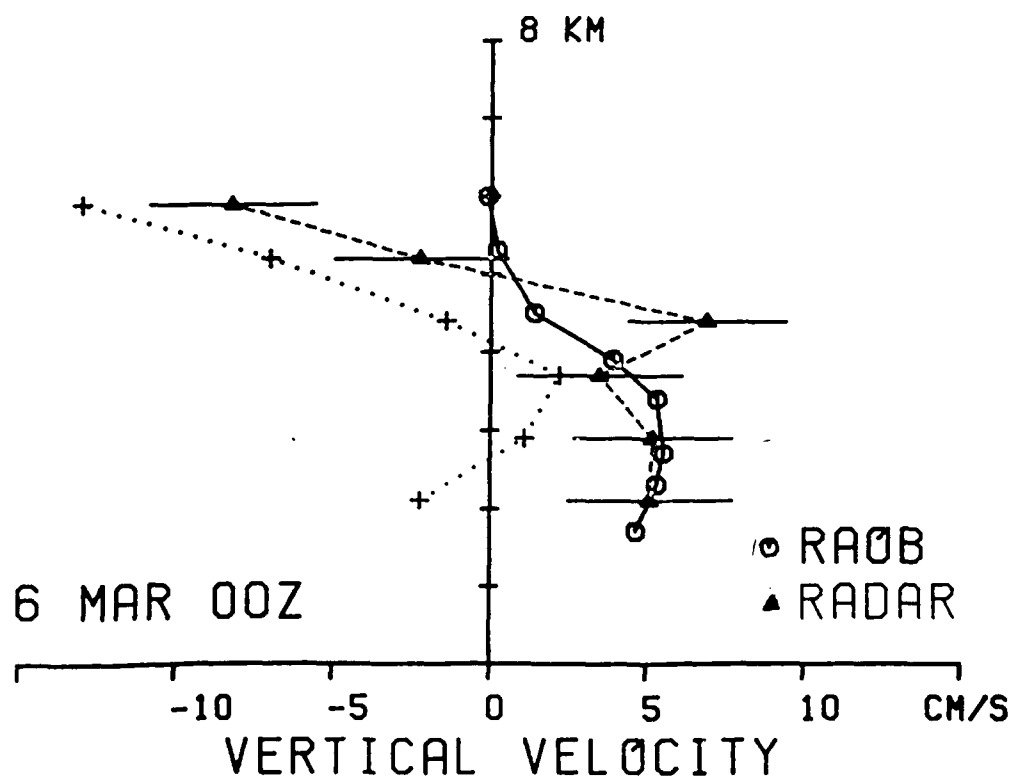
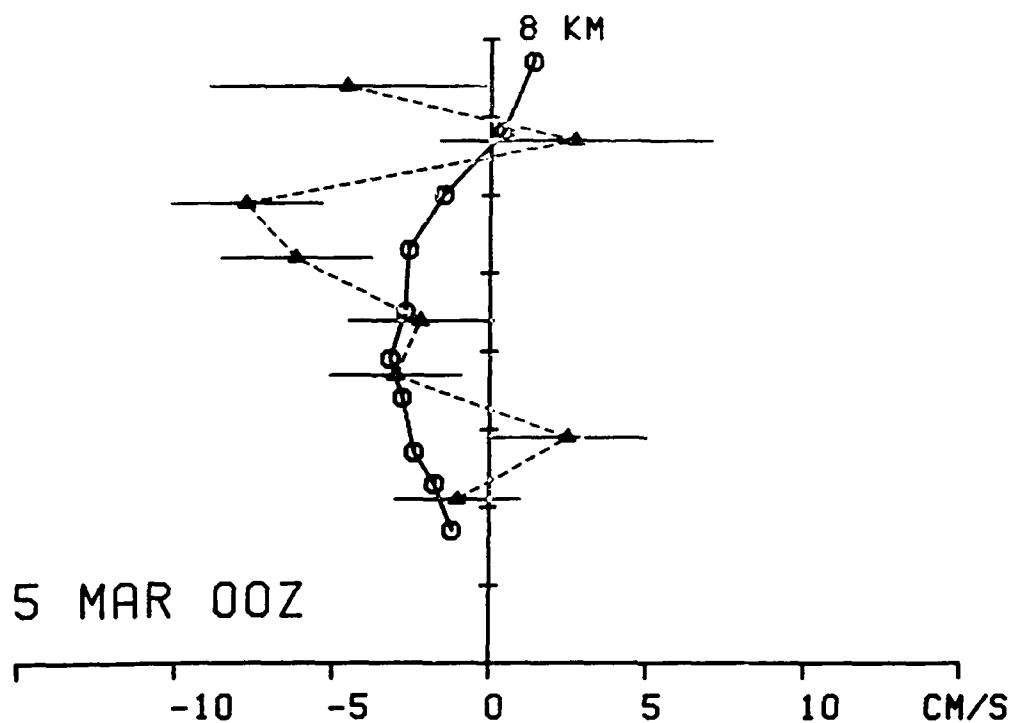


Figure 5. Vertical motions computed using the continuity equation and horizontal winds from the radiosonde station triangle around Flatland compared with 6-hourly mean radar motions. See text.

1200 UT, MARCH 18, 1987

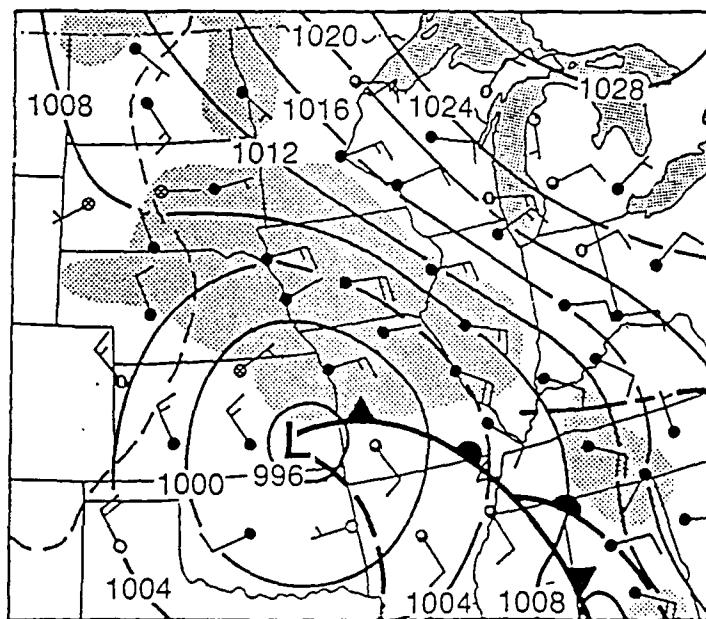


Figure 6. Synoptic weather map for 18 March 1987, 12 UTC.

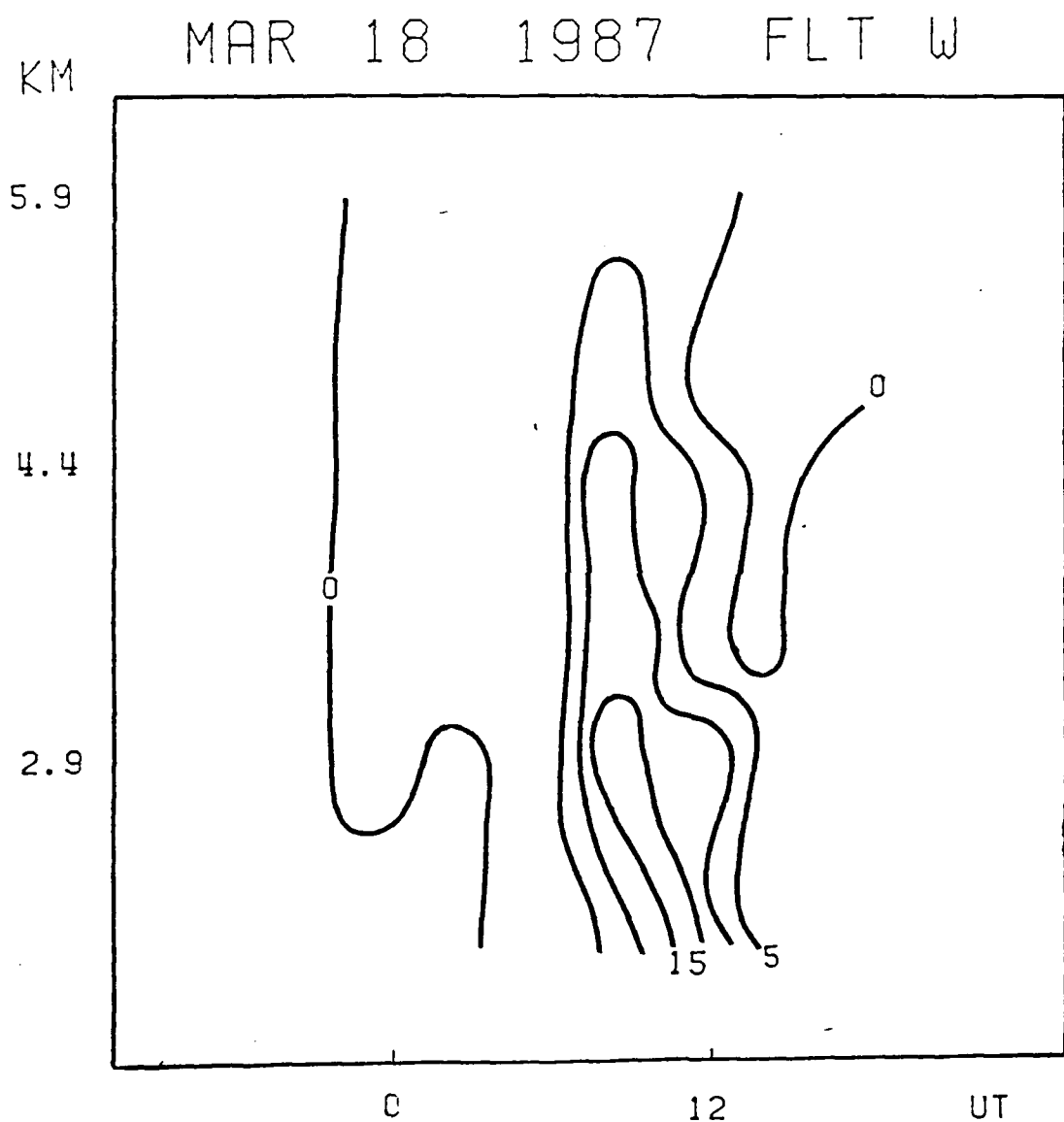


Figure 7. Vertical motions over Flatland on 18 March 1987.  
Upward is positive.

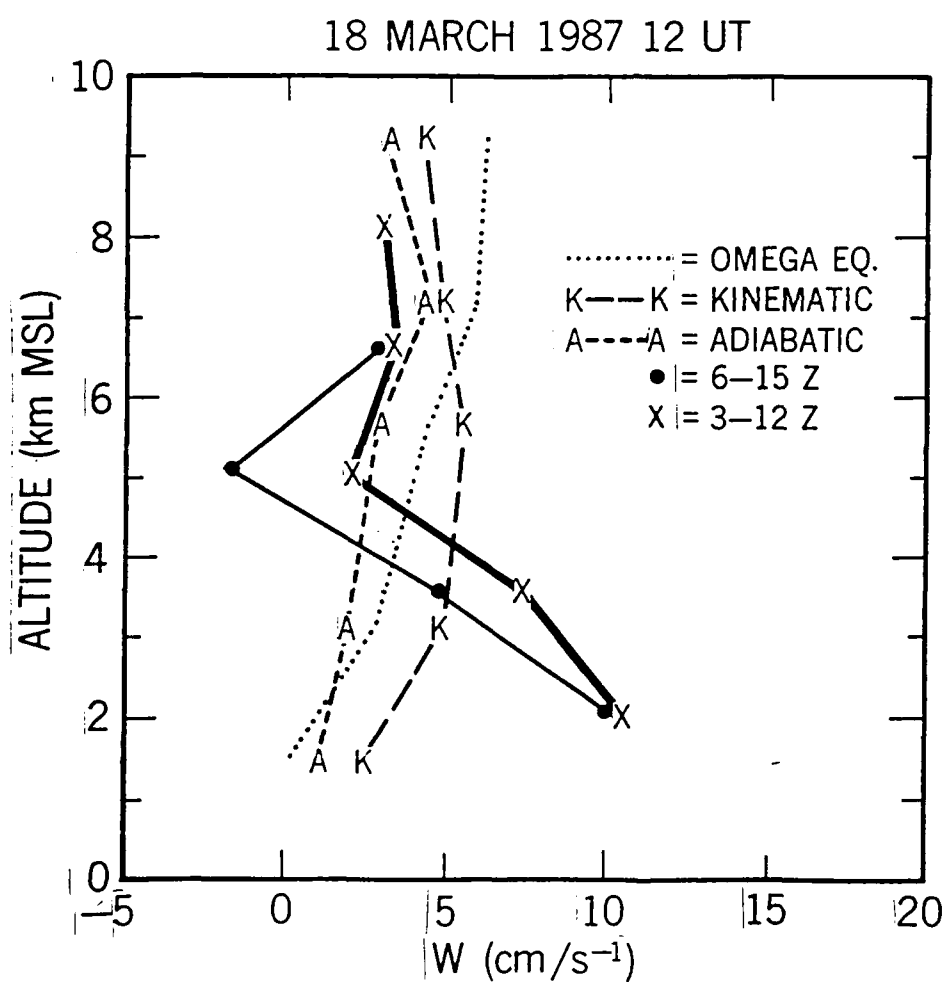


Figure 8. Vertical motions computed from NMC gridded analyses compared with 9-hourly mean radar motions. See text.

A simple model for the enhanced frequency spectrum of vertical  
velocity based on tilting of atmospheric layers by lee waves

Kenneth S. Gage

Aeronomy Laboratory  
National Oceanic and Atmospheric Administration  
Boulder Colorado 80303

Gregory D. Nastrom

Department of Earth Sciences  
St. Cloud State University  
St. Cloud, Minnesota 56301

This paper is concerned with the interpretation of the enhanced frequency spectrum of vertical velocity that has been observed at many locations under strong wind conditions in the vicinity of rough terrain. These enhanced frequency spectra are considerably more energetic than the vertical velocity spectra observed under low-wind conditions, and their shape resembles the shape of the oblique spectra observed by the same radars. In this paper we present the composite spectra of horizontal and vertical velocity observed over a range of wind conditions by the Platteville, Colorado radar, located in the lee of the Colorado Rockies. The vertical velocity spectra show clearly the increase in magnitude and change in spectral slope that occurs as the troposphere becomes increasingly disturbed. We compare the observations with a simple model that relates the magnitude of the vertical velocity spectrum to the horizontal velocity spectrum and the effective tilt of atmospheric layers. Our results show that it is possible to simulate the observed vertical velocity spectrum with effective tilts in the range of 2.5 to 10 degrees. Recent observations of vertical velocity spectra from the Flatland radar, located in flat terrain in central Illinois, do not exhibit this behavior, which leads us to conclude that lee waves are responsible for the enhancement in the Colorado spectra.

## 1. INTRODUCTION

Much has been learned in recent years concerning the nature of the observed spectrum of mesoscale variability in the free atmosphere. Major progress has been made, for example, through spectral analysis of time series of Doppler radar observations of horizontal and vertical velocities. The frequency spectra determined from radar observations have been compared with spectral models for internal waves and quasi-two-dimensional turbulence [VanZandt, 1982, 1985; Scheffler and Liu, 1985; Gage and Nastrom, 1985a,b].

While there is still considerable debate concerning the nature of the spectrum of horizontal velocities, there is general agreement that the vertical velocity spectra in undisturbed conditions are almost entirely due to internal waves. This view is supported by the climatological study of the frequency spectra of vertical motions reported by Ecklund et al. [1986] and the detailed analysis of vertical velocity observations from the Flatland radar [Green et al., 1988; VanZandt et al., 1989].

Although the vertical velocity spectrum seems to result from internal waves, the horizontal velocity spectrum may be expected to have contributions from both internal waves and quasi-two-dimensional turbulence as discussed in Gage and Nastrom [1985a,b; 1986] and Gage [1989]. Recently, this subject has received increased attention from the oceanographic community in the recent work of Müller et al. [1988], who estimate the relative contributions of internal waves and vortical modes to the ocean current spectra observed during IWEX. The coexistence of waves and quasi-two-dimensional turbulence is anticipated in the analysis of stratified turbulence contained in Riley et al. [1981] and Lilly [1983]. The subject of turbulence in stratified fluids has recently been reviewed by Hopfinger [1987].

This paper is concerned with the explanation of the enhanced frequency spectra of vertical motions that are often observed near mountains under

strong wind conditions. We hypothesize that these enhanced spectra of vertical motions are due to a contamination of the vertical motions by a component of the quasi-horizontal motions that occur on isentropic surfaces. According to this hypothesis, when isentropic surfaces are tilted as they are by lee waves, the vertical beam of the Doppler radar observes a component of the quasi-horizontal motions. This hypothesis is tested by employing a simple model that relates the observed vertical velocity spectrum to the observed horizontal velocity spectrum. Observations taken by the Platteville, Colorado radar are used for this purpose.

## 2. THE ENHANCED FREQUENCY SPECTRUM OF VERTICAL MOTIONS

A clear illustration of the enhanced frequency spectrum of vertical motions is shown in Figure 1. These spectra were reported by Ecklund et al. [1985] and were taken in southern France during the ALPEX experiment. The enhanced spectra contrast dramatically with the relatively flat spectra of vertical velocity observed under quiet conditions shown in Figures 1 and 2. Furthermore, the quiet-time spectra observed during ALPEX closely resemble vertical velocity spectra observed elsewhere under similar conditions [Ecklund et al., 1986]. They also resemble the Flatland vertical velocity spectra reported by VanZandt et al. [1989] observed under most conditions.

The possibility that the enhanced frequency spectrum of vertical motions might be due to Doppler shifting of an internal wave spectrum by strong winds needs to be considered. Both Scheffler and Liu [1986] and Fritts and VanZandt [1987] have analyzed the effect of mean winds on a spectrum of internal waves. Recently, VanZandt et al. [1989] have shown that the relatively small changes of vertical velocity spectra that are observed at Flatland can be explained by Doppler shifting.

The fact that enhanced vertical velocity spectra are not observed at Flatland is a strong argument that the enhanced vertical velocity spectra observed at other locations is due to the influence of terrain and not to

4

Doppler shifting. In the remainder of this paper, we examine the enhanced vertical velocity spectra that are observed at Platteville, Colorado in the lee of the Rocky Mountains.

### 3. FREQUENCY SPECTRA OF VERTICAL AND HORIZONTAL MOTIONS

#### OBSERVED AT PLATTEVILLE, COLORADO

The Platteville radar has been in continuous operation since the early 1980's. It was originally constructed as a prototype for the Poker Flat MST radar [Ecklund et al., 1979] and has been operated in recent years by NOAA's Wave Propagation Laboratory. The spectra presented in Figure 3 and Figure 4 are composite spectra averaged by season and stratified by the standard deviation of vertical velocity. At Platteville, there is a close relationship between the background wind speed and the vertical velocity variance as evident in Figure 3 and Figure 4.

Composite vertical velocity spectra for the winter season at Platteville, Colorado are shown in Figure 3. These spectra show clearly the enhancement in spectral magnitude and systematic variation of spectral slope that accompanies increasing winds at this location. The dashed curve indicates a spectral slope of  $-5/3$ . With increasing wind speed the observed vertical velocity spectra approach the  $-5/3$  spectral slope. Only those time periods when both horizontal and vertical wind components were measured are used here, although the results are very similar when all available data are used.

Corresponding composite zonal wind spectra at 5.8 km for the winter season as stratified by vertical velocity variance are shown in Figure 4. These spectra also show a systematic but less pronounced variation with background wind speed. Note that the magnitude of the horizontal velocity spectra are in all cases considerably larger than the magnitude of the corresponding vertical velocity spectra. Again, the dashed line shows the  $-5/3$  slope for comparison with the observed spectra.

#### 4. A SIMPLE MODEL FOR THE ENHANCED VERTICAL VELOCITY SPECTRUM

The simple model used here to explain the enhanced vertical velocity spectrum is based on the idea that in stably stratified flows the velocity field is comprised of both internal waves and potential vorticity modes [Riley et al., 1981; Lilly, 1983; Müller, 1984; Herring and Metais, 1989]. The potential vorticity modes are comprised of quasi-horizontal eddies that follow very closely isentropic surfaces in the stratified fluid. Accordingly, when the isentropic surfaces are horizontal and undisturbed, vertical motion will be due only to internal waves. The horizontal motion field, however, will be comprised of both internal waves and vortical modes. When isentropic surfaces are tilted, the vortical modes will also be tilted to conserve potential vorticity so that there will now be a vertical component to the vortical motion.

The consequences of the model on observations by a vertically directed radar are simple and straightforward. When isentropic surfaces are flat, the radar will observe only the internal gravity wave field and vortical motions will not be observed. However, when isentropic surfaces are tilted, as they may be by mountain lee waves, the radar will observe a component of the vortical motion.

The process can be quantified as follows. If the effective tilting angle is  $\delta$ , the observed vertical velocity spectrum  $\Phi_{ww}(\omega)$  is related to the horizontal velocity spectrum  $\Phi_{uu}(\omega)$  by

$$\Phi_{ww}(\omega) = \sin^2 \delta \Phi_{uu}(\omega) + [\Phi_{ww}(\omega)]_{\text{internal waves}} \quad (1)$$

Thus if  $\delta$  were known it would be possible to estimate the vertical velocity spectrum from the observed horizontal velocity spectrum since the internal wave spectrum is fairly well known. From the Platteville observations, we can deduce the effective tilting angle that satisfies (1).

## 5. VERTICAL VELOCITY SPECTRA DEDUCED FROM THE SIMPLE MODEL

Vertical velocity spectra can be deduced from the observed horizontal velocity spectrum by first determining the effective tilting angle. The effective tilting angle is determined by the value of  $\delta$  required to reduce the horizontal velocity spectrum to the observed magnitude of the vertical velocity spectrum. For example, Figure 5 shows that  $\delta = 10^\circ$  brings the observed horizontal velocity spectrum for  $U = 17 \text{ ms}^{-1}$  into near coincidence with the observed vertical velocity spectrum. Note that only when the effective tilt angle is less than about  $5^\circ$  does the internal wave spectrum become important in (1) for these observations.

Model vertical velocity spectra for the various background horizontal velocities in Figure 4 are shown in Figure 6. Comparison of the two sets of spectra shows excellent agreement. The effective tilt angles that are consistent with the model fall in the range of  $2.5^\circ - 10^\circ$ . This magnitude of tilt is easily produced by lee waves that possess horizontal wavelengths of order ten kilometers and vertical displacements ranging from several hundred meters to greater than one kilometer [Gage, 1986]. Of course, in the absence of mountain lee waves tilting would not be sufficient to produce the enhanced vertical velocity spectrum. On the synoptic scale isentropic surfaces are generally tilted less than a few tenths of a degree. Propagating internal waves can cause tilting of perhaps a few degrees which could cause a slight enhancement in the observed magnitude of vertical velocity spectra at very low frequencies even over flat terrain.

## 6. CONCLUSIONS

A simple model has been used to simulate the enhanced frequency spectra of vertical motion observed at Platteville, Colorado under disturbed conditions. If it is hypothesized that the horizontal velocity spectrum is primarily due to quasi-horizontal motions associated with potential vorticity modes, the magnitude and shape of the observed vertical velocity spectrum can be explained by tilting of isentropic surfaces due to lee waves.

While the simple model proposed here is reasonably consistent with observations at Platteville, more stringent tests are required before too much confidence can be placed in the result. For example, independent estimates of the slope of isentropic surfaces associated with lee waves expected under various background wind conditions would strengthen the analysis. Alternatively, observations taken simultaneously at more than one oblique zenith angle would help with the evaluation of how much of the horizontal velocity spectra is associated with vortical modes and how much is due to internal waves.

## 7. REFERENCES

- Ecklund, W. L., D. A. Carter, and B. B. Balsley. Continuous measurement of upper atmospheric winds and turbulence using a VHF Doppler radar: Preliminary results, J. Atmos. Terr. Phys., 41, 933-944, 1979.
- Ecklund, W. L., B. B. Balsley, D. A. Carter, A. C. Riddle, M. Crochet, and R. Garelo. Observations of vertical motions in the troposphere and lower stratosphere using three closely-spaced ST radars, Radio Sci., 20, 1196-1206, 1985.
- Ecklund, W. L., K. S. Gage, G. D. Nastrom, and B. B. Balsley. A preliminary climatology of the spectrum of vertical velocity observed by clear-air Doppler radar, J. Clim. Appl. Meteor., 25, 885-892, 1986.
- Fritts, D. C. and T. E. VanZandt. Effects of Doppler shifting on the frequency spectrum of atmospheric gravity waves, J. Geophys. Res., 92, 9723-9732, 1987.
- Gage, K. S. and G. D. Nastrom. On the spectrum of atmospheric velocity fluctuations seen by MST/ST radar and their interpretation, Radio Sci., 20, 1339-1347, 1985a.
- Gage, K. S. and G. D. Nastrom. Evidence for coexisting spectra of stratified turbulence and internal waves in mesoscale atmospheric velocity fields, Preprint Vol., 7th Symp. on Turbulence and Diffusion, Nov 12-15, Boulder, CO, 176-179, 1985b.
- Gage, K. S. Implications of tilting of stable layers on atmospheric measurements by clear-air Doppler radars, Preprint Vol., 23rd Conf. on Radar Meteorology, Sept 22-26, Snowmass, CO, A. M. S., Boston, MA, 33-37, 1986.
- Gage, K. S. (1989), "The structure and dynamics of the free atmosphere as observed by VHF/UHF radar", Radar in Meteorology, Chapt. 28a, D. Atlas, ed., Amer. Meteorol. Soc., Boston, MA, (in press).
- Green, J. L., K. S. Gage, T. E. VanZandt, W. L. Clark, J. M. Warnock and G.D.Nastrom. Observations of vertical velocity over Illinois by the Flatland radar, Geophys. Res. Lett., 15, 269-272, 1988.

- Herring, J. R. and O. Metais. Numerical experiments in forced stably stratified turbulence, J. Fluid Mech., 1989, (in press).
- Hopfinger, E. J. Turbulence in stratified fluids: A review, J. Geophys. Res., 92, 5287-5303, 1987.
- Lilly, D. K. Stratified turbulence and the mesoscale variability of the atmosphere, J. Atmos. Sci., 40, 749-761, 1983.
- Müller, P. Small-scale vortical motions, Proc. of Hawaiian Winter workshop, P. Müller and R. Pujale, eds., 249-261, Institute of Geophysics, Honolulu, HI, 1984.
- Müller, P., R.-C. Lien, and R. Williams. Estimates of potential vorticity at small scales in the ocean, J. Phys. Ocean., 18, 401-416, 1988.
- Riley, J. J., R. W. Metcalfe, and M. A. Weissman (1981). Direct numerical simulation of homogeneous turbulence in density-stratified fluids, Nonlinear Properties of Internal Waves, B. J. West, ed., Amer. Inst. of Physics, 76, 79-112.
- Scheffler, A. O. and C. H. Liu. On observations of gravity wave spectra in the atmosphere by using MST radar, Radio Sci., 20, 1309-1322, 1985.
- Scheffler, A. O. and C. H. Liu. The effects of Doppler shift on gravity wave spectra observed by MST radar, J. Atmos. Terr. Phys., 48, 1225-1231, 1986.
- VanZandt, T. E. A universal spectrum of buoyancy waves in the atmosphere, Geophys. Res. Lett., 9, 575-578, 1982.
- VanZandt, T. E. A model for gravity wave spectra observed by Doppler sounding systems, Radio Sci., 20, 1323-1330, 1985.
- VanZandt, T. E., G. D. Nastrom, J. L. Green and K. S. Gage. The spectrum of vertical velocity from Flatland radar observations, Preprint Vol., 24th Conf. on Radar Meteorology, Tallahassee, FL. Amer. Meteorol. Soc., Boston, MA, 717-720, 1989.

## FIGURE CAPTIONS

- Figure 1. The frequency spectrum of vertical velocity observed in southern France during ALPEX for active and quiet days. (After Ecklund et al., [1985]).
- Figure 2. The frequency spectrum of vertical velocity observed in southern France during ALPEX for quiet days. (After Ecklund et al., [1985]).
- Figure 3. The frequency spectrum of vertical velocity observed at Platteville, CO during the winter season at 5.8 km. Spectra shown are composite spectra averaged over several years and stratified by vertical velocity variance.
- Figure 4. The frequency spectra of zonal wind speed observed at Platteville, CO during the winter season at 5.8 km. The spectra represent the same period of observation as the spectra in Figure 3 and are stratified in a similar manner.
- Figure 5a. An illustration of the deduction of the vertical velocity spectrum from the observed horizontal velocity spectrum using (1). Also shown is the observed vertical velocity spectrum for  $\bar{u} = 17 \text{ ms}^{-1}$  for comparison.
- Figure 5b. Same as for Figure 5a except for  $\bar{u} = 14 \text{ ms}^{-1}$ .
- Figure 5c. Same as for Figure 5a except for  $\bar{u} = 9 \text{ ms}^{-1}$ .
- Figure 5d. Same as for Figure 5a except for  $\bar{u} = 4 \text{ ms}^{-1}$ .
- Figure 6. Frequency spectra of vertical velocity derived from the observed horizontal velocity according to (1). These spectra should be compared with the observed spectra in Figure 3.

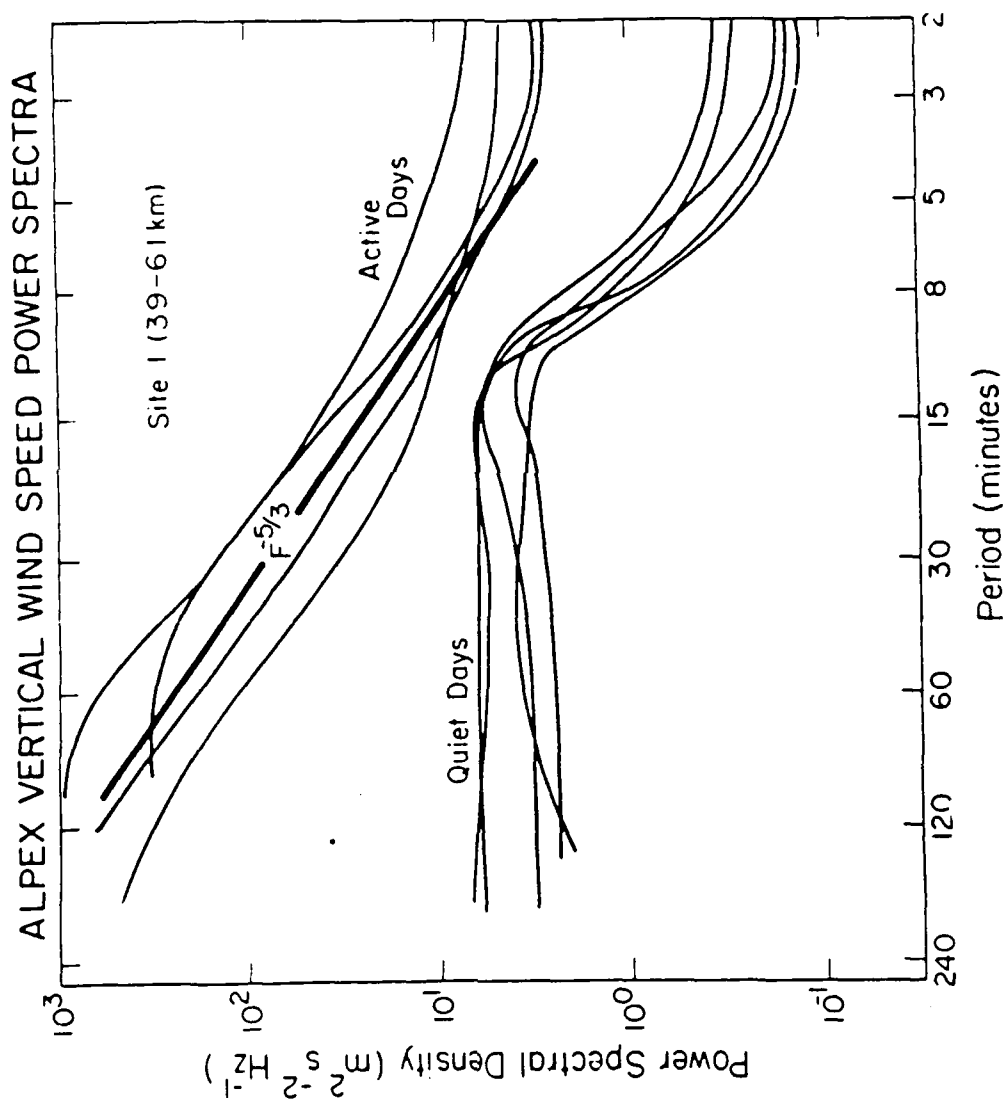


Fig. 1

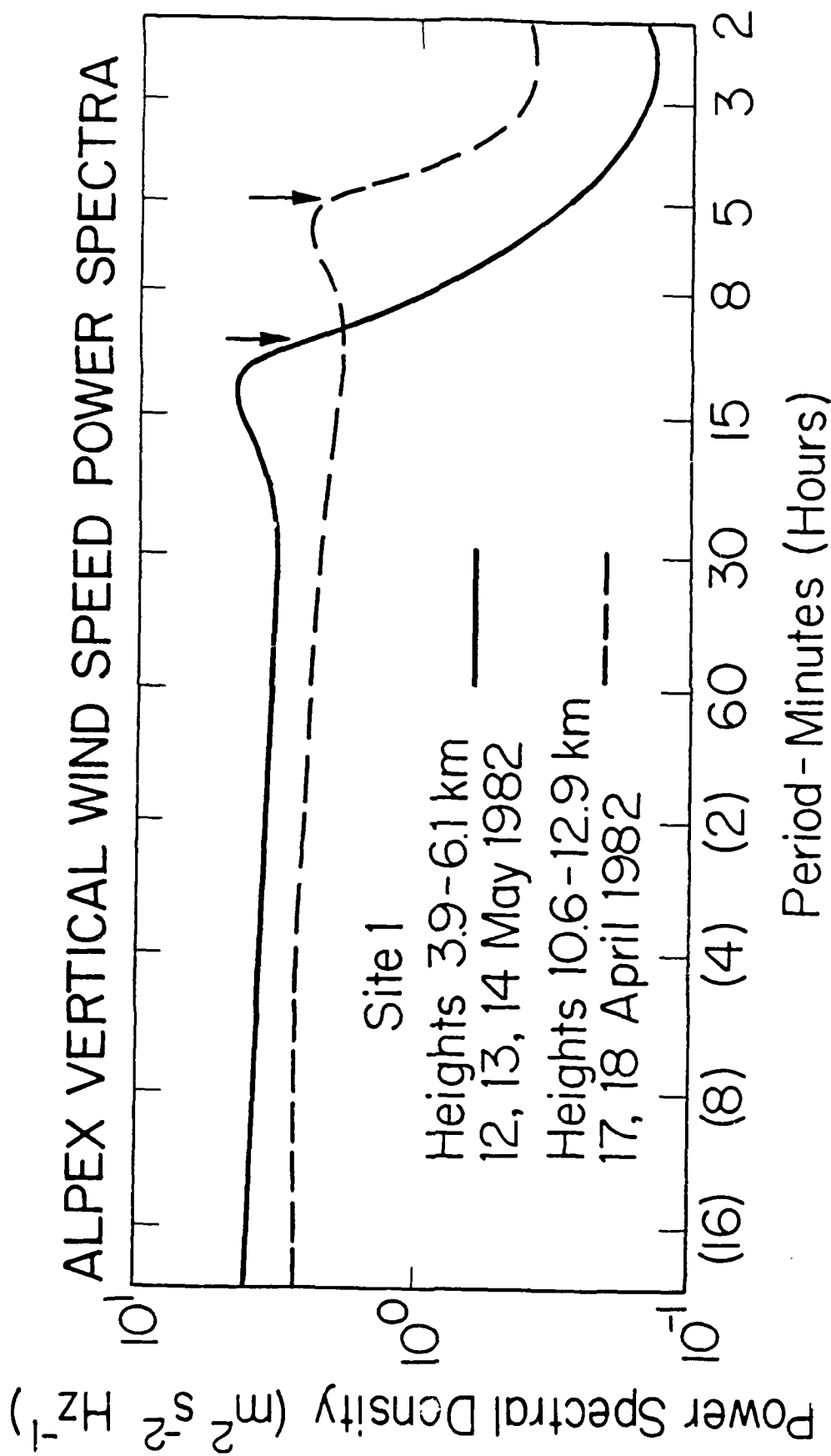


Fig. 2

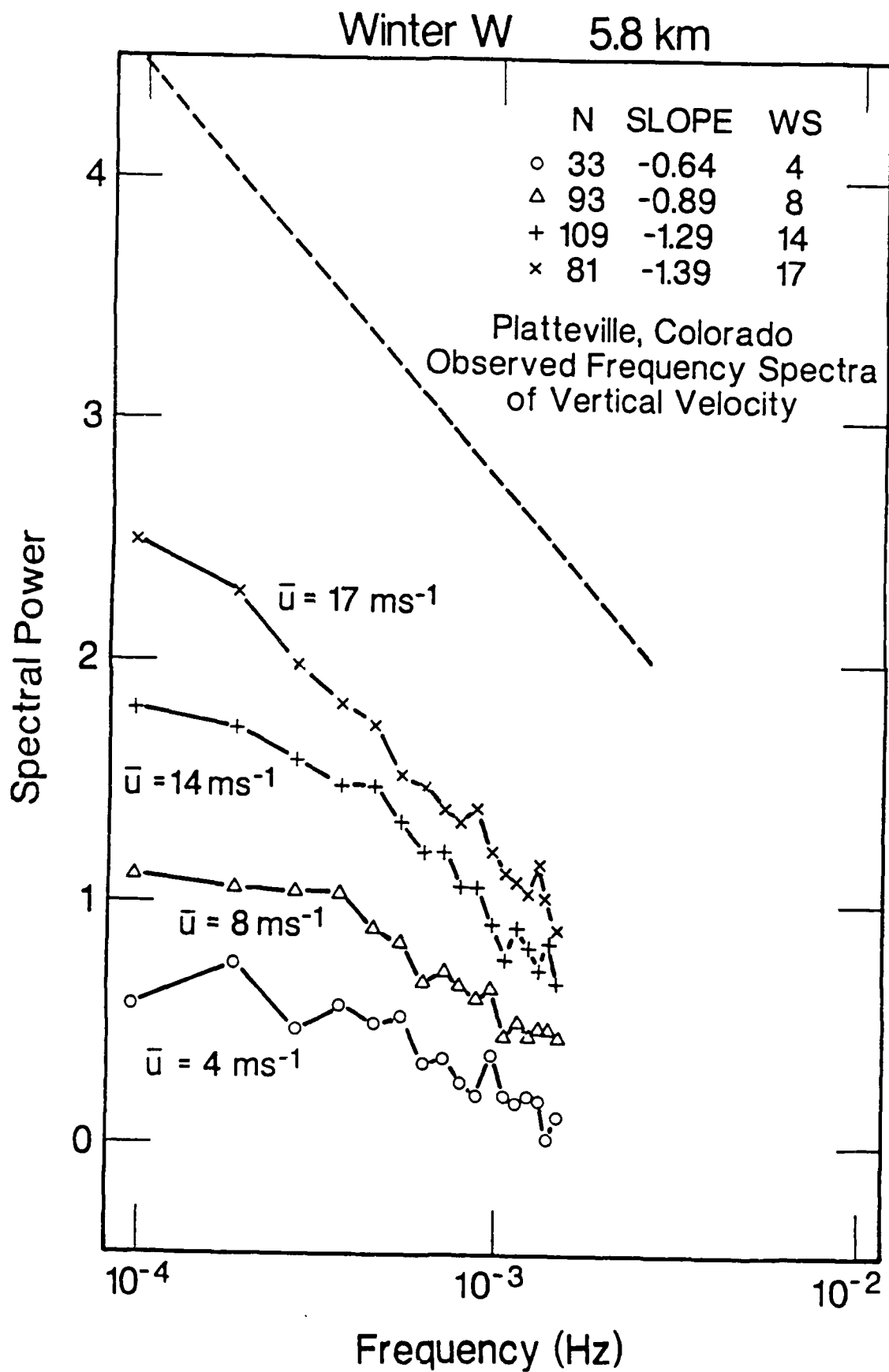


Fig. 3

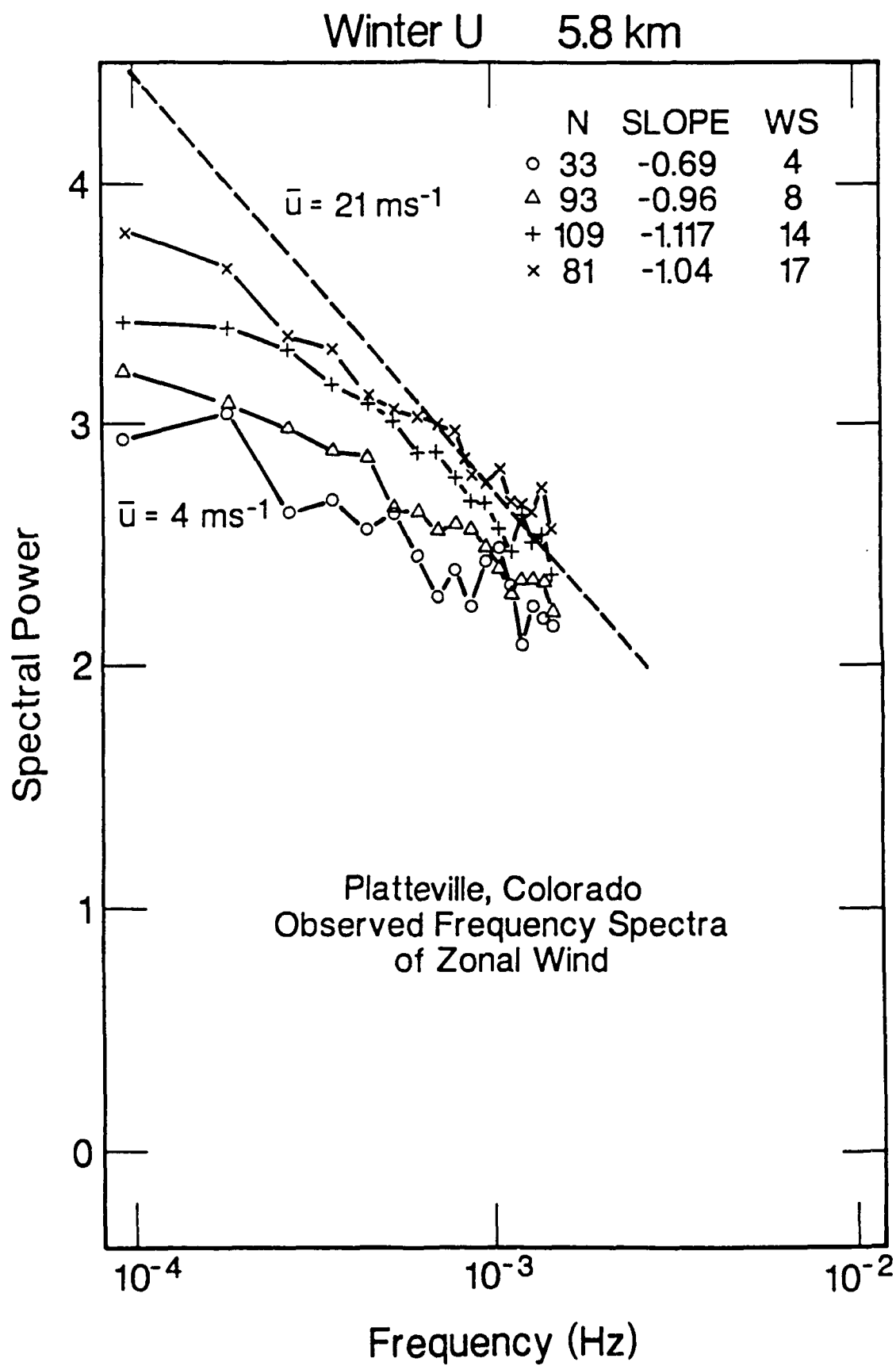


Fig. 4

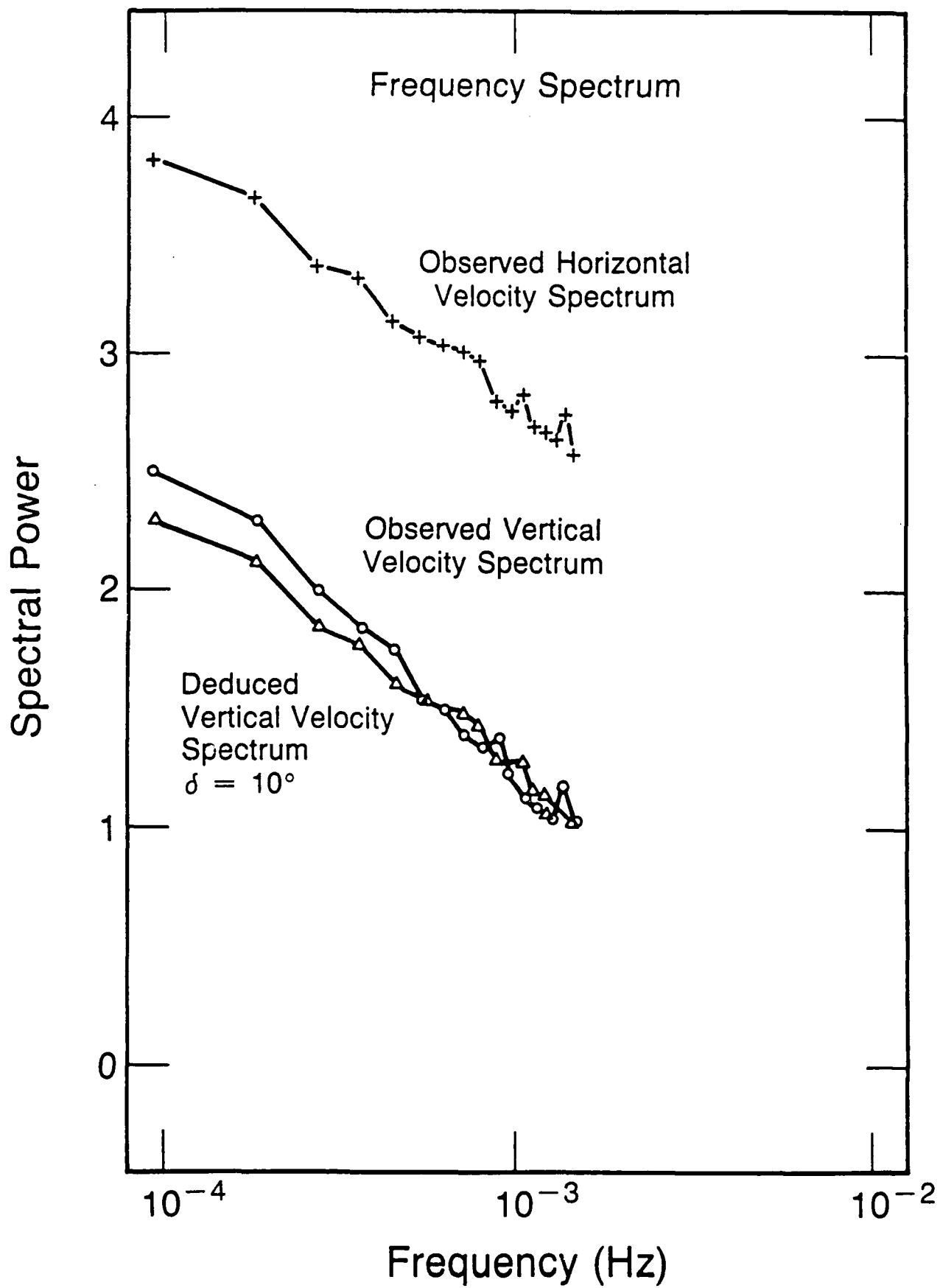


Fig. 5a

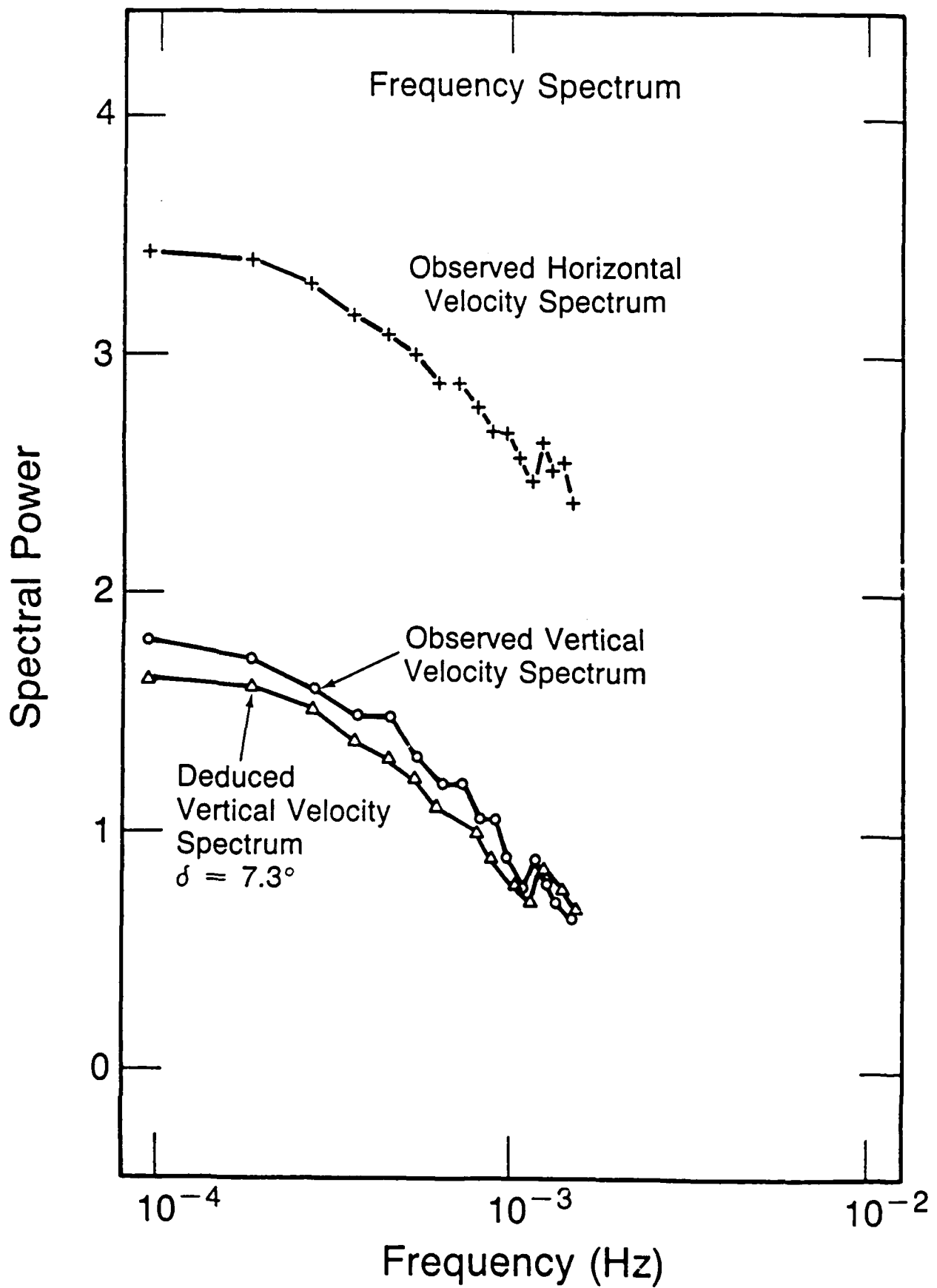


Fig. 5b

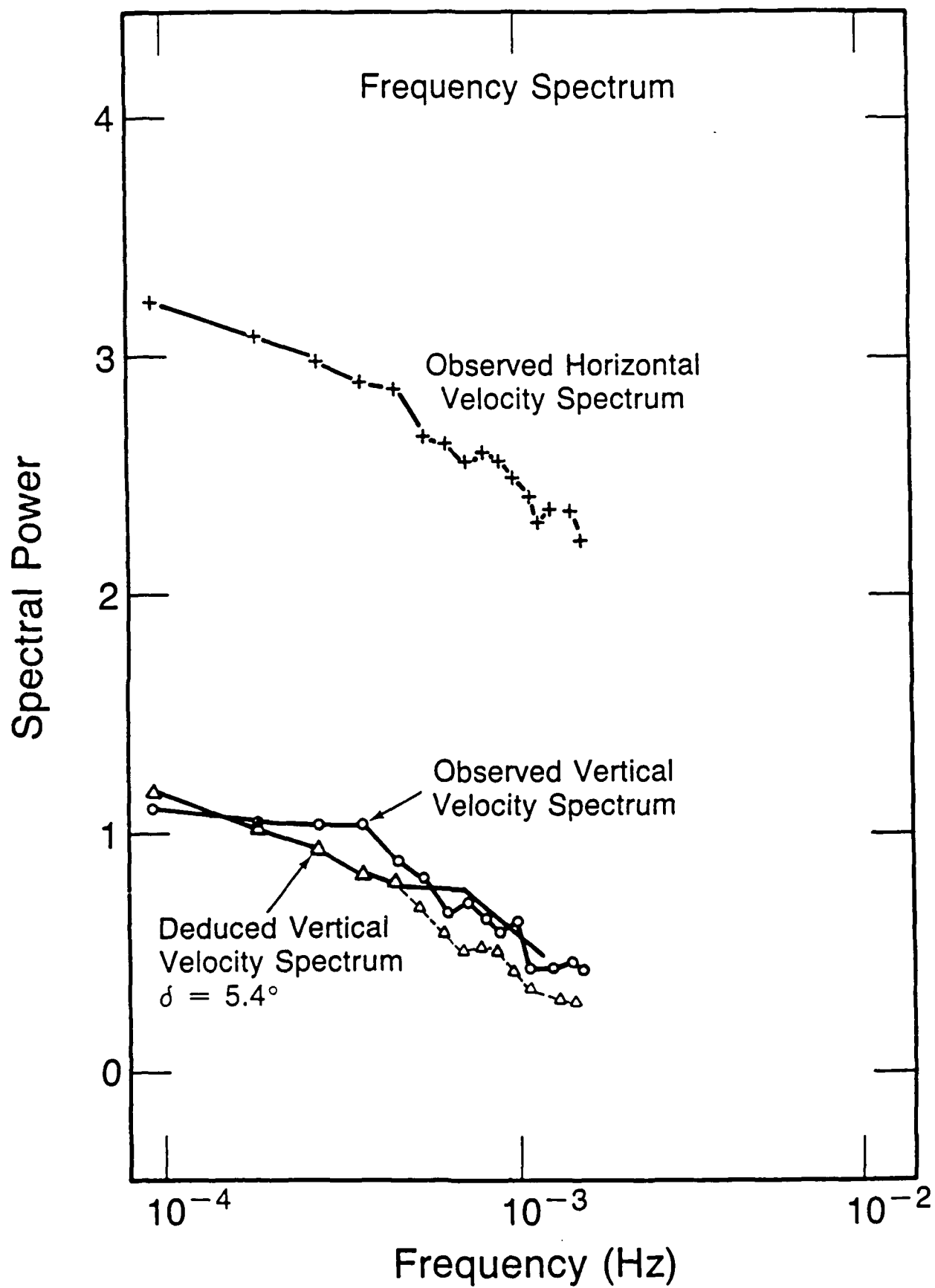


Fig. 5c

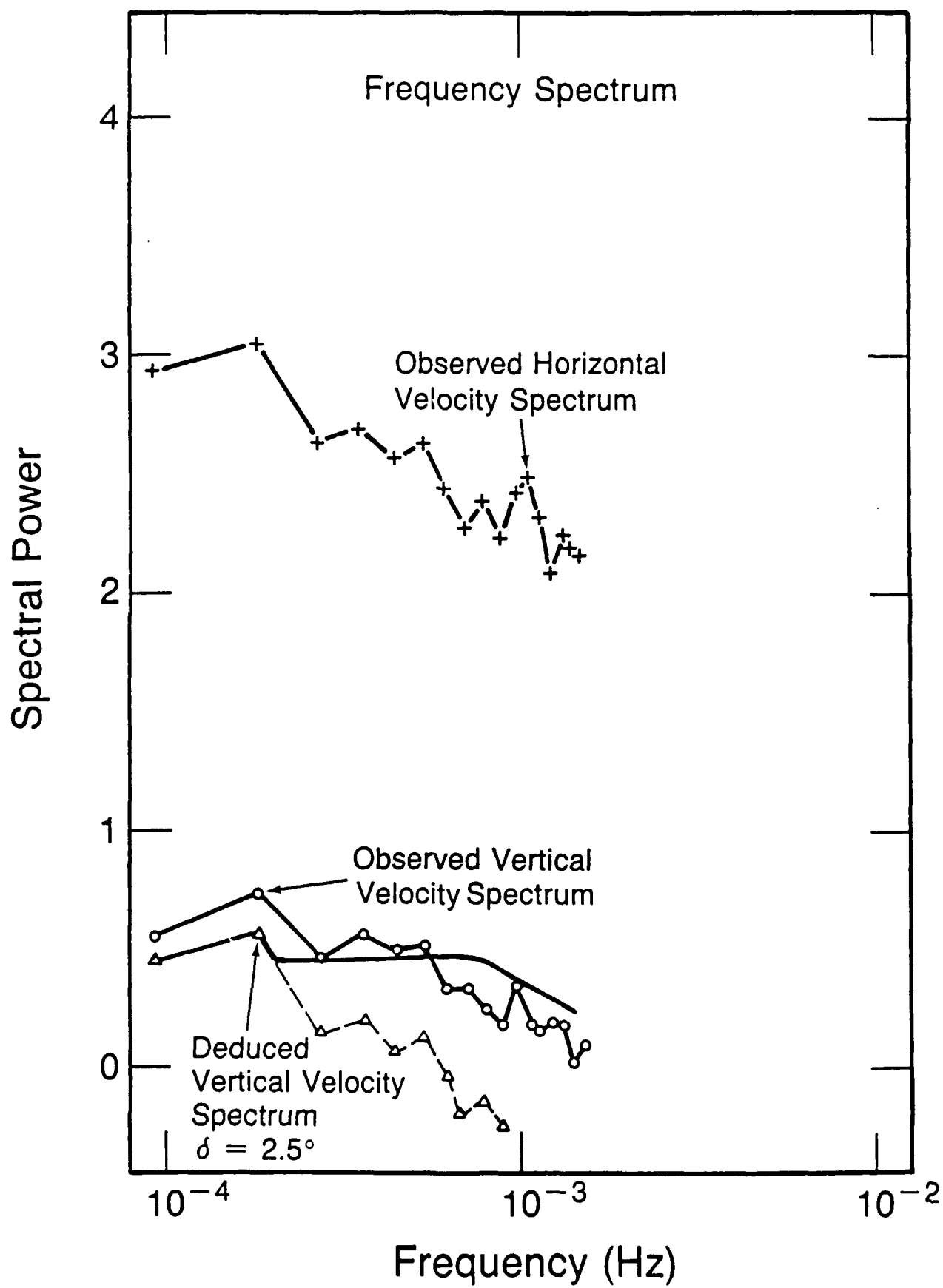


Fig. 5d

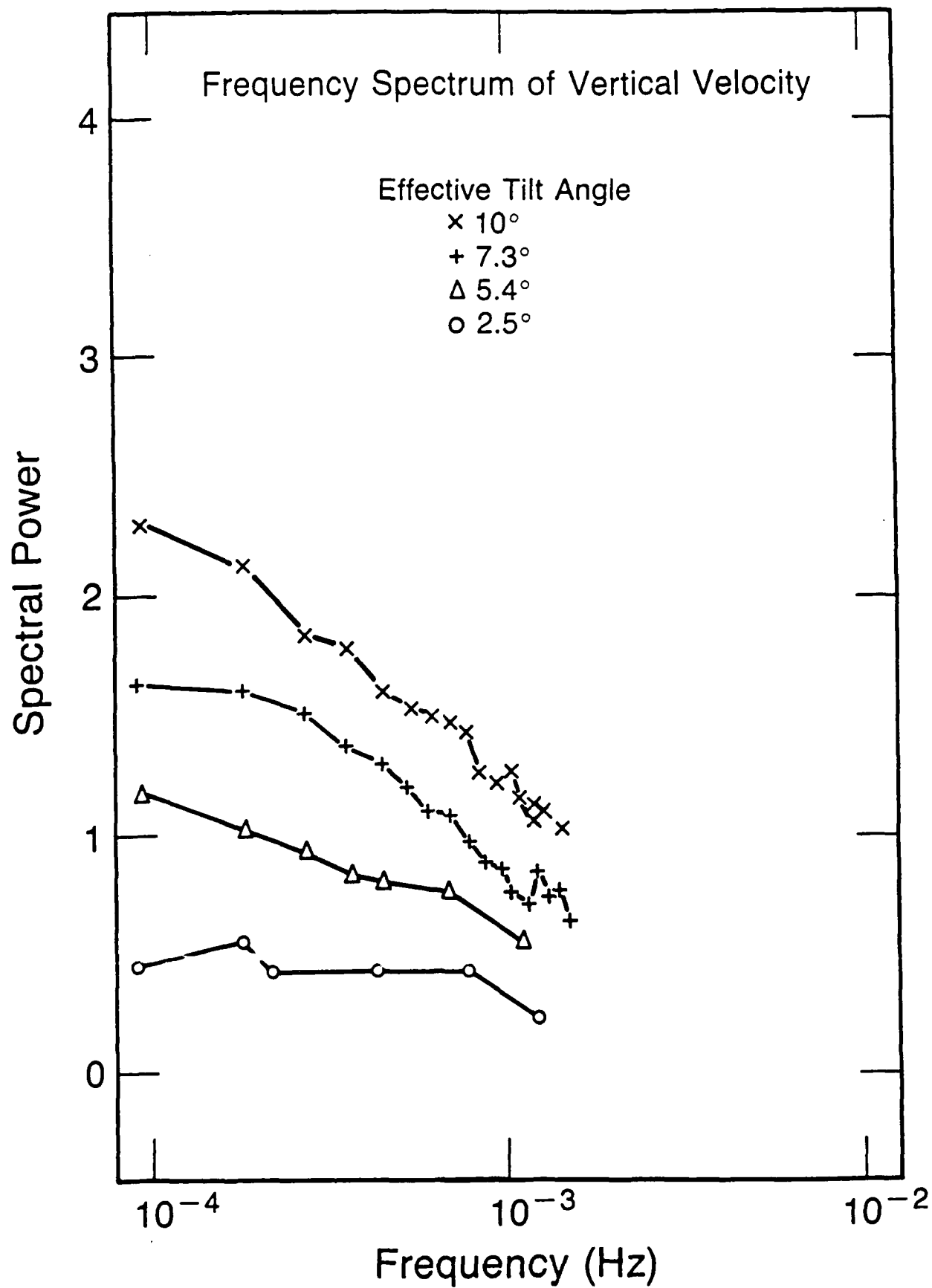


Fig. 6

THE EFFECTS OF SAMPLING STRATEGY ON ESTIMATES  
OF THE MEAN VERTICAL VELOCITY

G. D. Nastrom  
St. Cloud State University, St. Cloud, MN 56301

K. S. Gage and W. L. Ecklund  
Aeronomy Laboratory, NOAA, Boulder, CO 80303

ABSTRACT

Whenever the time series of a variable is not sampled continuously, a fraction of its variance is missed. This fraction contributes to the uncertainty of the mean value determined from the available sample. In the case of vertical velocity, where a relatively large fraction of the variance is due to high frequency motions, the effect of even small gaps in the sampling is very important. Measurements from the Flatland VHF radar are used to study this effect. Quasi-continuous data are sampled with several strategies, and it is found that the strategy with the smallest gap between data samples gives the smallest uncertainty of the mean vertical velocity. It is found that the time between statistically independent samples of vertical velocity at Flatland is 5.1 minutes in the troposphere.

## 1. INTRODUCTION

Clear-air Doppler radars can provide profiles of the vertical velocity over a station on a nearly continuous basis, and at many research sites these data are recorded at intervals on the order of a minute. In some cases it is necessary to use data samples spaced at greater intervals than at the reporting frequency and in recent years there have been several studies which have used time-means of the vertical velocity. For example, Nastrom, et al.(1985), compared time-means of vertical velocity from MST radar measurements with large-scale values based on radiosonde data; and Larsen, et al.(1988), compared them with ECMWF model forecasts of vertical velocity. Cornish (1988) mentioned the difficulty of obtaining long-term mean values at the Arecibo observatory, and Balsley, et al. (1988), in a much more extensive study, used time mean vertical velocities to study tropical motions at 7°N. Strauch, et al. (1987), studied the importance of including the effects of large vertical motions in the measurements of the horizontal wind components from obliquely directed radar beams. For purposes such as these it is important to use the sampling strategy which yields the mean value of vertical velocity with the smallest possible uncertainty under given experimental constraints and to estimate the

magnitude of the uncertainty of the mean once a sampling strategy is selected.

Because the spectrum of atmospheric vertical velocity covers a complete range of frequencies, some variance will be missed whenever the temporal sampling is not continuous. This unresolved, or missed, variance contributes to the uncertainty of mean values based on the available observations, along with other effects such as aliasing of the observed frequency spectrum. In this paper we examine the effects of various temporal sampling strategies on estimates of the time-mean vertical velocity from MST radar measurements.

## 2. DATA

Data used for this study are vertical velocities from the Flatland VHF radar. The radar operating parameters and examples of the data are given by Green, et al. (1988). Briefly, during the period of record used here, March through May, 1987, the radar was operated with one beam which was pointed vertically. Doppler spectra were averaged for about 2.5 minutes and then recorded on tape. Mean velocities at 2.5-minute intervals were computed from these average spectra. The available data are thus quasi-continuous in time as only a few seconds gap was missed each data processing and recording cycle. In practice, some

observations are missing due to insufficient signal-to-noise ratio of the doppler spectrum, or other problems such as contamination by reflections from aircraft. Also, there are occasional short gaps due to equipment malfunction. For the analyses of frequency spectra and the autocorrelation function given here a segment of data was not used at a given height if a gap longer than 10 minutes occurred.

### 3. STATISTICAL FEATURES OF THE VERTICAL VELOCITY

The fluctuations of vertical velocity at Flatland have the most energy at high frequencies, as can be seen in the frequency spectrum (Figure 1) which shows that most of the energy falls between about 10 and 30 minutes period. The coordinates in Figure 1 are area preserving, i.e., the variance in a given frequency band is proportional to the area under the curve. From comparisons with a model of a spectrum of gravity waves subjected to doppler shifting by horizontal winds, Van Zandt, et al. (1989), conclude that the observed spectrum of vertical velocity at Flatland is due mostly to gravity waves. This is in contrast to the spectra of vertical velocity at locations in or near mountains which show the effects of standing lee wave activity (Ecklund, et al., 1986; Gage and Nastrom, 1989).

Because a large portion of the variance at Flatland is due to relatively high frequency variations we should expect

that a relatively high sampling rate will be required to avoid large uncertainties in mean values computed from the observations. In Figure 1 we note that the peak variance is found at about 12 minutes period, and in order to avoid serious sampling problems we might expect that observations should be taken more often than about half this period, i.e., every 6 minutes or so. Another, more rigorous, estimate of the time between independent samples can be obtained from analysis of the autocorrelation function as discussed next.

Figure 2 shows the autocorrelation function,  $R(t)$ , at Flatland at 5 km for lags less than about 15 minutes and, for comparison, the  $R(t)$  functions at Poker Flat, Alaska, from Nastrom and Gage (1983).  $R(t)$  can be used to estimate the effective time between independent samples ( $T$ ) using the relation (Leith, 1973)

$$T = 2 \int_0^{\infty} R(t) dt \quad (1)$$

where  $t$  is the lag. An important application of  $T$  is in computing statistical significance levels (Mitchell, et al., 1966) from time series of observed data. Nastrom and Gage (1983) found that at Poker Flat  $T$  ranged from about 15

minutes for the curves labeled "winter 1" and "summer", which represent active periods, to about 9 minutes for the curve labeled "winter 2", which represents quiet periods. There were not enough cases to prepare a summer curve for quiet periods, and only the curve for active times is shown. The curve labeled "Flatland" was prepared by averaging the autocorrelation functions from each 6-hour period available. The data within each 6-hour period were linearly interpolated to 153-second intervals and residuals from a linear trend line fit by least squares were then used to compute  $R(t)$ . Note that the average curve at Flatland decreases more rapidly than all of the curves from Poker Flat, suggesting that the vertical velocity at Flatland has a relatively short "memory". The semi-logarithmic plots in Figure 2 show that an appropriate analytic model after about lag 5-minutes is  $R(t) = c \exp(-vt)$ , where  $v$  defines the rate of decrease. At shorter lags the observed curves fall above this model, suggesting that the observed autocorrelation function is a mixed first-order moving average, first-order autoregressive process as discussed in more detail by Nastrom and Gage (1983). Using (1) with this model of  $R(t)$  we estimate that  $T$  at Flatland is 5.1 minutes, which is less than the estimate for any of the curves at Poker Flat. Also, we note that this estimate (5.1 minutes) is near that of 6 minutes inferred above from Figure 1. This result does not mean that observations should be taken only each 5.1 minutes at Flatland, but rather that, on the

average, independent information is gained only at this rate. In fact, considerable uncertainty of the mean is found when only every-other observation is used (i.e., with data spaced about 5.1 minutes), as discussed next.

#### 4. EFFECTS OF SAMPLING STRATEGY ON MEAN VERTICAL VELOCITY

The analysis approach we will use will be to form averages over one-, two-, three-, and six-hour periods using the complete set of observations. These averages will be used as the standards for comparison. Next, the data set will be degraded to simulate various sampling strategies and the mean values thus obtained will be compared with the "true" mean values based on complete data. This procedure will give estimates of the uncertainty of measurement due to temporal sampling strategy. There are, of course, other sources of uncertainty, such as system limitations and the effects of spatial averaging, which might be important in practice and which are beyond the scope of this study.

Four schemes were used to illustrate the effects of a strategy which uses incomplete sampling. Three of them use one-half of the data but in varying sized segments: the first uses alternate observations, the second uses data for every-other 10 minutes, and the third uses data for every-other 30 minutes. Each of these could simulate a strategy applied in a field experiment where, for example, the radar

was used to gather vertical data half of the time and oblique data half of the time. The fourth strategy uses data for the first 12 minutes of each hour, similar to the observation cycle of the data used by Larsen, et al. (1988). The results from these strategies will be labeled "alt obs", "0-10 min", "0-30 min", and "12 min" in Figures 3 and 4 and in Table 1.

RMS differences between mean values based on these four sampling strategies and the "true" mean computed from all available data are given in Figure 3 as functions of averaging period. Two patterns are evident in Figure 3: first, the RMS differences decrease with increasing averaging time. This decrease is consistent with the notion that the degraded observation cycles are sufficient to resolve long-period variations reflected in the left-hand tail of the spectrum in Figure 1, and that the variance due to longer periods thus contributes to the uncertainty of the mean only for shorter averaging periods.

The second pattern seen in Figure 3 is that larger gaps between data samples lead to larger uncertainty of the estimates of the mean. This effect reflects the increased spectral leakage caused by longer gaps, an effect discussed by Baer and Tribbia (1976). They found that there is reduced spectral fidelity for all frequencies higher than the frequency corresponding to the longest gap in a data

sequence. The reduced spectral fidelity in the present context leads to greater uncertainty of the estimate of the mean value.

Finally, we note that the uncertainty of the estimate of the mean is relatively very large when only 12 minutes of data per hour are used. For a one-hour averaging period the RMS difference from the true mean is nearly  $9 \text{ cm s}^{-1}$  for this strategy, which is over half as large as the standard deviation of all data (about  $14 \text{ cm s}^{-1}$ ).

Other statistical quantities can be used to illustrate the patterns seen in Figure 3. For example, Figure 4 shows the mean deviation, defined as the average absolute value of the difference between the true mean and that from the various sampling strategies, in a format similar to Figure 3. The patterns are consistent with those in Figure 3, although the numerical values of this measure of uncertainty are only about two-thirds as large as the RMS values.

Another measure of the capability of one estimate of the mean to track the true mean is the linear correlation coefficient,  $r$ . Table 1 gives the values of  $r$  over  $N$  pairs of means with the true mean for the same averaging times and sampling strategies used in Figures 3 and 4. The percentage of variance in one variable explained by another is given by  $100 r^2$ . Applying the results in Table 1 shows that for all

averaging periods the strategy of using alternate 2.5-minute data intervals accounts for 90 percent or more of the variance of the true mean in all cases here, while using every-other 10-minute period accounts for over 80 percent of the variance for averaging periods of 2 hours or more. At the extreme, using only the first 12 minutes of each hour the estimates of the means account for less than 50 percent of the variance of the true mean except for the 6-hour averaging period. These results show that the uncertainty of estimates of the mean vertical velocity is minimized when the average length of gaps in the data is minimized.

## 5. CONCLUSIONS.

The following conclusions are based on analysis of vertical velocities measured by the Flatland MST radar during the spring of 1987:

1. The autocorrelation function of vertical velocity resembles that expected for a mixed first-order moving-average, first-order autoregressive process.

2. The average time between independent samples in the data from Flatland used here is about 5 minutes.

3. The uncertainty of the mean value of vertical velocity decreases as the averaging period used to compute the mean increases regardless of the sampling strategy used.

4. The uncertainty of the mean value of vertical velocity increases as the length of gaps in the data increases. Because of this effect, every effort should be made to minimize gaps in samples of vertical velocity in future field programs.

These results are concerned only with temporal sampling, and in practice other effects such as instrument errors may require attention. In particular, these results do not include any sampling uncertainties which might arise from spatial variability. It remains as a future experiment to compare averages from nearby stations as functions of averaging time, sampling strategy, and other variables to study such effects.

Acknowledgements. The Flatland Radar is a joint project of the National Science Foundation and the National Oceanic and Atmospheric Administration. One of us (GDN) was partially supported by the Air Force Office of Scientific Research.

## 5. REFERENCES.

Baer, F., and J. J. Tribbia, Spectral fidelity of gappy data, Tellus, 28, 215-227, 1976.

Balsley, B. B., W. L. Ecklund, D. A. Carter, A. C. Riddle and K. S. Gage, Average vertical motions in the tropical atmosphere observed by a radar wind profiler on Pohnpei (7°N Latitude, 157° Longitude), J. Atmos. Sci, 45, 396-405, 1988.

Cornish, C. R., Observations of vertical velocities in the tropical upper troposphere and lower stratosphere using the Arecibo 430-MHz radar, J. Geophys. Res, 93, 9419-9431, 1988.

Ecklund, W. L., K. S. Gage, G. D. Nastrom, and B. B. Balsley, A preliminary climatology of the spectrum of vertical velocity observed by clear-air doppler radar, J. Clim. Appl. Meteor., 25, 885-892, 1986.

Gage, K. S., and G. D. Nastrom, A simple model for the enhanced frequency spectrum of vertical velocity based on tilting of atmospheric layers by lee waves, Radio Sci., this issue, 1989.

Green, J. L., K. S. Gage, T. E. Van Zandt, W. L. Clark, J. M. Warnock, and G. D. Nastrom, Observations of vertical velocity over Illinois by the Flatland radar, Geophys. Res. Lett., 15,269-272, 1988.

Larsen, M. F., J. Rottger, and T. S. Dennis, A comparison of operational analysis and VHF wind profiler vertical velocities, Mon. Wea. Rev., 48-59, 1988.

Leith, C., The standard error of time-average estimates of climatic means, J. Appl. Meteor., 12, 1066-1069, 1973.

Mitchell, J. M., Jr., B. Dzerdzevskii, H. Flohn, W. L. Hofmeyr, H. H. Lamb, K. N. Rao, and C. C. Wallen, Climatic Change, WMO Technical Note No. 79, Secretariat of the WMO, Geneva, 79 pp, 1966.

Nastrom, G. D., and K. S. Gage, A brief climatology of vertical air motions from MST radar data at Poker Flat, Alaska, Preprints, 21st Conf. on Radar Meteorology, Edmonton, 135-140, Am. Meteor. Soc., Boston, 1983.

Nastrom, G. D., W. L. Ecklund, and K. S. Gage, Direct measurement of large-scale vertical velocities using clear-air doppler radars, Mon. Wea. Rev., 113, 708-718, 1985.

Strauch, R. G., B. L. Weber, A. S. Frisch, C. G. Little, D. A. Merritt, K. P. Moran, and D. C. Welsh, The precision and relative accuracy of profiler wind measurements, J. Atmos. Ocean. Tech., 4, 563-571, 1987.

VanZandt, T.E., G.D. Nastrom, J.L. Green, and K.S. Gage, The spectrum of vertical velocity from Flatland Radar Observations. Preprints, 24th Conference on Radar Meteorology, American Meteorological Society, Tallahassee, March 27-31, 1989.

Table 1. Correlation of mean values from different sampling strategies with the "true" mean value.

AVERAGING PERIOD	1 hr	2 hrs	3 hrs	6 hrs
N	1951	652	652	308
ALT OBS	0.94	0.95	0.96	0.97
0-10 MIN	0.87	0.90	0.91	0.94
0-30 MIN	0.82	0.86	0.88	0.90
12 MIN	0.62	0.68	0.73	0.80

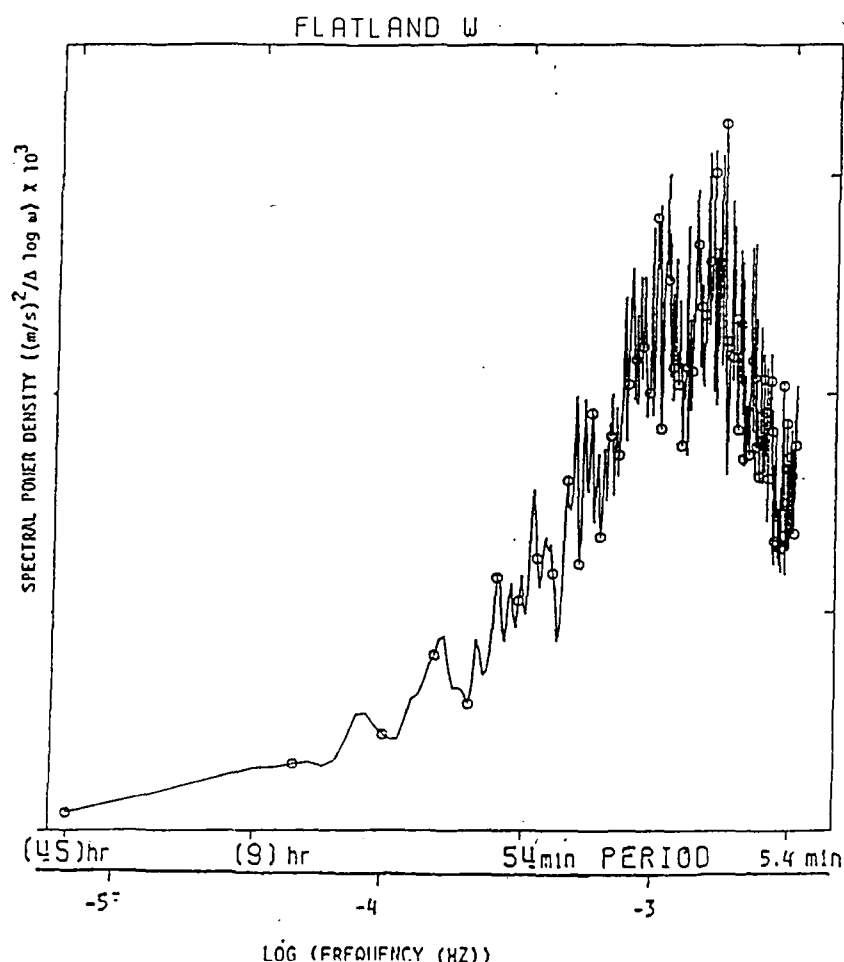


Figure 1. Average of 34 spectra of vertical velocity over 48-hour data periods at Flatland during March through September, 1987, in area preserving coordinates.

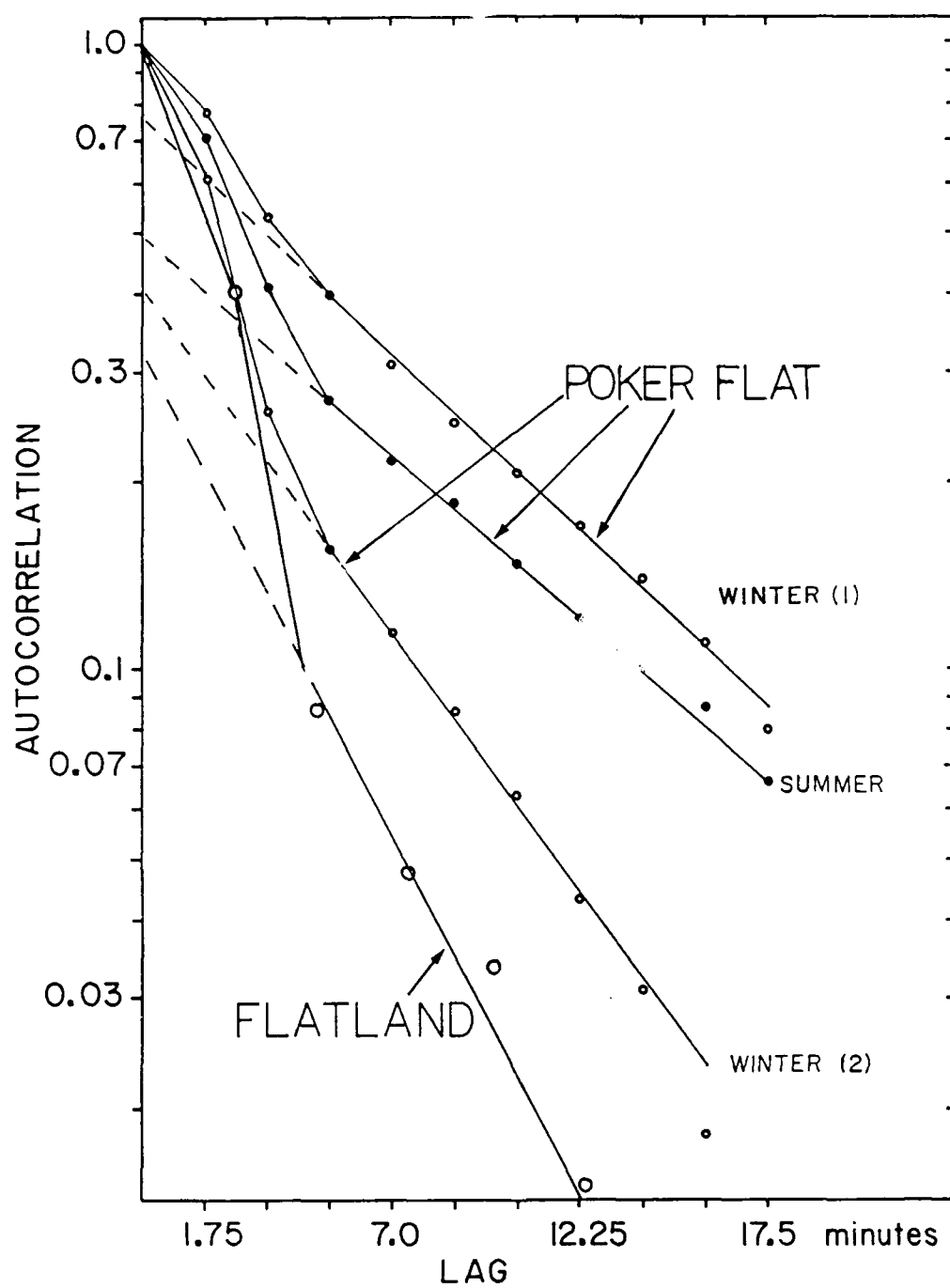


Figure 2. Autocorrelation function of vertical velocity at Flatland and at Poker Flat. See text.

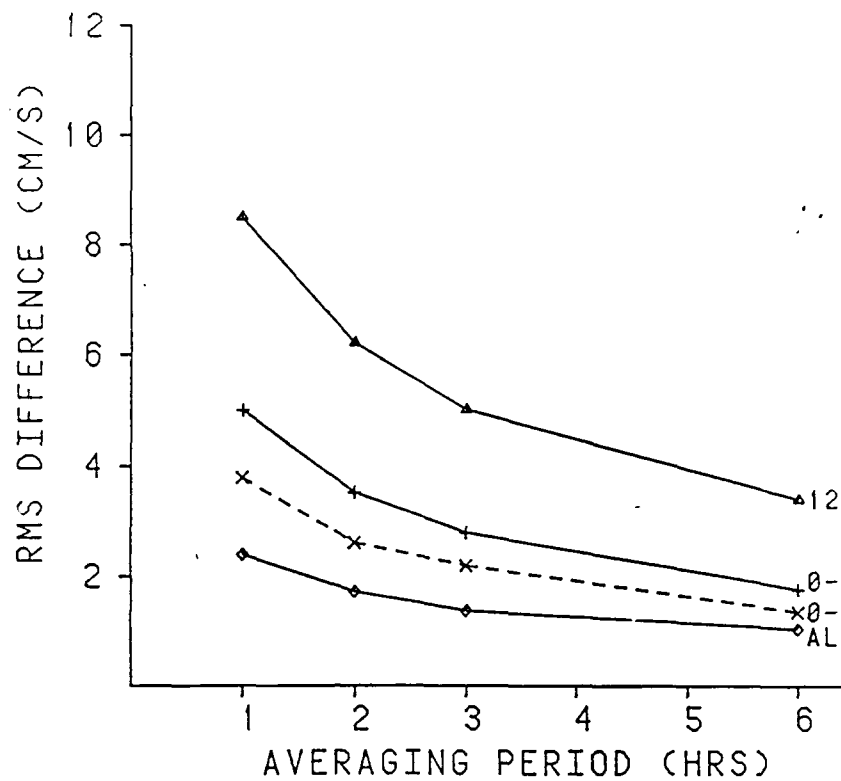


Figure 3. RMS difference of mean vertical velocity as a function of averaging time for various sampling strategies from the mean based on complete data.

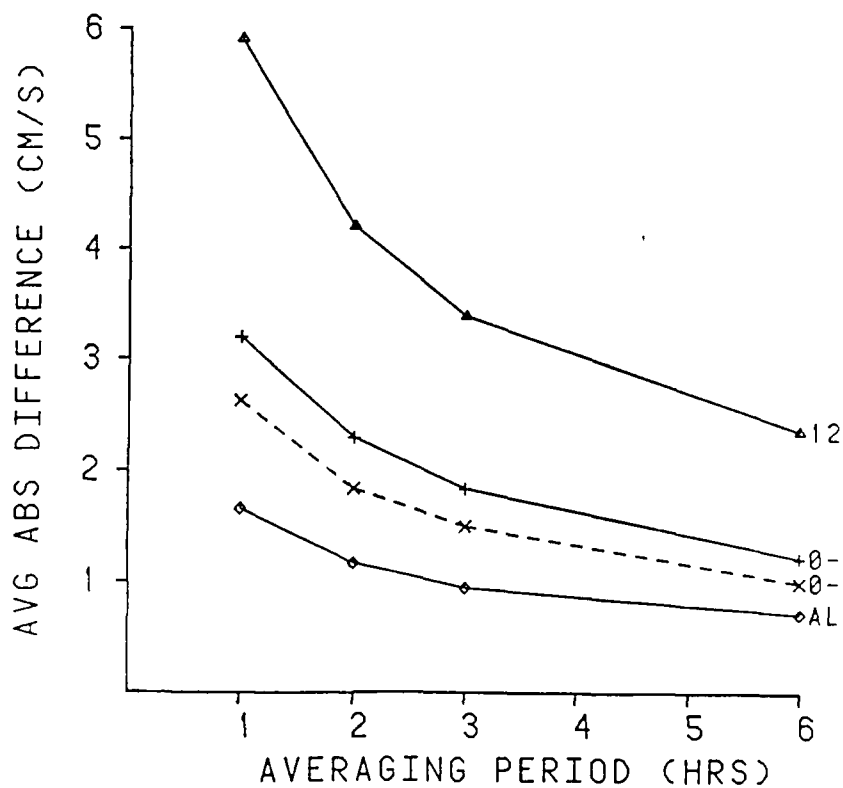


Figure 4. As in Figure 3, except for the mean deviation, i.e., the average absolute value of the differences in the means.

5.4.1 COMPARISON AMONG CLEAR-AIR RADAR, THERMOSONDE AND OPTICAL MEASUREMENTS  
AND MODEL ESTIMATES OF  $C_n^2$  MADE IN VERY FLAT TERRAIN OVER ILLINOIS

J.M. Warnock<sup>1</sup>, R.R. Beland<sup>2</sup>, J.H. Brown<sup>2</sup>, W.L. Clark<sup>1</sup>, F.D. Eaton<sup>3</sup>,  
L.D. Favier<sup>3</sup>, K.S. Gage<sup>1</sup>, J.L. Green<sup>1</sup>, W.H. Hatch<sup>3</sup>, J.R. Hines<sup>3</sup>,  
E.A. Murphy<sup>2</sup>, G.D. Nastrom<sup>4</sup>, W.A. Peterson<sup>3</sup>, and T.E. VanZandt<sup>1</sup>

<sup>1</sup>Aeronomy Laboratory  
National Oceanic and Atmospheric Administration/ERL  
Boulder, CO 80303

<sup>2</sup>Air Force Geophysics Laboratory  
Hanscom Air Force Base  
Bedford, MA 01731

<sup>3</sup>Atmospheric Science Laboratory  
White Sands Missile Range, NM 88002

<sup>4</sup>Department of Earth Sciences  
St. Cloud State University  
St. Cloud, MN 56301

INTRODUCTION

An experimental campaign was conducted in June 1988 at the Flatland VHF clear-air Doppler Radar site, which is located in very flat terrain far removed from mountains near Champaign-Urbana, Illinois, to measure height profiles of the refractivity turbulence structure parameter  $C_n^2$  and related turbulent parameters. Three different techniques were used<sup>n</sup> to measure profiles of  $C_n^2$ : the Flatland radar (GREEN et al., 1988), a stellar scintillometer (OCHS et al., 1977), and thermosonde balloon flights (BROWN et al., 1982). Both the radar and scintillometer measured  $C_n^2$  remotely by sensing the effect of the fluctuations of refractive index on the propagation of electromagnetic waves. At radio wavelengths the humidity and its gradient as well as the temperature gradients contribute significantly to the refractive index, whereas at optical wavelengths only the temperature fluctuations are important. In contrast to the remote sensors, the thermosonde measures the temperature fluctuations directly by measuring the RMS temperature difference between two very fast temperature sensors separated by a meter. The balloon instrument also made measurements of the height profile of the standard thermodynamic parameters (pressure, temperature, and humidity), plus wind speed and direction. Model estimates of  $C_n^2$  were calculated from the thermodynamic and wind measurements using the numerical methods described by WARNOCK AND VANZANDT (1980). In addition, optical measurements were made of the transverse coherence length (EATON et al., 1988), and of the isoplanatic angle (EATON et al., 1985). Both these parameters depend on a weighted integrated value of  $C_n^2$  through the atmosphere.

Comparisons among these measurements taken simultaneously in simple topography provide a unique opportunity to compare these different measurement techniques and to contrast these measurements with previous comparisons made in rough terrain (e.g., GOOD et al., 1982; GREEN et al., 1984; EATON et al., 1988). In this paper we present some preliminary results, which emphasize the radar measurements.

## EXPERIMENTAL SET UP

### Thermosonde System

The thermosonde system consisted of two parts, which were mounted below an ascending balloon (BROWN et al., 1982). One part was a standard VIZ digital microsonde, the other was a micro-thermo bridge thermosonde linked to the microsonde. The thermosonde measured the RMS temperature fluctuations between two unheated fine wire tungsten probes separated horizontally by one meter. The noise level of the instrument is about  $0.002^{\circ}\text{C}$ , and the data were recorded every four seconds giving about a 20-meter height resolution. The microsonde makes excellent height-resolution measurements of the standard thermodynamic parameters (pressure, temperature, and relative humidity), and wind speed and direction. The thermodynamic data were recorded every four seconds, which gave about a 20 m height resolution. The wind speed and direction were determined by using the Loran-C navigator system, and the data were recorded every ten seconds, which gave about a 50 m height resolution. A 1200-gram meteorological balloon was used to lift the instrument package with an ascent rate of about 5 m/s. The package was suspended from 90 to 180 meters below the balloon to ensure that the turbulent wake from the two meter balloon did not affect the measurements.

### Flatland Radar

The Flatland radar (GREEN et al., 1988) is located about 8 km west of the Champaign-Urbana Airport [ $40.05^{\circ}\text{N}$ ,  $88.38^{\circ}\text{E}$ , 212 m above mean sea level (MSL)]. This clear-air Doppler radar (also called wind profiler or ST radar) operates at a frequency of 49.8 MHz (6.02 m wavelength), with peak and average power of about 10 kw and 150 watts, respectively. The pulse length and the range resolution are selectable from 150 to 2400 m. All the data reported in this paper were taken with a pulse length of 1.5 km and over-sampled with a range resolution of 750 m. In this experiment, the antenna beam was tilted twenty degrees off the vertical toward the east or south directions. With this tilt angle, echoes due to specular scattering were essentially eliminated, so that unambiguous  $C_n^2$  measurements were obtained.

### Optical Systems

Three optical systems were used in this study: a stellar scintillometer, an isoplanometer (EATON et al., 1985), and a transverse coherence length system (EATON et al., 1988). The isoplanometer measures the isoplanatic angle  $\theta_o$ , which is the maximum angular extent of an extended object that can be viewed through turbulence, and the transverse coherence system measures the transverse coherence length  $r_o$ , which is related to the spread of a star image due to turbulence. The scintillometer, described below, measures a height profile of  $C_n^2$ , whereas both the isoplanometer and transverse coherence systems measure an optical quantity which is related to the weighted integrated value of  $C_n^2$  through the atmosphere, i.e.,  $\theta_o$  (radians) and  $r_o$  (meters) are

$$\theta_o = 0.528 \left[ k^2 \int_0^{\infty} C_n^2(z) z^{5/3} dz \right]^{-3/5}$$

$$r_o = 2.1 \left[ 1.46 k^2 \int_0^{\infty} C_n^2(z) dz \right]^{-3/5}$$

where  $k$  is the wavenumber of the light and  $z$  is the height above ground.

## Stellar Scintillometer Model II

The stellar scintillometer Model II was developed by the Wave Propagation Laboratory of NOAA (OCHS et al., 1977). To operate the system, a star of second magnitude or brighter and within  $45^\circ$  of the zenith is selected. The system is sensitive to spatial wavelengths ranging from 5 to 15 cm, and measures seven different height regions of optical turbulence ranging from 2.2 to 18.5 km above ground level (AGL). The height weighting functions for these seven heights are broad, and are broadest at the highest altitudes.

## Surface Measurements

An instrumented tower was installed near the telescope domes. In addition to the standard meteorological measurements, the temperature structure parameters  $C_T^2$  and the solar radiation were measured. The temperature, dew point temperature, wind speed and direction, and  $C_T^2$  measurements were made at both one and four meters above the surface, and the pressure and solar radiation were each measured at one height, one and four meters, respectively.

## Model Estimates of $C_n^2$

Model calculations of  $C_n^2$  were made from the microsonde upper air data; i.e., pressure, temperature, humidity, and wind speed and direction. The basic model concepts are given by VANZANDT et al. (1981). Since then, the model has been extended and revised considerably. We used the latest version described by WARNOCK et al. (1985), and used the numerical techniques described by WARNOCK AND VANZANDT (1985), to evaluate the model estimates. To compare the model estimates with results from previous comparisons with the Sunset and Stapleton radars, which are located in and near the mountains, respectively (WARNOCK et al. 1986; 1988), we used identical values of all the model parameters and constants except one: the constant in the equation giving the distribution of wind shear. This parameter quantifies the shear environment in the range of scales important in the onset of turbulence flow; therefore, the evaluation of this parameter allows the shear environment at these scales above the Flatland radar to be contrasted with its value above rough terrain.

## Description of Campaign

This experimental campaign was conducted at the Flatland radar site from 6 to 15 June 1988. The scintillometer and isoplanometer systems shared a single telescope; the scintillometer operated at night and the isoplanometer operated during the day and in twilight. Thermosonde balloon launches were usually made after noontime and before midnight local time. A typical schedule was to launch a few packages in the afternoon and a few after dark. The radar operated during clear and cloudy conditions, whereas the optical systems operated during clear sky conditions. The optical telescopes were located about forty meters northeast of the center of the radar antenna, and the thermosonde launch site was about sixty meters east of the antenna center.

## PRELIMINARY RESULTS

Measurements made by both the radar and scintillometer remote sensors are average values over both time and space. Five-minute data averages were used in this paper by both systems, and the height profiles measured by both systems are relatively smooth. In contrast, each thermosonde in situ measurement is an average over four seconds, which gives about a 20-meter height resolution. The four-second thermosonde data displays many very thin large peaks in  $C_n^2$ . *(Large peaks)* Frequently, the measured  $C_n^2$  values fall to the observing noise level. Thus, to compare the thermosonde profile with the others we smoothed the thermosonde data. We used a Gaussian filter with  $\sigma = 0.5$  km and truncated the filter at  $\pm 2.5 \sigma$ .

Figures 1 through 3 show height profiles of the  $C^2$  measurements from the radar, thermosonde, and scintillometer together with two model estimate profiles. All the radar data used in this preliminary study were taken with the antenna pointed  $20^\circ$  towards the east. The thermosonde and model profiles have been smoothed with the same Gaussian filter. One model profile gives the total  $C^2$  including the humidity terms; this model, called model (radar), is compared to the radar data. The other model, called model (dry), omits the humidity terms; it is compared to the scintillometer and thermosonde profiles. Note that the dry and radar model profiles merge together at about ten km and are identical at higher altitudes.

Figure 1 shows the first example in this data set that has data from all three instruments. Recall that the thermosonde, scintillometer, and dry model profiles form one set of profiles, and that these three profiles are to be compared with each other; whereas the radar and radar model are a separate set of profiles. The agreement among the profile in each set is very good to excellent. The radar data are on the model (radar) curve except for the lowest point at 4.85 km; at that height the model (radar) is smaller than radar measurement. The next example, shown in Figure 2, is a daytime example, so there are no scintillometer data. Figure 3 shows the next nighttime example. In both cases the model (radar) is smaller than the radar data for the lowest two to three range gates. The data from the other range gates fit the model (radar) well.

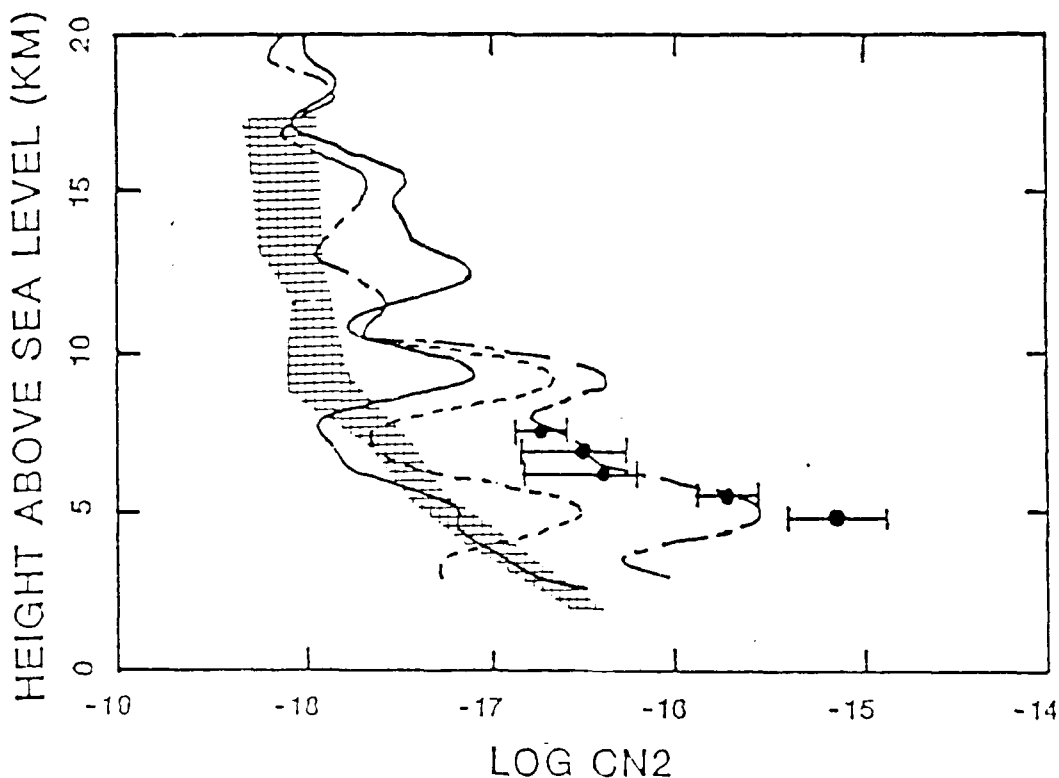


Figure 1. Height profile of  $\text{Log } C^2$  for 02-03 hours, 8 June 1988 UT. The large solid dot is the median of the radar data for the hour, and the horizontal bars give the extreme values of the radar measurements for the hour. The solid line is the thermosonde profile; the balloon was launched at 02:04 UT. The hatched area gives the range of scintillometer measurements over the hour. The long-short dashed line is the model (radar) profile, and the dashed line is model (dry), which is to be compared with the thermosonde and scintillometer profiles.

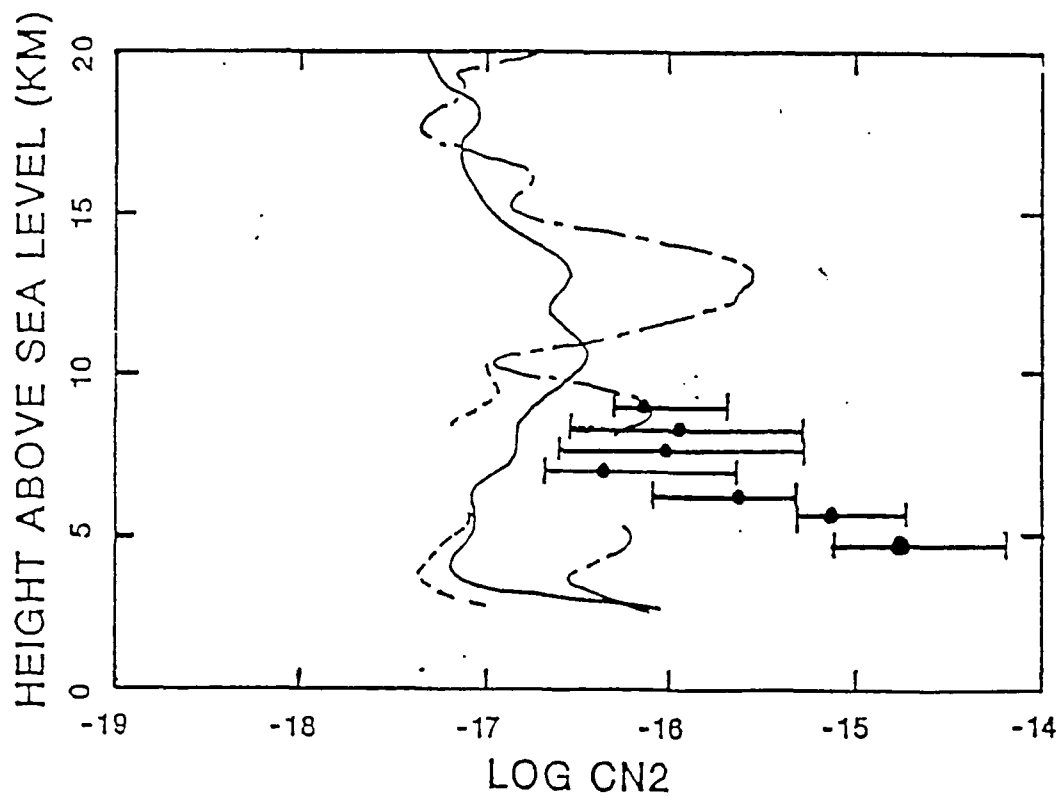


Figure 2. Same as for Figure 1 except for 18-19 hours, 10 June 1988 UT; the thermosonde balloon was launched at 17:12 UT. Because this was a daytime flight, there are no scintillometer data.

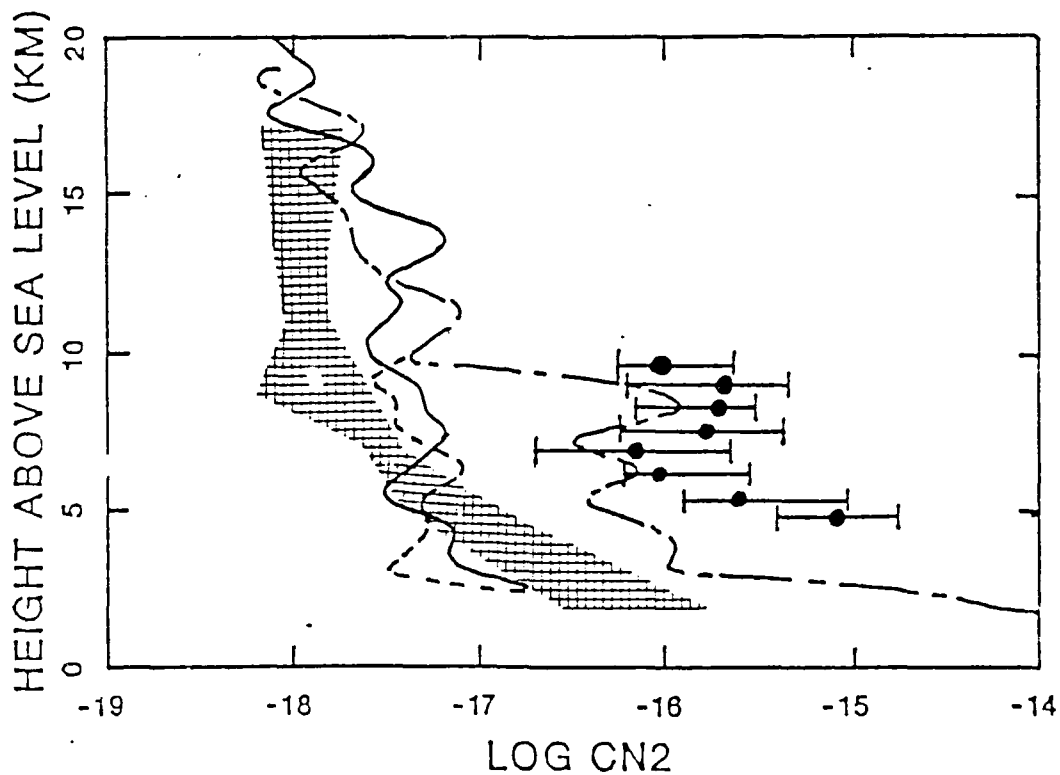


Figure 3. Same as for Figure 1 except for 00-01 hours, 11 June 1988 UT; the balloon was launched at 00:44 UT.

Figure 2 is not a typical example of the thermosonde measurements made during the day. For flights later in the afternoon, the thermosonde data were much larger than the nighttime measurements. This day/night effect is not yet understood.

All observational methods used in this study make several fundamental assumptions to derive a  $C_n^2$  value from the raw data. The most important assumption is that the mixing is due to turbulent flows, and, further, that the turbulent flows are homogeneous and isotropic and that the observing scales are in the inertial subrange. Since the measurements and model estimates used in this preliminary study are generally consistent, these simplifying assumptions and analysis in terms of the  $C_n^2$  structure parameter are generally useful. The relative importance of convective mixing, viscous damping at scales smaller than the inner scale, and anisotropic turbulent fluctuations will require further research.

#### SUMMARY AND CONCLUSIONS

An experimental campaign was conducted at the Flatland clear-air VHF radar site located near Champaign-Urbana, Illinois, in June 1988 to measure height profiles of the refractivity turbulence structure parameter  $C_n^2$  and related turbulent parameters. This Flatland site was chosen because it is located in very flat terrain far removed from mountains, so that orographic effects are minimized. Three different techniques were used to measure the height profiles of  $C_n^2$ . The 50 MHz clear-air Doppler Flatland radar and a stellar scintillometer measured the profile remotely, and high resolution in situ measurements of  $C_n^2$  were obtained from over 20 thermosonde balloon flight. The balloon instruments also measured the standard thermodynamic and wind data with excellent height resolution.

Model estimates were calculated from the standard balloon data and compared with the measurements. Because the radar measurements are sensitive to humidity and its gradient, whereas the thermosonde and scintillometer are not, two model profiles were calculated. One model profile included the humidity terms, called model (radar), and the other, called model (dry), did not.

During the nighttime, all the measurements and model profiles are generally consistent. There are two exceptions that occur systematically through the data set. One difference is that the model (radar) values of  $C_n^2$  near five kilometers are consistently lower than the values measured by the radar. Another difference is that the scintillometer measurements at about 14 km are always smaller than the thermosonde and model estimates, and are near the instrumental noise level.

In all the nighttime cases, identical values of all the model parameters and constants were used in the model calculations. Furthermore, these values were identical to those used in previous studies using the Sunset and Stapleton radars except for one very important parameter. This parameter is the constant in the distribution function of wind shears. Its value at Sunset and Stapleton was 50% greater than its value at Flatland. This suggests that the wind shears at scales of the fine structure are smaller over Flatland than over mountainous terrain.

#### ACKNOWLEDGMENTS

This work was partially supported by the National Science Foundation under grant ATM-89512513.

## REFERENCES

- Brown, J.H., R.E. Good, P.M. Bench, and G.E. Faucher (1982), Sonde experiments for comparative measurements of optical turbulence, AFGL-TR-82-0079, AD-All8740, Air Force Geophysics Laboratory, Hanscom Air Force Base, MA.
- Eaton, F.D., W.A. Peterson, J.R. Hines, and G. Fernandez (1985), Isoplanatic angle direct measurements and associated atmospheric conditions, Appl. Opt., 24, 3264-3273.
- Eaton, F.D., W.A. Peterson, J.R. Hines, K.R. Peterman, R.E. Good, R.R. Beland, and J.H. Brown (1988), Comparisons of VHF radar, optical and temperature fluctuation measurement of  $C_n^2$ ,  $r_o$ , and  $\theta_o$ , Theor. Appl. Climatol., 39, 17-29.
- Good, R.E., B.J. Watkins, A.F. Quesada, J.H. Brown, and G.B. Lorient (1982), Radar and optical measurements of  $C_n^2$ , Appl. Opt., 21, 3373-3376.
- Green, J.L., J. Vernin, T.E. VanZandt, W.L. Clark, and J.M. Warnock (1984), A comparison of optical and radar measurements of  $C_n^2$  height profiles, Preprint volume, 22nd Conf. on Radar Meteorol., Sept. 10-13, Zurich, Switzerland, 470-475.
- Green, J.L., K.S. Gage, T.E. VanZandt, W.L. Clark, J.M. Warnock, and G.D. Nastrom (1988), Observations of vertical velocity over Illinois by the Flatland radar, Geophys. Res. Lett., 15, 269-272.
- Ochs, G.R., T.-I. Wang, and T. Merrem (1977), Stellar scintillometer Model II for measurement of refractive-turbulence profiles, NOAA Tech. Memo ERL WPL-25.
- VanZandt, T.E., K.S. Gage, and J.M. Warnock (1981), An improved model for the calculation of profiles of  $C_n^2$  and  $\epsilon$  in the free atmosphere from background profiles of wind, temperature, and humidity. Preprint volume, 20th Conf. on Radar Meteorol., Nov. 30-Dec. 3, Boston, MA, 129-135.
- Warnock, J.M., and T.E. VanZandt (1985), A statistical model to estimate the refractivity turbulence structure constant  $C_n^2$  in the free atmosphere, NOAA Tech. Memo ERL AL-10.
- Warnock, J.M., T.E. VanZandt, and J.L. Green (1985), A statistical model to estimate mean values of parameters of turbulence in the free atmosphere. Preprint volume, 7th Symp. on Turbulence and Diffusion, Nov. 12-15, Boulder, CO, 156-159.
- Warnock, J.M., J.L. Green, and W.L. Clark (1986), Study of  $C_n^2$  and its variability measured by the Sunset clear-air : Preprint volume, 23rd Conf. on Radar Meteorol., Sept. 22-26, Snowmass, CO, 34-37.
- Warnock, J.M., N. Sengupta, and R.G. Strauch (1988), Comparison between height profiles of  $C_n^2$  measured by the Stapleton UHF clear-air Doppler radar and model calculations. Preprint volume, 8th Symp. on Turbulence and Diffusion, Apr. 26-29, San Diego, CA, 267-270.

# VHF Radar Measurements of the Vertical Momentum Flux

G. D. Nastrom

Control Data Corporation  
Minneapolis, MN 55440

and

J. L. Green

Aeronomy Laboratory, National Oceanic and Atmospheric Administration  
Boulder, CO 80303

## 1. INTRODUCTION

The capability of ST radars to provide direct measurements of the momentum flux presents an opportunity for major advances in atmospheric science. Some of the issues, needs, and techniques surrounding the measurement of momentum flux are discussed by Fritts (1984) and Schoeberl (1984), among others. The vertical momentum flux was first measured using the two-beam technique by Vincent and Reid (1983), who used mesospheric observations. They also presented the body force due to the vertical divergence of the vertical momentum flux. Cornish and Larsen (1984) examined the vertical momentum flux at 14.5 km over Arecibo, but did not look into the momentum flux divergence. It appears that no other results from the troposphere and stratosphere are available.

The purpose of this paper is to present preliminary results of momentum flux and momentum flux divergence calculations made using data from the Sunset radar. In an attempt to illustrate changing conditions, we present results from a day when the background wind speeds aloft changed abruptly. The results given here are examples taken from a more complete study of momentum flux values under a variety of synoptic weather conditions.

## 2. DATA AND METHOD

The Sunset Radar (Green, et al., 1985) is located in a narrow mountain canyon 15 km west of Boulder, Colorado, and is just east of the continental divide. The array antenna of this VHF (ST) pulsed Doppler radar can be steered in the east-west or north-south vertical plane. During the experiment reported here, five antenna beam positions were used: vertical and 15° to the east, west, north, and south. Three consecutive observations were

made at each beam position at 90-second intervals and then the beam was moved. A full cycle could thus be made each 20 minutes. The relative locations of the radar volumes are illustrated in Figure 1.

The synoptic situation early in the day chosen, January 28, 1985, was characterized by light winds throughout the height region sampled by the radar (from about 4 to 14 km). After about 15 UT a weak jet stream moved over Sunset with winds at 10 km over the radar increasing from 10 ms<sup>-1</sup> to over 30 ms<sup>-1</sup> by 18 UT. Winds at all levels above 4 km were primarily from the west; surface wind data were not available.

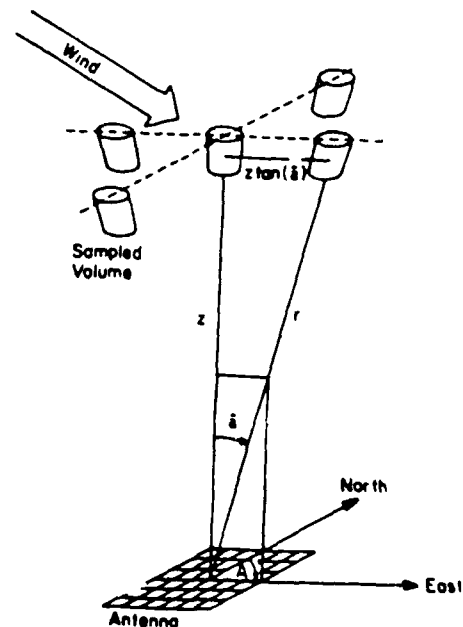


Figure 1. Schematic depiction of the radar beams positions at Sunset.

The upper air soundings at Denver, about 50 km southeast, show the tropopause rose from about 9 km to 10 km through the day. A strong inversion which was present in the lower troposphere, near 650 mb, early in the period dissipated after 1200 UT. Further, the temperature profile in the lower stratosphere late in the period was characterized by wave-like perturbations.

The method of Vincent and Reid (1983) was used for this calculation. The vertical momentum flux,  $\overline{u'w'}$  or  $\overline{v'w'}$ , is found from

$$\overline{u'w'}(z) = [\overline{V^2(\hat{a}, R)} - \overline{V^2(-\hat{a}, R)}] / (2 \sin 2\hat{a})$$

where  $V$  is the radial velocity,  $\hat{a}$  is the antenna beam angle,  $R$  is the range and  $z$  is the altitude. Altitudes from 4 to 14 km were sampled at 1 km intervals. Decreasing signal-to-noise sometimes rendered the upper level useless. The calculation was made at a given height only if all beam positions were sampled every cycle during a full hour. Averaging periods of one hour and three hours were used; the results are similar except that the three-hourly values are obviously smoothed, thus, we have chosen to present the one-hour results in order to capture as much detail of the effects of transients as possible.

### 3.0 RESULTS

Figure 2 shows the hourly momentum flux from 00-18 UT. Values for the meridional component ( $\overline{v'w'}$ ) are typically a few tens of  $\text{cm}^2/\text{s}^2$  from about 00-09 UT, and then increase in magnitude to on the order of one  $\text{m}^2/\text{s}^2$  after 09 UT. The most notable event is found below 5 km at 10-12 UT, when  $\overline{v'w'}$  reached over  $-20 \text{ m}^2/\text{s}^2$ . The values for the zonal component ( $\overline{u'w'}$ ) are usually less than a few  $\text{m}^2/\text{s}^2$  before 09 UT, although a few magnitudes exceed 10  $\text{m}^2/\text{s}^2$ . These results can be compared with the aircraft measurements given by Lilly and Kennedy (1973). They report

horizontally averaged momentum flux values of about 8 dynes/ $\text{cm}^2$  (which corresponds with 2  $\text{m}^2/\text{s}^2$  for mean density of  $5 \times 10^{-4} \text{ gcm}^{-3}$ ); although their traces of integrated momentum flux show large variability, indicating local values range far from the mean. At 10-12 UT a maximum

is found in  $\overline{u'w'}$  at the same location where a minimum was found in  $\overline{v'w'}$ .

After 12 UT the values of  $\overline{u'w'}$  generally exceed 10  $\text{m}^2/\text{s}^2$  above 8 km, with a local minimum found at 11 km at 18 UT.

Figure 3 shows the vertical flux divergence of meridional and zonal momentum. These results were computed from the data in Figure 2 by taking differences across layers 1 km apart. No smoothing has been applied in an effort to preserve as much detail in the results as possible. The units used,  $10^{-3} \text{ ms}^{-2}$ , correspond to 3.6 m/s/hour (e.g., the contour labelled  $10 \times 10^{-3} \text{ ms}^{-2}$  is the same as 36 m/s/hour). In Figure 3, large values of zonal and meridional momentum flux divergence occur near 6 km at 10-12 UT. Otherwise, the meridional values are nearly all less than about 3 units. Alternating periods of large zonal values are found above 10 km at 14-18 UT. After about 11 UT the contours of zero zonal momentum flux divergence slope upward to the right, while at the same time the contours of zero meridional flux slope downward to the right. The significance of this pattern, if any, is not yet clear.

### 4. CONCLUSION

We have presented preliminary results of the momentum flux and flux divergence during a transient episode, as a jet stream moved over the radar. The zonal and meridional momentum flux and flux divergences displayed remarkable continuity with altitude in time, increasing in intensity as lee waves and other gravity wave activity developed while the jet stream approached. The momentum flux values observed compare favorably with aircraft measurements made over similar topography, at least during the early part

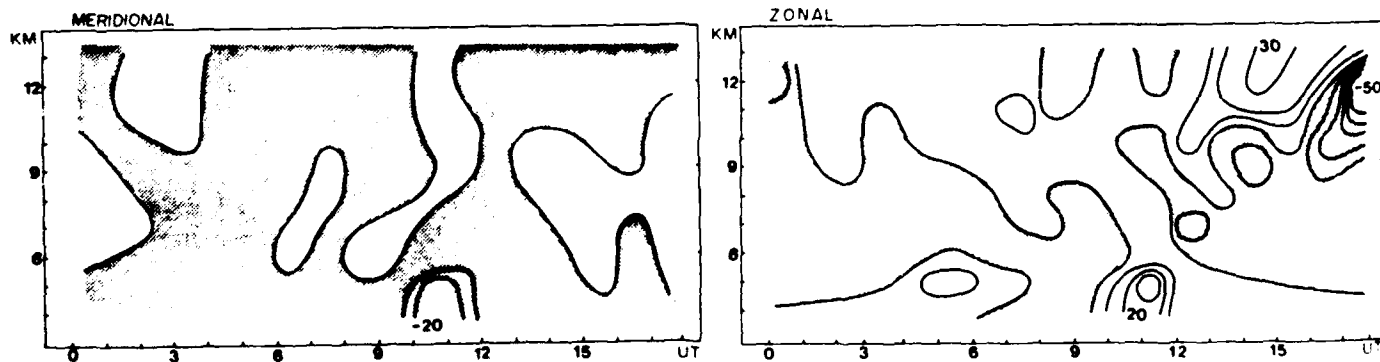


Figure 2. Time-height section of the vertical momentum flux at Sunset on January 28, 1985. Units:  $\text{m}^2/\text{s}^2$ . (a) meridional (b) zonal.

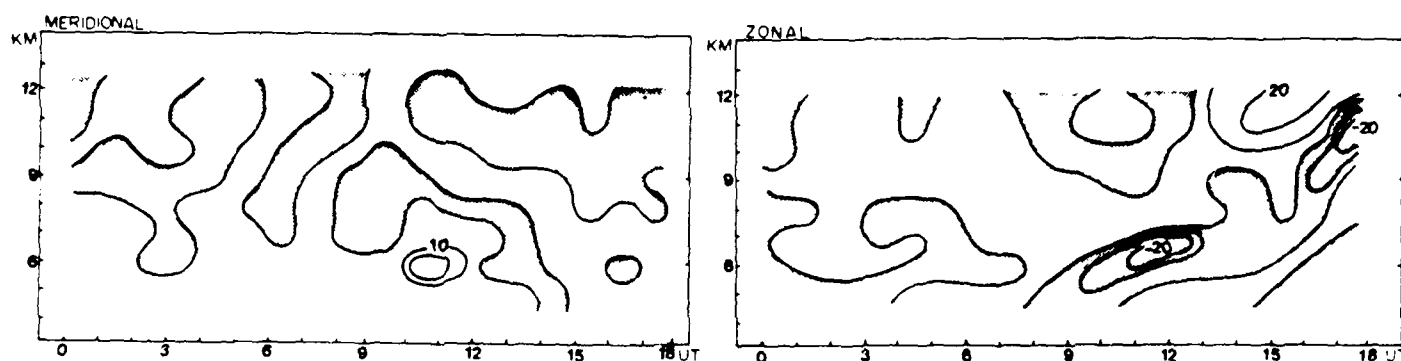


Figure 3. Time-height section of the vertical divergence of the vertical momentum flux at Sunset on January 28, 1985. Units:  $10^{-3} \text{ m/s}^2$ . (a) meridional (b) zonal.

of the day. The accelerations due to the momentum flux divergence seem rather large at first glance, especially for the late part of the day. However, we note that there may be compensating forces due to effects not considered here, such as transverse circulations or, likely more important, scales of motion too small to be resolved by these data.

#### REFERENCES

- Cornish, C.R., and M.F. Larsen, 1984: Use of the VAD technique and measurements of momentum flux in the stratosphere at Arecibo, Handbook for MAP, vol. 14, 208-210.
- Fritts, D.C., 1984: Momentum flux measurements; techniques and needs. Handbook for MAP, vol. 14, 216-218.
- Green, J.L., J.M. Warnock, W.L. Clark and T.E. VanZandt, 1986: Recent results at the Sunset Radar. Handbook for MAP, vol. 20.
- Lilly, D.K., and P.J. Kennedy, 1973: Observations of a stationary mountain wave and its associated momentum flux and energy dissipation: J. Atmos. Sci., 30, 1135-1152.
- Schoeberl, M.R., 1984: Techniques for the study of gravity waves and turbulence, Handbook for MAP, vol. 14, 179-182.
- Vincent, R.A., and I.M. Reid, 1983: HF Doppler measurements of mesospheric gravity wave momentum fluxes. J. Atmos. Sci., 40, 1321-1333.

FURTHER DISCUSSION OF THE DYNAMICAL PROCESSES THAT CONTRIBUTE TO THE  
SPECTRUM OF MESOSCALE ATMOSPHERIC MOTIONS

K. S. Gage

Aeronomy Laboratory  
National Oceanic and Atmospheric Administration  
Boulder, Colorado 80303

G. D. Nastrom

Control Data Corporation  
Minneapolis, Minnesota 55440

1. INTRODUCTION

In recent years much progress has been made in determining the spectrum of mesoscale atmospheric motions. The frequency spectra of vertical and horizontal velocities have been determined in the free atmosphere by means of the nearly continuous measurement of radial velocity by wind-profiling Doppler radar (Balsley and Carter, 1982; Gage and Nastrom, 1985; Ecklund et al., 1986). In addition, wind measurements by commercial aircraft collected during the NASA Global Atmospheric Sampling Program (GASP) have been analyzed to yield wavenumber spectra in the upper troposphere and lower stratosphere that cover scales ranging from a few km to 10,000 km (Nastrom and Gage, 1985).

The synthesis of the observed atmospheric spectra into a dynamical framework has proceeded along several lines. Two conceptual models have been proposed to explain the nature of the spectra. The first is analogous to the Garrett-Munk spectrum of internal waves in the ocean. The second relies on a combination of the internal wave spectrum and a spectrum of quasi-horizontal motions presumably associated with the vorticity bearing mode of fluid motions. This vortical mode possesses vertical variation and is often referred to as quasi-two-dimensional or stratified turbulence. In the following sections we shall briefly review the current status of these two competing models of mesoscale atmospheric spectra and present some new results of an analysis of the dependence of frequency spectra of horizontal velocity upon background wind speed that may provide a basis for evaluating the relative contributions of waves and turbulence to the spectrum of horizontal motions in the atmosphere.

2. BACKGROUND

The idea that the spectrum of mesoscale atmospheric motions might be due to an incoherent spectrum of internal wave motions analogous to the Garrett-Munk spectrum in the ocean appears to have originated with the work of Dewan (1979) and VanZandt (1982). VanZandt examined the observed atmospheric spectra of horizontal motions and showed that it was possible to construct a universal model of the atmospheric spectrum in the spirit of Garrett-Munk that fit the atmospheric observations quite well. However, since little information was available at the time on the

magnitude and shape of the spectrum of atmospheric vertical motions, the VanZandt model did not take them into account. Subsequently, as summarized in Ecklund et al. (1986), it now appears that a rather flat, nearly universal spectrum of vertical velocity exists in the atmosphere at least under light wind conditions. The possibility that this vertical velocity spectrum is nearly universal has been reinforced by recent results of the Flatland radar (Green et al., 1988) that show that in the absence of significant orography flat vertical velocity frequency spectra are obtained under a wide range of atmospheric conditions. However, the magnitude of this observed vertical velocity spectrum is not consistent with the VanZandt (1982) model spectrum as was pointed out by Gage and Nastrom (1985).

The original VanZandt model spectrum was normalized to fit the observed atmospheric horizontal velocity spectrum. If the observed vertical velocity spectrum is assumed to be an internal wave spectrum, it is possible to calculate the horizontal velocity spectrum of internal waves by employing the polarization relations and dispersion relation for internal waves. The spectrum of horizontal motions due to internal waves using this approach is shown in Fig. 1. Also shown in Fig. 1 are observed horizontal velocity spectra. In these examples, the observed horizontal velocity spectra contain more energy than the model spectrum at all frequencies. While this suggests that other processes besides internal waves may be responsible for the spectrum of horizontal motions, it must be kept in mind that up to this point no attempt has been made to account for Doppler shifting effects. Recently Scheffler and Liu (1986) and Fritts and VanZandt (1987) have been able to model the influence of mean wind speeds on internal wave spectra and their results show that the effect of Doppler shifting on atmospheric internal waves is not negligible.

The possibility that the observed atmospheric spectrum of horizontal motions may be dominated by processes other than internal waves was considered by Lilly (1983) and Gage and Nastrom (1985a, 1985b). These authors suggested that the horizontal velocity spectrum may be a manifestation of the vortical mode of fluid motions also known as stratified turbulence or quasi-two-dimensional turbulence. Lilly based his analysis on earlier work by Riley et al. (1981) that showed that at low Froude numbers it was possible through a scaling analysis to separate the equations of motion into

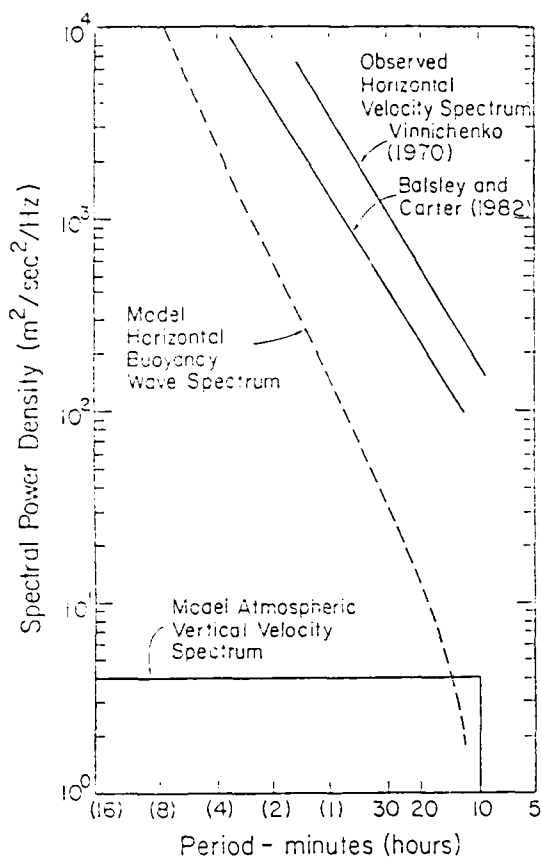


Fig. 1. Comparison of observed frequency spectra of horizontal motions with the frequency spectrum of horizontal buoyancy wave motions consistent with a model tropospheric vertical velocity spectrum.

a set of equations governing wave motions and another set of equations governing turbulence. Physically, at low Froude number in a stratified fluid it should be possible to decompose the motion field into waves and stratified turbulence. The possibility that the observed atmospheric velocity spectra contain contributions from waves and quasi-two-dimensional stratified turbulence has been considered by Gage and Nastrom (1985a, 1985b).

Both points of view discussed above accept the idea that the spectrum of vertical motions is largely determined by a spectrum of internal waves. Only in the importance attached to quasi-two-dimensional turbulence do the points of view differ. Doppler shifting effects may provide a way to differentiate waves and turbulence. The calculations of Scheffler and Liu (1986) and Fritts and VanZandt (1987) provide a means to quantify the Doppler shifting effect of a mean velocity on a spectrum of internal waves. The Taylor-transformation can be used to relate frequency spectra of turbulence to the wave number spectra of atmospheric motions

### 3. THE EFFECT OF A MEAN WIND ON INTERNAL WAVE AND TURBULENCE SPECTRA

According to the analysis of Scheffler and Liu (1986) and Fritts and VanZandt (1987) the influence of a mean wind on the spectrum of internal waves can be parameterized by the quantity

$$\beta = \frac{\bar{U} m_*}{N} \quad (1)$$

where  $m_*$  is a characteristic vertical wavenumber,  $\bar{U}$  is the mean wind speed, and  $N$  is the Brunt-Vaisala frequency. The influence of the mean wind on the spectrum of horizontal velocity for internal waves is illustrated in Fig. 2 which is taken from Fritts and VanZandt (1987). Figure 2 shows that qualitatively the influence of the mean wind is to increase the spectral amplitude at the high frequency end of the spectrum and to decrease the spectral amplitude at the low frequency end of the spectrum. The net effect of the mean wind is to increase (make less negative) the spectral slope above  $-2$  which is the slope of the model spectrum without Doppler shifting. Note that this change in spectral slope is in the sense required to fit the observed spectral slope in Fig. 1. Note also that only those waves with a component of their phase velocity in the direction of the mean wind are Doppler shifted.

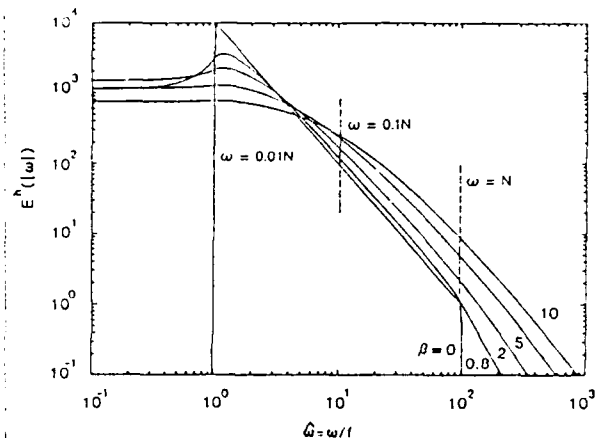


Fig. 2. Doppler shifting effect of a mean wind on a model buoyancy wave spectrum of horizontal velocity. (After Fritts and VanZandt, 1987.)

The Taylor transformation can be used to determine the frequency spectrum of turbulence seen by a fixed observer when a known wavenumber spectrum is advected past at a given velocity. The frequency spectrum is given by

$$E(f) = 2\pi E(k)/\bar{U} \quad (2)$$

where

$$f = \bar{U}k/2\pi \quad (3)$$

To determine the dependence of the wind speed, we adopt the model wavenumber spectrum contained in Fig. 3. This model wavenumber spectrum is a good approximation to the climatological GASP spectrum (Nastrom and Gage, 1985). Using Eqs. (2) and (3) we calculate the frequency spectra pertinent to various advection velocities as illustrated in Fig. 4. Note that unlike the wave spectra in Fig. 2, the turbulence spectra in Fig. 4 retain their original spectral slope. Their spectral magnitude increases uniformly at all frequencies with increasing advection velocity. Actually, over mountainous terrain, the GASP spectra are modified somewhat (Nastrom et al., 1987) and these modifications should be taken into account in a more complete analysis.

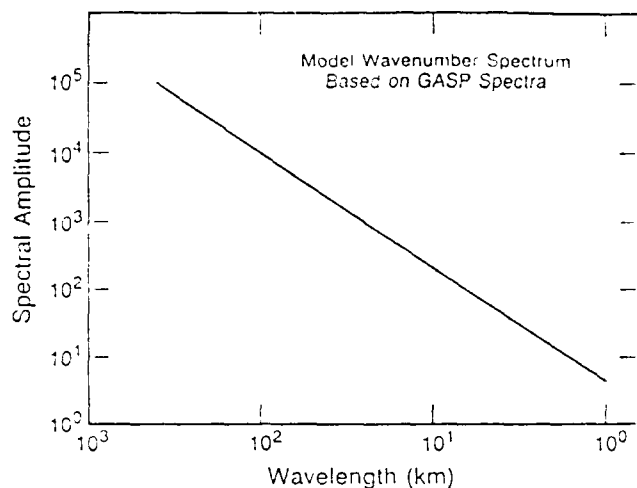


Fig. 3. Model horizontal wavenumber spectrum of horizontal velocity based on GASP spectra.

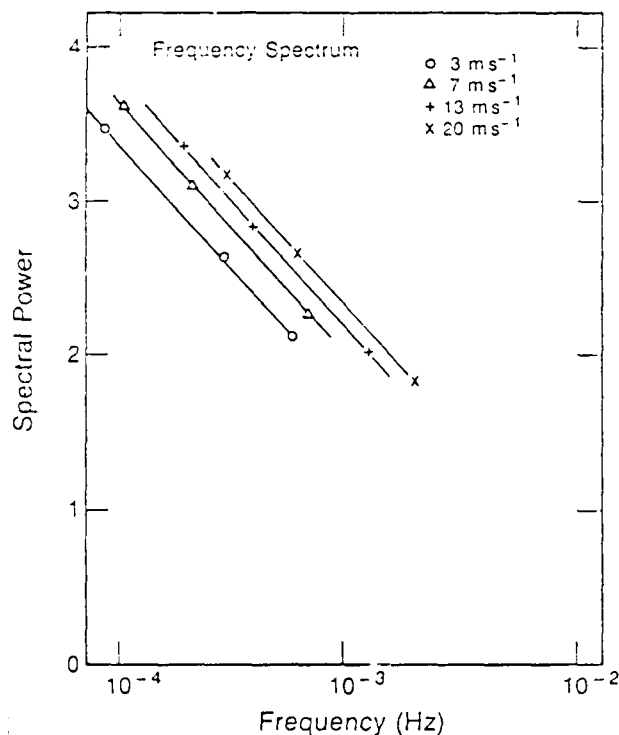


Fig. 4. Doppler shifted frequency spectra of horizontal velocity determined by Taylor transformation of the model wavenumber spectrum contained in Fig. 3.

#### 4. THE OBSERVED DEPENDENCE OF THE FREQUENCY SPECTRUM OF HORIZONTAL VELOCITY UPON WIND SPEED AT PLATTEVILLE, COLORADO

The 50 MHz Doppler radar located at Platteville, Colorado, has been observing horizontal and vertical velocities routinely since 1981. For the purposes of the present paper accumulated data from 1981-1984 were analyzed to determine the dependence of the frequency spectra upon background wind speed. The frequency spectrum of the observed winds were calculated for 3 hour and 9 hour periods and data were stratified according to mean horizontal wind speed. Composite spectra

were formed for each wind speed interval. Composite 3-hour spectra for the zonal wind are shown in Fig. 5. These spectra show a general increase in spectral amplitude with increasing wind speed. Spectral shape does not appear to be greatly affected by increasing mean winds over the range 2 to 20  $\text{ms}^{-1}$ .

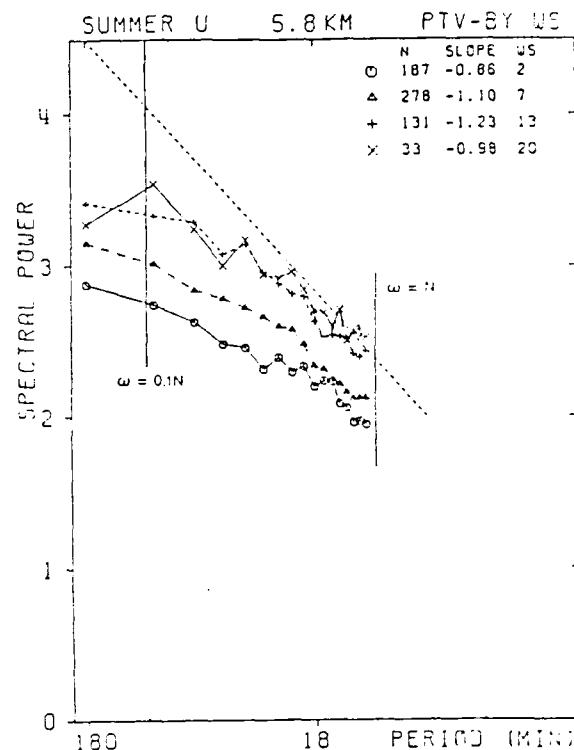


Fig. 5. Observed 3-hour frequency spectra of horizontal zonal velocity at Platteville, Colorado during summer months stratified by wind speed.

#### 5. COMPARISON OF THE OBSERVED DEPENDENCE OF THE HORIZONTAL VELOCITY SPECTRUM ON MEAN VELOCITY WITH THE WAVE AND TURBULENCE MODELS

In this section we compare quantitatively the dependence of the observed frequency spectrum of horizontal velocity upon mean wind speed with the Doppler shifting effect discussed in Section 3. This is accomplished by determining the change in spectral amplitude with changing wind speed. Since we are concerned primarily with the relative magnitudes of the spectra, all changes in spectral amplitude are determined relative to the spectral amplitude of the non-Doppler shifted (or lowest wind speed) spectrum. Changes in the spectral amplitude are determined as a function of wind speed at several frequencies. The frequencies chosen for the comparison are the Brunt-Vaisala frequency  $N$ , a frequency equal to  $.1N$ , and a frequency equal to  $.01N$ . The observed frequency spectrum does not extend to low enough frequencies to compare with the wave and turbulence models at  $.01N$  but the changes in spectral amplitude for the models have been included here for completeness.

In order to determine the changes in spectral amplitude for the wave model it is necessary to assign a value to the characteristic

wavenumber  $m_*$ . We have for this purpose adopted a value of  $m_* = .75 \times 10^{-3}$  cpm which is consistent with values anticipated by Fritts and VanZandt (1987). For the troposphere pertinent to the summertime Platteville spectra contained in Fig. 5, we adopt  $N = 1.67 \times 10^{-3}$  cps. With these choices for  $m_*$  and  $N$ ,  $\beta = .45U$ .

The results of the comparisons are contained in Fig. 6. Altogether there are six curves plotted in Fig. 6. Each curve gives the spectral density ratio as a function of wind speed. Curves with positive (negative) slope have increasing (decreasing) spectral amplitude with increasing wind speed. Two curves are plotted for the observed change in spectral amplitude corresponding to frequencies of  $N$  and  $.1N$ , respectively. These curves show a modest increase in slope with decreasing frequency. The turbulence model result does not depend on frequency so that only a single curve is drawn. This curve has a positive slope intermediate to the slopes of the two curves for the observed spectra. Three curves are plotted for the wave model. These curves show the dependence upon wind speed of the model wave spectrum for frequencies of  $N$ ,  $.1N$  and  $.01N$ , respectively. The slopes for the three curves decrease rather markedly with decreasing frequency. This is the opposite sense of the more modest change noted previously for the observed spectra.

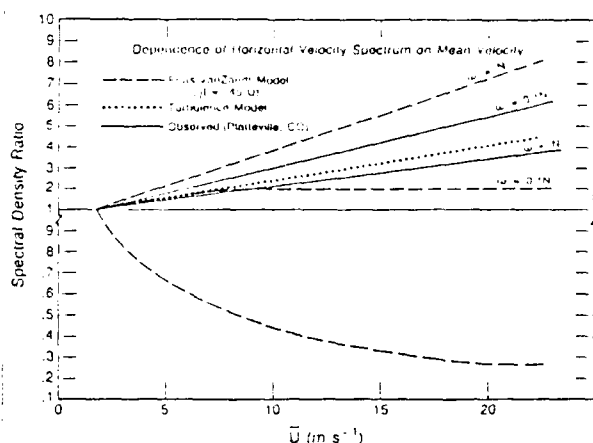


Fig. 6. Comparison of the observed dependence of the horizontal velocity spectrum on wind speed with wave and turbulence models.

## 6. CONCLUDING REMARKS

In this paper we have considered the dynamical processes that may be responsible for the observed mesoscale atmospheric wind spectra. We have addressed the issue of whether the observed spectrum of horizontal velocity is due primarily to waves or turbulence by comparing the dependence of the observed horizontal velocity spectra on wind speed with the Doppler shifting effect anticipated for a model wave spectrum and for a model turbulence spectrum. The results show that the observed spectra do not follow either the turbulence model or the wave model very closely. However, the turbulence model seems to fit the observations more closely than does the wave model.

The wave and turbulence models employed here must be considered as approximate and the results shown are necessarily of a statistical nature. The observations are limited to a single location and may not be typical of other locations. For these reasons the results presented here must be regarded as preliminary.

## 7. REFERENCES

- Balsley, B.B., and D.A. Carter, 1982: The spectrum of atmospheric velocity fluctuations at 8 km and 86 km, *Geophys. Res. Lett.*, **9**, 465-468.
- Dewan, E.M., 1979: Stratospheric spectra resembling turbulence, *Science*, **204**, 832-835.
- Ecklund, W.L., K.S. Gage, G.D. Nastrom, and B.B. Balsley, 1986: A preliminary climatology of the spectrum of vertical velocity observed by clear-air Doppler radar, *J. Climate and Appl. Meteorol.*, **25**, 885-892.
- Fritts, D.O., and T.E. VanZandt, 1987: The effects of Doppler shifting on the frequency spectra of atmospheric gravity waves, *J. Geophys. Res.*, **92**, 9723-9732.
- Gage, K.S., and G.D. Nastrom, 1985a: On the spectrum of atmospheric velocity fluctuations seen by MST/ST radar and their interpretation, *Radio Sci.*, **20**, 1339-1347.
- Gage, K.S., and G.D. Nastrom, 1985b: Evidence for coexisting spectra of stratified turbulence and internal waves in mesoscale atmospheric velocity fields, Preprint Vol. 7th Symp. on Turbulence and Diffusion, Nov. 12-15, Boulder, Colorado, pp 176-179.
- Green, J.L., G.D. Nastrom, K.S. Gage, T.E. VanZandt, W.L. Clark, and J.M. Warnock, 1988: Observations of vertical velocity over Illinois by the Flatland radar, accepted by *Geophys. Res. Lett.*
- Lilly, D.K., 1983: Stratified turbulence and the mesoscale variability of the atmosphere, *J. Atmos. Sci.*, **40**, 749-761.
- Nastrom, G.D., and K.S. Gage, 1985: A climatology of atmospheric wavenumber spectra observed by commercial aircraft, *J. Atmos. Sci.*, **42**, 950-960.
- Riley, J.J., R.W. Metcalfe, and M.A. Weissman, 1981: Direct numerical simulations of homogeneous turbulence in density-stratified fluids, *Nonlinear Properties of Internal Waves*, **76**, ed. B.J. West, pp 79-112, American Institute of Physics, New York.
- Scheffler, A.O. and C.H. Liu, The effect of Doppler shift on gravity wave spectra observed by MST radar, *J. Atmos. Terr. Phys.*, **48**, 1225-1231.
- VanZandt, T.E., 1982: A universal spectrum of buoyancy waves in the atmosphere, *Geophys. Res. Lett.*, **9**, 575-578.

UTILIZATION OF A SINGLE CLEAR-AIR DOPPLER RADAR BEAM TO MEASURE VERTICAL DIVERGENCE

by

W.L. Clark,<sup>1</sup> G.D. Nastrom,<sup>2</sup> K.S. Gage,<sup>1</sup> J.L. Green,<sup>1</sup> R.G. Strauch,<sup>3</sup> and J.M. Warnock<sup>1</sup>

<sup>1</sup>Aeronomy Laboratory, National Oceanic and Atmospheric Administration, Boulder, Colorado 80303

<sup>2</sup>Meteorology Research, Control Data Corporation, Minneapolis, Minnesota 55440

<sup>3</sup>Wave Propagation Laboratory, National Oceanic and Atmospheric Administration, Boulder, Colorado 80303

## 1. INTRODUCTION

Clear-air Doppler radars, also called wind profilers, have the almost unique capability to profile the vertical air motion over the radar on a nearly continuous basis. Clark et al. (1986) point out that 9w/9z, the vertical divergence component, may easily be obtained from these measurements through simple height differencing. This technique is sensitive to all scales of motion and should be complementary to values of horizontal velocity divergence determined from the NWS rawinsonde network or those obtained from the future clear-air Doppler radar networks (see Chadwick and Hassel, 1987), using techniques similar to those of Zamora et al. (1987).

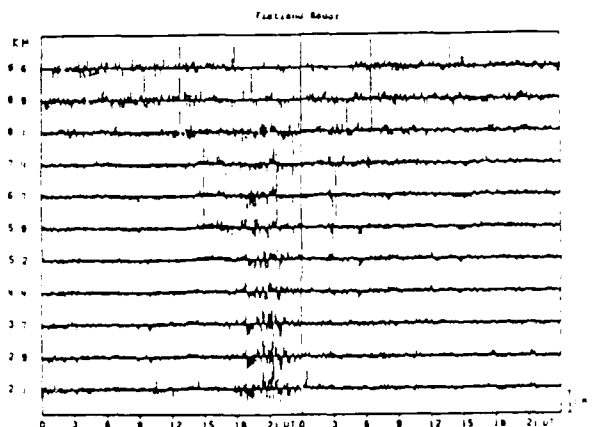
Vertical divergence observations seemingly associated with the passage of a front are described in Clark et al. (1986). However, these observations were made at the Sunset radar in the foothills of the Colorado Rocky Mountains and were complicated by orographic effects (such as lee waves) and the convective activity accompanying the front.

Here we present a case study of the vertical motion and vertical divergence observed during the passage of a cold front under more favorable conditions. The data presented are from the Flatland radar (Green et al., 1988) which is located in the extremely flat terrain near Champaign, Illinois, far from any mountains, and there was little convective activity associated with the frontal passage.

## 2. CASE STUDY

The NWS 500 mbar charts at 1200 UT April 29 and 30 show strong north-westerly flow, increasing north of the radar, and associated with a center of low pressure to the north-east. This condition is often associated with subsidence and clear skies. A cold front passed over the Flatland radar at about 0200 UT on the 30th of April. This front advanced steadily from the North at about 30km/hr (8 m/s). The NWS surface analysis charts show the front 390km north of the radar at 1200 UT April 29, over the Flatland radar around 0200 UT, and 330km south of the radar at 1200 UT April 30, 1987. There was no precipitation associated with this system as it passed over the radar. The weather observer at Willard airport, 8km east of the radar, reported clear skies except for scattered clouds at 3km (10,000 feet) from 1045-1545 UT

on the 29th, and again from 2345-0245 UT on the 30th. The observer was off duty between 0445 UT until 1045 UT the next day, but at 1145 UT scattered clouds at 3km were again noted, while at 1245 UT there were clear skies. The basically clear skies are consistent with the expectation of subsidence associated with the upper level north-westerly flow.



April 29-30, 1987

Figure 1. Vertical velocity time series from the Flatland radar covering April 29-30, 1987. The horizontal axis is marked in hours UT, while the vertical axis shows the height of each time series in km MSL. The velocity scale is shown at the lower right.

The vertical velocity data for the 48-hour period centered on the frontal passage is presented at full time resolution in Figure 1. Focussing our attention on the lower heights the traces show variability roughly within a range of plus or minus 20cm/s. An exception to this occurs between the hours of 1800 to 2400 UT on the 29th. During this more active period, w ranges between plus or minus about 50cm/s, and close examination with a straight edge shows that the excursions lasting a few minutes or more are basically in phase at all heights below 7 or 8 km. From the airport observations described above, we know that the sky was clear during this period, so that the oscillations are unlikely to be due to convective activity. A more likely explanation is that these features are shear generated gravity waves launched from the jet stream to the north. The large

amplitude upward excursion between 0000 and 0100 UT on the 30th, however, is seen only at the lowest height, 2.1km MSL. It may well be associated with a weak pre-frontal cumulus and is not inconsistent with the scattered clouds observed during this time at Willard airport.

For the detection of large-scale features in the flow, we clearly need to remove local scale features and signals from propagating waves. In Figure 2 we show the results of simple running mean filtering. The top panel shows the results of contouring 1 hour means of  $w$ . The center panel in Figure 2 shows  $\partial w / \partial z$ , determined from the difference of the  $w$  values at adjacent heights. To the extent that the vertical divergence is compensated by the horizontal velocity convergence, we can say that the light solid lines represent horizontal velocity convergence, while the dashed represent horizontal divergence. The bottom panel was obtained from the  $\partial w / \partial z$  data in the middle panel by performing a 3 height running mean in a simple attempt to reduce the amplitude of small-vertical scale features.

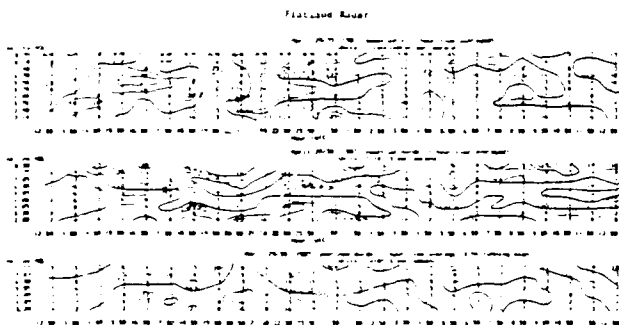


Figure 2. The top panel shows contours of hourly mean  $w$ , in  $10\text{cm/s}$  intervals, where light solid lines represent upward motion, dashed lines downward, and the thick solid line no vertical motion. The middle and lower panels show  $\partial w / \partial z$  in  $10^{-4}\text{s}^{-1}$  contour intervals, where the light solid lines represent vertical velocity divergence, the dashed lines represent vertical convergence, and the solid line depicts the transition. The lower panel is the same as the middle panel, except that the data has been smoothed by a 3-height running mean.

### 3. DISCUSSION

The hourly mean vertical velocity contours in Figure 2 show basically downward motion, consistent with the pattern of flow shown in the NWS 500 mbar analysis. Superimposed are periods of upward motion, which are not yet accounted for in our study. The front itself is apparently unobserved in these lower tropospheric observations, indicating that it must be a shallow feature, perhaps confined to the boundary layer. This is consistent with the fact that its southward progression is not reflected in the 500 mbar wind pattern. The pattern of vertical divergence shows the tendency of the atmosphere to arrange itself in layers of alternating divergence and convergence. This is especially noticeable after 0200 UT on the 30th. The decreased vertical scale of this layering associated with the active period believed due to trapped gravity waves is also

evident in the middle panel of Figure 2.

### 4. SUMMARY

The vertical velocity divergence term is easily measurable with clear-air Doppler radars. The divergence pattern observed depends on the dominating signal of the various atmospheric events occurring simultaneously above the radar. For example, in the case study presented here, propagating gravity waves seemed to clearly dominate the data for a six hour interval. During other times the source of the signal seems associated with the pattern of upper atmospheric flow.

**Acknowledgements.** This work was partially supported by the National Science Foundation under grant ATM-8512513. We gratefully acknowledge helpful consultation with T.E. VanZandt of the NOAA Aeronomy Laboratory.

### 5. REFERENCES

- Chadwick, R.B., and N. Hassel, 1987: The next generation surface-based atmospheric sounding system. Preprint Vol., Third International Conference on Interactive Information and Processing Systems for Meteorology, Oceanography, and Hydrology. AMS, 15-21.
- Clark, W.L., J.L. Green, and J.M. Warnock, 1986: The use of a vertical beam clear-air Doppler radar to measure horizontal divergence of the wind field. Preprint Vol., 23rd Conf. on Radar Meteorology, Snowmass, Colo., Sept. 22-26, American Meteorological Society, Boston, 38-40.
- Green, J.L., G.D. Nastrom, K.S. Gage, T.E. VanZandt, W.L. Clark, and J.M. Warnock, 1988: Observations of vertical velocity over Illinois by the Flatland radar. Submitted to *Geophys. Res. Lett.*
- Zamora, R.J., M.A. Shapiro, C.A. Doswell, III, 1987: The diagnosis of upper tropospheric divergence and ageostrophic wind using profiler observations. *Mon. Wea. Rev.*, **115**, 871-884.

# MEASUREMENT OF VERTICAL VELOCITY USING CLEAR-AIR DOPPLER RADARS

by

T.E. VanZandt,<sup>1</sup> J.L. Green,<sup>1</sup> G.D. Nastrom,<sup>2</sup> K.S. Gage,<sup>1</sup> W.L. Clark,<sup>1</sup> and J.M. Warnock<sup>1</sup>

<sup>1</sup>Aeronomy Laboratory, National Oceanic and Atmospheric Administration, Boulder, CO 80303

<sup>2</sup>Meteorology Research, Control Data Corporation, Minneapolis, MN 55440

## 1. INTRODUCTION

Since the development of the clear-air Doppler radar technique (also called the wind-profiling or MST-radar technique) at Jicamarca, Peru (Woodman and Guillen, 1974), and Sunset, Colorado (Green et al., 1975), it has been applied to a wide range of meteorological problems (see, e.g., Liu and Kato, 1985). Despite this rapid progress, research on some important problems has been frustrated by the fact that most clear-air Doppler radars are near mountains. The resulting orographic effects act as geophysical noise on observations of other processes. These effects are especially serious for studies of the vertical component of motion. For example, Ecklund et al. (1982) found that when the wind flowed over the mountains, the variance of the vertical velocity was strongly correlated with the wind speed. Nastrom et al. (1985) found that they could extract the small synoptic-scale vertical velocity only when the horizontal wind was not from the direction of nearby mountains. Following their suggestion, we have constructed a new clear-air Doppler radar, called the Flatland radar, in very flat terrain near Champaign-Urbana, Illinois. We find that the vertical velocity field over very flat terrain is indeed quite different from that near rough terrain, and we present observations that suggest that the vertical velocity due to other processes, such as synoptic-scale motions and gravity waves, can be studied by clear-air Doppler radars in very flat terrain.

## 2. EXPERIMENTAL DESIGN

The Flatland Radar is located at 40.5°N, 88.4°W, 212m above mean sea level (MSL), about 8km west of the Champaign-Urbana Airport. The radar operates at a frequency of 49.8MHz (wavelength, 6.02m), with a pulse length and the range resolution of 750m. The 3dB, two-way beamwidth is 3.2°. To minimize contamination of vertical velocity measurements by horizontal winds, the antenna was carefully leveled to within 0.02° from the vertical. The Doppler spectra have a velocity resolution of 5cm s<sup>-1</sup> and an unaliased velocity range of  $\pm 3.2$  ms<sup>-1</sup>. The Flatland radar has been measuring the vertical velocity every 153 seconds almost continuously since March 2, 1987. The second phase of the Flatland radar, with steerable oblique beams to measure both components of the horizontal wind, will be implemented in early 1988. A more detailed description of the radar and some preliminary results are given in Green et al., 1988.

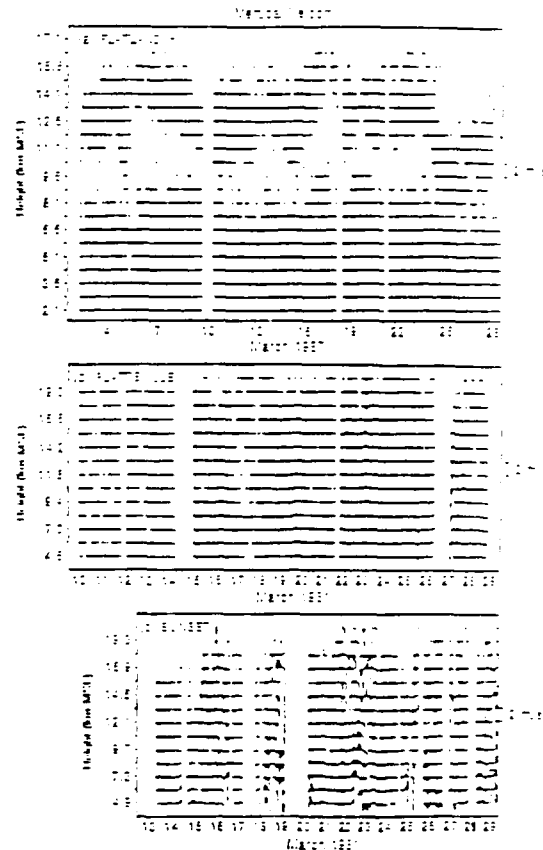


Figure 1. Radar vertical velocities averaged over fifteen-minute periods: (a) Flatland radar during March 1987; (b) Platteville radar during March 1981. (Panels (b) and (c) are from Ecklund et al., 1982.)

## 3. RESULTS

Figure 1 presents time series of 15-minute averages of the vertical velocity in each range gate of three radars, each located in a different kind of terrain. Panel (a) is from the Flatland radar and panels (b) and (c) are from the Platteville and Sunset radars in Colorado, 80 and 16km east of the crest of the Front Range (~4000m MSL), respectively. In the Flatland time series the smaller upper height limit and the data gaps around 10km are thought to be due to a smaller signal-to-noise ratio.

In the Colorado time series in Figures 1(b) and 1(c) there is a striking alternation of "active" periods with large variance and "quiet" periods with relatively small variance. Ecklund et al. (1982) showed that the variance is highly correlated with the strength of the 5km zonal wind flowing over the Front Range, and they concluded that the active periods are mostly due to mountain waves. In contrast, the variance in the Flatland time series in Figure 1(a) is nearly always small, comparable with that during the quiet periods at Platteville and even smaller than the quiet periods at Sunset.

Mountains have similar effects on short-period vertical motions. Figure 2 shows frequency spectra during spring 1987 from the 5.2km range gate at Flatland, plotted with thick curves, together with spectra taken in southern France during ALPEX (Ecklund et al., 1985), plotted with thin curves. The spectra are stratified into quiet days, when the lower-tropospheric winds were light, less than  $\sim 5$  m/s, and active days, when the winds were greater than  $\sim 20$  m/s. On quiet days both the ALPEX and Flatland spectra are flat to periods just less than the buoyancy frequency at about 10 minutes. The Flatland active-days spectrum is similar, but flatter and slightly raised. But at ALPEX the strong winds were northerly mistral winds that passed over nearby low mountains, and the ALPEX active-day spectra are much steeper, with a slope as negative as  $-5/3$  (indicated by the thick straight line) and with amplitudes much larger at all frequencies.

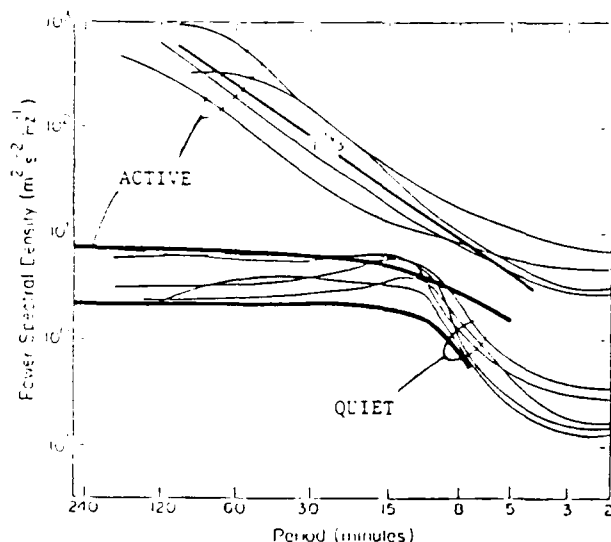


Figure 2. Frequency spectra of vertical velocity fluctuations. The two thick curves are from Illinois (Flatland) and the thin curves, from southern France (ALPEX). The heavy straight line labeled  $F^{-5/3}$  is an approximation to the ALPEX active-days spectra. The Flatland spectra are from the 5.2km range gate and are the average of 13 and 9 spectra, respectively. The ALPEX spectra are the average of four 750m range gates centered from 3.85 to 6.10km.

Moreover, the slight change in shape of the Flatland spectra with increasing wind speed is not inconsistent with the change predicted due to

Doppler shifting of an intrinsic gravity wave spectrum by the background wind (Fritts and VanZandt, 1987). This suggests that under these conditions the vertical motions are predominantly due to propagating gravity waves, with only small contributions from other processes.

#### 4. CONCLUSIONS

These results show that vertical motions near rough terrain are often dominated by orographic effects, at all periods ranging from minutes to many hours. The absence of such effects over very flat terrain suggests that clear-air Doppler radars can be used to study vertical velocities due to other processes, including synoptic-scale motions and propagating gravity waves.

**Acknowledgements.** This work was partially supported by the National Science Foundation under grant ATM-8512513. The radar is constructed at the Bondville Field Site of the Department of Electrical Engineering and Computer Science of the University of Illinois. S. Henson provided local maintenance and operation of the radar, and S.D. Mayor helped with initial data processing. We gratefully acknowledge helpful consultations with B. Ackerman, B.B. Balsley, S.A. Bowhill, D.A. Carter, W.L. Ecklund, E. Kudeki, and C.H. Liu.

#### 5. REFERENCES

- Ecklund, W.L., K.S. Gage, B.B. Balsley and J.L. Green, 1982: Vertical wind variability observed by the VHF radar in the lee of the Colorado Rockies, *Mon. Wea. Rev.*, **110**, 1451-1457.
- Ecklund, W.L., B.B. Balsley, D.A. Carter, A.C. Riddle, M. Crochet and R. Garelo, 1985: Observations of vertical motions in the troposphere and lower stratosphere using three closely spaced ST radars, *Radio Sci.*, **20**, 1196-1206.
- Fritts, D.C., and T.E. VanZandt, 1987: Effects of Doppler shifting on the frequency spectra of atmospheric gravity waves, *J. Geophys. Res.*, **92**, 9723-9732.
- Green, J.L., J.M. Warnock, R.H. Winkler and T.E. VanZandt, 1975: Studies of winds in the upper troposphere with a sensitive VHF radar, *Geophys. Res. Lett.*, **2**, 19-21.
- Green, J.L., G.D. Nastrom, K.S. Gage, T.E. VanZandt, W.L. Clark, and J.M. Warnock, 1988: Observations of vertical velocity over Illinois by the Flatland radar, submitted to *Geophys. Res. Lett.*
- Liu, C.H. and S. Kato, 1985: Forward: Technical and scientific aspects of MST radars, *Radio Sci.*, **20**, 1129.
- Nastrom, G.D., W.L. Ecklund and K.S. Gage, 1985: Direct measurement of large-scale vertical velocities using clear-air Doppler radars, *Mon. Wea. Rev.*, **113**, 708-718.
- Woodman, R.F. and A. Guillen, 1974: Radar observations of winds and turbulence in the stratosphere and mesosphere, *J. Atmos. Sci.*, **31**, 493-505.

## SOURCES OF GRAVITY WAVES AS SEEN IN VERTICAL VELOCITIES MEASURED BY THE FLATLAND VHF RADAR

G.D. Nastrom<sup>1</sup>, M. R. Peterson<sup>2</sup>, J. L. Green<sup>3</sup>, K. S. Gage<sup>3</sup>,  
T. E. VanZandt<sup>3</sup>

1. Dept. of Earth Sciences, St. Cloud State Univ., St. Cloud  
MN 56301
2. Meteorology Research Center, Control Data, Minneapolis  
MN 55440
3. Aeronomy Laboratory, NOAA/ERL, Boulder, CO 80303

### 1. INTRODUCTION

The capability of clear-air doppler radars to monitor the air velocity vector over a station on a continuous basis enables studies of a variety of features not adequately sampled by other currently available or past measurement systems (such as balloons). In particular, studies of atmospheric gravity waves using conventional data sources have been impeded due to their relatively short time scales, from a few minutes to a few hours, and many questions remain unanswered. Vertical velocity data from radar sites located in or near mountains all show alternating quiet and active periods of vertical velocity variance (e.g., Ecklund, et al., 1982); the quiet periods are believed to reflect a gravity wave spectrum, and the active periods are caused by the effect of standing lee waves launched by the atmospheric flow over rough terrain. The patterns of velocity observed during lee wave events are highly localized and it is not clear that general conclusions regarding mesoscale dynamics can be drawn from these episodes. In contrast to those results, the vertical velocities measured by the Flatland radar in Illinois represent a spectrum of freely propagating gravity waves subject to doppler shifting by the background wind (VanZandt, et al., 1989).

Processes which have been suggested as sources of gravity waves include flow over orography, unstable wind shears, and convection. There have been a few case studies which show the variance of the vertical velocity is effected by frontal passages and near thunderstorms and jet streams (e.g., Gage and Balsley, 1978; Ruster, et al., 1986), but in general it has been difficult to separate the effects of these processes from lee wave effects in radar data obtained near mountainous areas. The purpose of this paper is to describe the atmospheric processes which cause enhanced variance of the vertical velocity at Flatland where lee waves are not a problem.

### 2. DATA

The Flatland radar is located in very flat terrain near Champaign, Illinois, as described by Green, et al., 1988. In its final configuration the radar will provide horizontal and vertical wind measurements from several beams. The data available for this study are from the first phase of the radar system and include only the vertical velocity measurements. Data are recorded at time intervals of approximately 2 minutes at vertical levels separated by 0.75 km between 1.4 and 18.6 km. An example of a typical time series of vertical velocity as seen by the Flatland radar was presented in Green et al., 1988. Close inspection of such radar data reveals periods when the variance of vertical velocity is very small and other times when the variance is relatively large. We have studied the period from March, 1987, through May, 1988, and find the "quiet" periods correspond to days when no significant weather systems were located over east central Illinois and the region was often dominated by high pressure. Conversely the "active" periods can all be identified with some synoptic or mesoscale phenomenon. Although the difference between "quiet" and "active" periods seen at Flatland is much smaller than that at radar sites located in or near mountains where lee wave effects are important, their significance for atmospheric processes may be greater. It is during the active periods that enhanced gravity wave activity leads to significant fluxes of momentum and energy, and the divergences of these variables have direct bearing on the large-scale flow. Also, irreversible mixing processes associated with episodes of wave transience lead to exchange of passive tracers, especially in the presence of strong gradients such as near upper level fronts and tropopause folds. Thus, given the relatively large portion of the earth's surface affected by processes such as seen at Flatland at any given time, their net influence on the atmosphere may be large.

All instances of high variance were found to be associated with a particular event such as a frontal passage or a thunderstorm. There were no active periods

indicated in the radar data not associated with a significant weather event; likewise, inspection of the daily weather maps and satellite pictures showed that all weather events led to a signature in the radar data during this period. In order to illustrate these signatures we will next present specific cases when the variance was increased, relating characteristics of the data collected by the Flatland radar to the concurrent atmospheric conditions.

### 3. CASE STUDIES

9 March 1987. Dry cold front with light winds aloft. At 9/03 UTC a cold front was stretched across northern Illinois between Chicago and Urbana. Behind the front a massive high pressure dome of cold air centered in southern Manitoba pushed rapidly southward creating an Arctic outbreak. By 9/09 UTC the front had passed Urbana and was located over the southern tip of Illinois. Surface observations from the Champaign airport indicated frontal passage at approximately 9/05 UTC. However, no precipitation or convection was observed and only middle and high clouds were reported. At 500 mb a low pressure trough was situated over the southeastern U.S., and winds through the troposphere were generally weak and from the north over most of Illinois.

Inspection of the Flatland vertical velocities for this day (Figure 1) shows that at about 05 UTC there was a sudden increase of variance at all levels in the troposphere. It is evident that this disturbance in the vertical velocity field corresponds to the time the cold front passed the radar site. An interesting feature in this case is that near 11 km, just below the tropopause, the signal-to-noise ratio of radar echos was small before

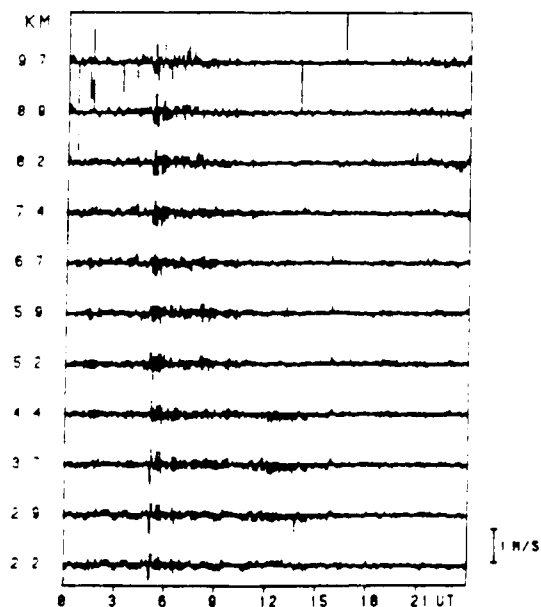


Fig. 1. Flatland vertical velocities ( $\text{cm s}^{-1}$ ) for 9 March 1987. Time resolution is roughly every 2.5 minutes.

frontal passage and rose sharply after the large negative spike in vertical velocity below 4 km near 05 UTC. Although the relationship of this phenomenon to the dynamics of the frontal system is not well understood, it is clearly an upper-level signature of the increased turbulence on the 3-m scale.

The amplitude of the oscillation in the troposphere appears to damp out with time after 9/09 UTC. Spectral analysis of the data between 06 and 09 UTC (Figure 2) shows the predominant period was 8.6 minutes in the troposphere. The Brunt-Vaisala period between 700 and 300 mb was about 9.0 minutes based on radiosonde soundings at Peoria and Salem. We note that these spectra closely resemble those expected for a spectrum of internal gravity waves in calm or very light wind conditions. In fact, the slightly positive slope of the spectra is consistent in the gravity wave model with the  $-5/3$  power law often observed for the horizontal velocity spectra.

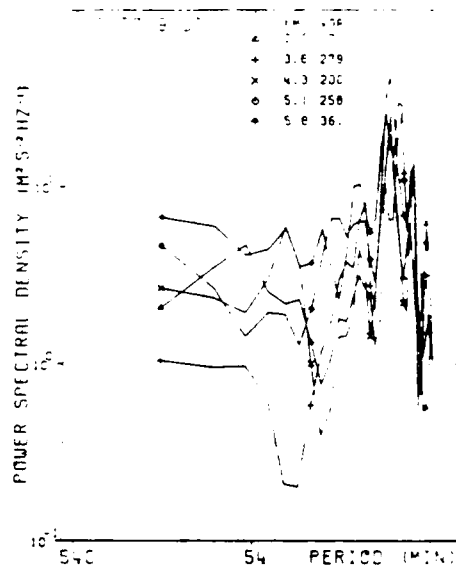


Fig. 2. Spectral analysis of vertical velocities for 06-09 UTC 9 March 1987.

The close association of the oscillations in Figure 1 with the frontal passage is in contrast with the results of Brodhum, et al. (1976), who reported that wave amplitudes at the surface, as seen by microbarographs, began to increase 4-5 hours before the passage of cold fronts. Gedzelman (1983) also reports that wave amplitudes are larger than average when extratropical cyclones are approaching. We believe that the unusual factor in the present case is that the winds aloft were very light.

14-15 April 1987. Cold front with precipitation. At 14/12 UTC a low at the surface was located over northwestern Missouri, with a warm front extending southeastward across central Illinois and southern Indiana and with a cold front curving south across Missouri (Figure 3a). Rainfall was recorded throughout the

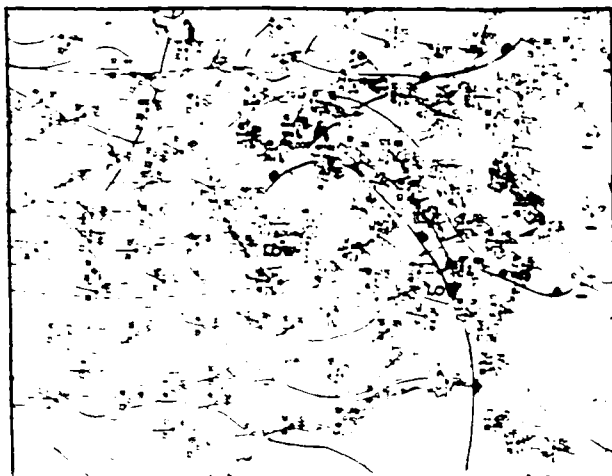


Fig. 3(a). Surface weather map for 14 April 1987, 1200 UTC.

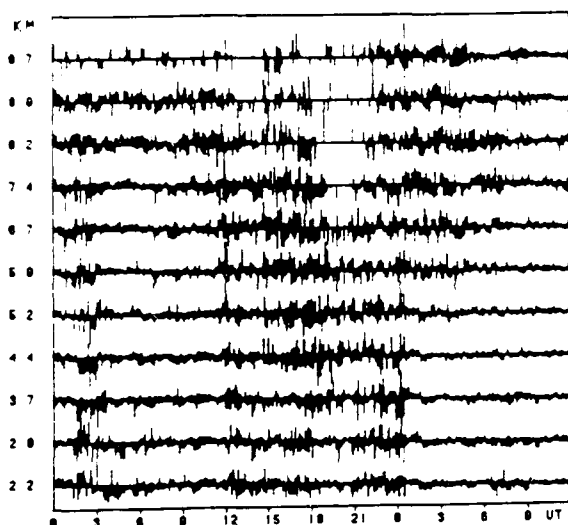


Fig. 3(b). As in Fig. 1, but for 14-15 April 1987.

Midwest during this period, and the weather surveillance radar at Marseilles, Illinois, indicated precipitation echos in the vicinity of Flatland from 14/12 - 15/12 UTC. Surface observations from Champaign showed thunderstorms at approximately 14/0230 UTC, after which no precipitation fell until approximately 14/12 UTC when rain began. The rain continued to about 16 UTC. The surface observations suggest the cold front passed over Champaign between 14/15 and 16 UTC, and by 15/00 UTC the front was located in central Indiana well to the east of the radar site.

The Flatland vertical velocities (Figure 3b) for this episode showed a more complicated pattern than in the previous case. In the present case the large variance in vertical velocity persisted for several hours, with increased variance between 14/02 and 03 UTC, corresponding to the thunderstorm reported at Champaign at

that time, followed by another active period that started at about 14/12 UTC and ended shortly after 15/00 UTC in the mid-troposphere. This period brackets the time the front passed Champaign, and it corresponds to the time rain was falling in the area. We conclude that the sequence of events in this case, with increased wave activity several hours before cold frontal passage, is consistent with that reported by Brodhum, et al. (1976), and Gedzelman (1983). This pattern is more frequently found in the Flatland data than that of the previous case.

20 May 1987. The next two cases demonstrate the increase in vertical velocity variance as seen by the radar in response to convective activity. On May 20 a weak front passed through central Illinois followed by thunderstorms later in the day. The surface map at 20/12 UTC depicted a stationary front just south of Chicago with a surface trough extending westward through central Illinois and northern Missouri, with a wind shift across the trough axis but no significant temperature or dew point discontinuity. Winds aloft over Illinois were light this day, and were generally southwesterly on the backside of a weak ridge centered over Indiana. Surface reports from Champaign airport indicated a wind shift at about 20/13 UTC, and beginning at about 19 UTC thunderstorm activity was reported in the area, both from surface reports and from the Marseilles weather radar. The passage of the trough is reflected in the Flatland data as an increase in variance at 13 UTC (Figure 4), coincident with the wind shift at the surface. Variances decreased between 20/14 and 18 UTC, then increased again at approximately 19 UTC, the same time thunderstorms were first reported, and persisted for several hours. These results expand those of Lu, et al. (1984), and others in showing thunderstorms near a front. The impulse-like signal near 20/13

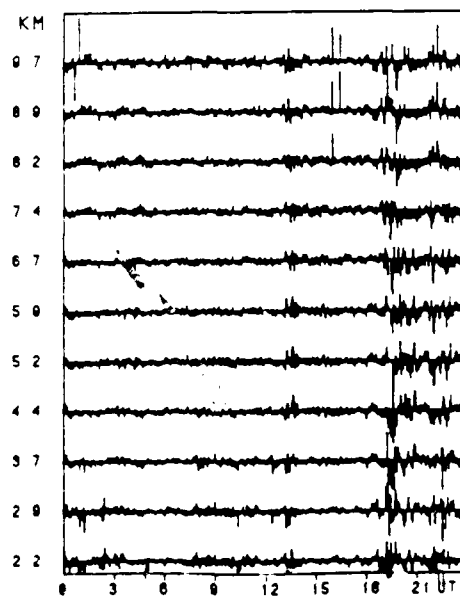


Fig. 4. As in Fig. 1, but for 20 May 1987.

UTC followed by an oscillation at all tropospheric heights is reminiscent of the 9 March case discussed earlier, and spectral analysis again showed a dominant period of oscillation just longer than the Brunt-Vaisala period.

**28 May 1987.** This case illustrates a less dramatic source of increased variance, namely, dry convective currents caused by afternoon heating of the surface. Surface reports from Champaign indicated temperatures in excess of 30° C and scattered clouds with bases at 1.5 km, rising to 6 km after 22 UTC. Vertical velocities for this day (Figure 5) showed increased variance between 18 and 22 UTC (12 to 16 local standard time), particularly below about 4 km. Because there was no organized activity occurring at this time at the surface or in the lower troposphere we conclude that the enhanced vertical motion seen here was related to surface heating. Inspection of the data for all summer reveals this type of enhanced variance is frequently seen in the afternoon hours on warm, sunny days.

The effects of afternoon convection are generalized in Figure 6 which shows the diurnal variation of the standard deviation over all data from June-August 1987. In the mid- and lower troposphere there is largest activity from 12-18 LT. Greatest values are below about 3 km, with only a slight maximum at higher levels. The increase at low altitudes is likely associated with convective plumes, while the increase at upper levels may be due to the convective waves launched at low levels discussed by Kuettner, et al. (1987).

#### 4. CONCLUSIONS

Several case studies of synoptic weather events and Flatland radar data have been presented. These were chosen to illustrate broad features although it must be noted that the time series of vertical velocity are different in each case despite a similarity in synoptic situations. However, several generalizations can be made: (1) All weather events resulted in a marked increase in the variance of vertical velocity, including thunderstorms, fronts, synoptic scale cyclones, upper level disturbances, and convection currents caused by surface heating. (2) There do not appear to be any instances of spurious or unexplained bursts of activity in the radar data. All cases of increased variance were found to be related to synoptic or mesoscale events. (3) Preliminary results indicate that tropospheric gravity waves associated with fronts and thunderstorms sometimes lead to quasi-monochromatic signatures in the radar data.

Results from the Flatland VHF radar are consistent with and expand upon past data from surface-based observations. The high temporal and spatial resolution of the radar data and the ability to measure all three wind components simultaneously offer

exciting possibilities in the future, especially in view of radiometric results such as those given by Dick, et al. (1987) and the detailed analyses suggested by these results.

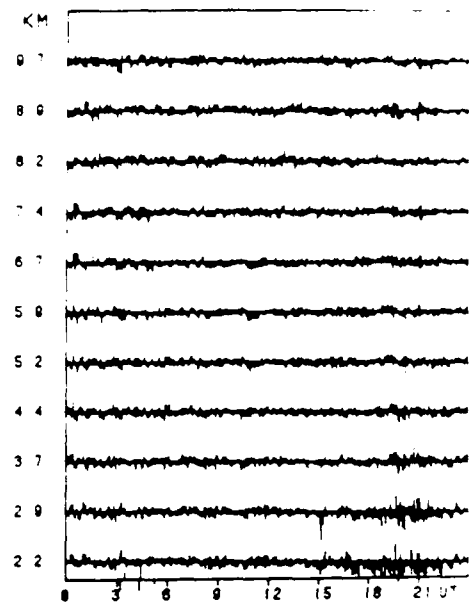


Fig. 5. As in Fig. 1, but for 28 May 1987.

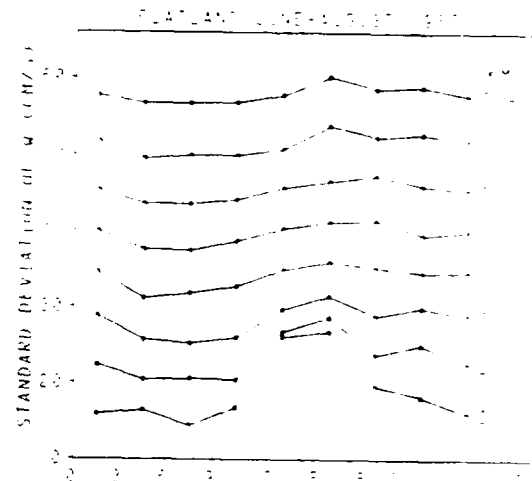


Fig. 6. Diurnal variation of the standard deviation of vertical velocity for all data collected from June - August 1987. The ordinate is offset by 5 cm s<sup>-1</sup> for each level in the vertical.

#### 5. REFERENCES

- Bruehl, J. D., D. C. Burt, and J. Neisser, 1978: Über Schwerkraft an der Kalbfriedrichsungen. *J. Geophys. Res.* 83, 10, 10, 10.
- Costa, P. E., R. Westwater, M. T. Decker, A. L. Bedard, and S. B. Smith, 1987: Improved microwave radiometric observations of the troposphere. *J. Geophys. Res.* 92, 10, 10, 10.
- Green, J. D., and J. D. Green, 1982: Vertical velocity observed by VHF radar in the lee of the Colorado Rockies. *Mon. Wea. Rev.* 110, 1451-1457.
- Green, J. D., and J. D. Green, 1978: Doppler radar probing of the troposphere. *Mon. Wea. Rev.* 106, 10, 10, 10.
- Green, J. D., 1983: Short-period atmospheric gravity waves: a study of their statistical properties and source mechanisms. *Mon. Wea. Rev.* 111, 10, 10, 10.
- Green, J. D., and J. D. Green, 1982: Vertical velocity observed by VHF radar in the lee of the Colorado Rockies. *Mon. Wea. Rev.* 110, 1451-1457.
- Kuettner, J., R. P. A. H. Decker, and J. D. Green, 1987: Ionospheric waves: observations of gravity wave signatures over the Colorado Rockies. *Mon. Wea. Rev.* 115, 10, 10, 10.
- Lee, J. D., J. D. Green, and J. D. Green, 1986: VHF radar observations of gravity waves associated with thunderstorms. *J. Atmos. Sci.* 43, 10, 10, 10.
- Neisser, J., J. D. Green, and J. D. Green, 1987: Gravity waves in the troposphere. *J. Geophys. Res.* 92, 10, 10, 10.
- Neisser, J., J. D. Green, and J. D. Green, 1988: The frequency and amplitude of gravity waves in the troposphere. *J. Geophys. Res.* 93, 10, 10, 10.

COMPARISONS OF REFRACTIVITY TURBULENCE ESTIMATES FROM THE FLATLAND VHF RADAR  
WITH OTHER MEASUREMENT TECHNIQUES

J.L. Green<sup>1</sup>, R.R. Beland<sup>2</sup>, J.H. Brown<sup>2</sup>, W.L. Clark<sup>1</sup>, F.D. Eaton<sup>3</sup>, L.D. Favier<sup>3</sup>, K.S. Gage<sup>1</sup>,  
W.H. Hatch<sup>3</sup>, J.R. Hines<sup>3</sup>, E.A. Murphy<sup>2</sup>, G.D. Nastrom<sup>4</sup>, W.A. Peterson<sup>3</sup>, T.E. VanZandt<sup>1</sup>, and J.M. Warnock<sup>1</sup>

<sup>1</sup> Aeronomy Laboratory, NOAA/ERL, Boulder, CO 80503

<sup>2</sup> Air Force Geophysics Laboratory, Hanscom Air Force Base, Bedford, MA 01731

<sup>3</sup> Atmospheric Science Laboratory, White Sands Missile Range, NM 88002

<sup>4</sup> Department of Earth Sciences, St. Cloud State University, St. Cloud, MN 56301

## 1. INTRODUCTION

The measurement of the refractivity structure parameter  $C_n^2$  is of fundamental importance to the understanding of the propagation of radio and optical waves through the atmosphere. It is, therefore, of considerable interest to the design and siting of many types of remote sensors and astronomical telescopes and to the study of atmospheric turbulence. Until recently, most of the clear-air radars were located near mountains, so that previous studies of  $C_n^2$  by clear-air radars and comparisons between radar measurements and other methods of measuring  $C_n^2$  were all made in rough terrain (e.g., Good et al., 1982; Green et al., 1984; Eaton et al., 1988). The resulting orographic effects may alter the turbulence intensity near the mountains as well as complicate the interpretation of the results. Therefore, an experimental campaign was conducted in June 1988 at the Flatland clear-air VHF radar site located in very flat terrain far removed from mountains near Champaign-Urbana, Illinois, to measure height profiles of the refractivity turbulence structure parameter  $C_n^2$  and related turbulent parameters.

Three different techniques were used to measure height profiles of  $C_n^2$ . The Flatland clear-air radar (Green et al., 1988), and a stellar scintillometer (Ochs et al., 1977), measured the profile remotely, and in situ measurements were obtained from over 20 thermosonde balloon flights (Brown et al., 1982). The balloon instrument also made measurements of the height profile of the standard thermodynamic parameters (pressure, temperature, and humidity), plus wind speed and direction. Model estimates of  $C_n^2$  were calculated from the thermodynamic and wind measurements using the numerical methods described by Warnock and VanZandt (1985). In addition, optical measurements were made of the transverse coherence length  $r_0$  (Eaton et al., 1988), and of the isoplanatic angle  $\theta_0$  (Eaton et al., 1985). Both these parameters depend on a weighted integrated value of  $C_n^2$  through the atmosphere.

Both the scintillometer and radar measurements of  $C_n^2$  are obtained remotely by sensing the effect of the fluctuations of refractive index on the propagation of electromagnetic waves; the scintillometer measures the optical scintillation from a star, whereas the radar measures backscatter from these fluctuations. At radio wavelengths the humidity and its gradient as well as the temperature gradients contribute significantly to the refractive index; whereas at optical

wavelengths only the temperature fluctuations are important. In contrast to the remote sensors, a thermosonde (Brown et al., 1982) measures the temperature fluctuations directly by measuring the RMS temperature difference between two very fast temperature sensors separated by a meter. Comparisons among these measurements taken simultaneously in simple topography, provide a unique opportunity to compare these different measurement techniques. In this paper we present some preliminary results, which emphasize the radar measurements.

## 2. EXPERIMENTAL SET UP

### 2.1 Flatland Radar

The Flatland radar (Green et al., 1988) is located about 8 km west of the Champaign-Urbana airport [40.05°N, 88.38°E, 212m above mean sea level (MSL)]. This clear-air Doppler radar (also called wind profiler, or ST radar) operates at a frequency of 49.8 MHz (6.02 m wavelength) with peak and average power of about 10 kw and 150 watts, respectively. All the data reported in this paper were taken with a pulse length of 1.5 km and over sampled with a range resolution of 750 m.

The antenna consists of two collocated dipole arrays covering a 57 x 57 m area, with a 3 dB, two-way beamwidth of 3.2 degrees. Each of the arrays is composed of strings of coaxial-collinear dipoles. In this experiment the antenna beam was tilted twenty degrees off the vertical toward the east or south directions. With this tilt angle, echoes due to specular scattering were essentially eliminated, so that unambiguous  $C_n^2$  measurements were obtained.

The signal received by the radar was sampled, coherently filtered, and Fourier transformed to produce Doppler power spectra in real time at the radar site. The Doppler spectra have 128 points with a velocity resolution of 5 cm/s and an unaliased radial  $\pm 3.2$  m/s. Three of these spectra were averaged together and recorded on magnetic tape. Several steps were required to derive  $C_n^2$  from the power spectra. First, the region in the spectrum that contained the signal had to be identified (e.g., Clark and Carter, 1980). Next, the signal-to-noise was obtained from the area under the signal of the power spectrum. We calibrated the signal-to-noise by calculating the noise power from radio astronomy cosmic noise charts and the system temperature. Finally, we calculated the radar reflectivity from the radar equation using the measured system parameters and recorded transmitted power (e.g., Green et al., 1979).

## 2.2 Stellar Scintillometer Model II

The stellar scintillometer Model II was developed by the Wave Propagation Laboratory of NOAA (Ochs et al., 1977). To operate the system, a star of second magnitude or brighter and within  $45^\circ$  of the zenith is selected. The system uses a Schmidt-Cassegrain telescope 35.5 cm in diameter to focus starlight from the star into an attached instrument package that sequentially measures the scintillation intensity at different spatial wavelengths ranging from 5 to 15 cm. Since particular spatial wavelengths observed in the scintillation pattern originate from specific altitude regions in the atmosphere, the surface-based measurements can be combined with weighting functions to obtain  $C^2_n$  height profiles. The system can measure seven different height regions of optical turbulence ranging from 2.2 to 18.5 km above ground level (AGL). The height weighting functions for these seven heights are broad, and are broadest at the highest altitudes.

## 2.3 Thermosonde System

The thermosonde system consisted of two parts, which were mounted below an ascending balloon (Brown et al., 1982). One part was a standard VIZ digital microsonde, the other was a micro-thermo bridge linked to the microsonde. A 1200 gram meteorological balloon was used to lift the instrument package with an ascent rate of about 5 m/s. The package was suspended from 90 to 180 meters below the balloon to ensure that the turbulent wake from the two meter balloon did not affect the measurements.

### 2.3.1 Thermosonde

The thermosonde measured the RMS temperature fluctuations between two unheated fine wire tungsten probes separated horizontally by one meter. The minimum detectable RMS temperature fluctuation was about  $0.002^\circ\text{C}$ , and the data were recorded every four seconds, giving about a 20-meter height resolution.  $C^2_n$  was calculated from the observed temperature fluctuations and the pressure and temperature observed by the microsonde.

### 2.3.2 Standard upper air data:

The microsonde makes excellent height-resolution measurements of the standard thermodynamic parameters (pressure, temperature, and relative humidity) and wind speed and direction. The thermodynamic data was recorded every four seconds, which gave about a 20 height resolution. The wind speed and direction were determined by using the Loran-C navigator system, and the data were recorded every 10 seconds, which gave about a 50 m height resolution. These data are useful in describing the meteorological conditions during the campaign, and are the input for the  $C^2_n$  model calculations described below.

## 2.4 Model Estimates of $C^2_n$

Model calculations of  $C^2_n$  were made from the standard upper air data, i.e., pressure, temperature, humidity, and wind speed and direction. These data are described in section 2.3.2 above. The basic model concepts are given by VanZandt et al. (1981). Since then, the model has been extended and revised considerably. We used the latest version described by Warnock et al. (1985), and used the numerical techniques

described by Warnock and VanZandt (1985) to evaluate the model estimates. To compare the model estimates with results from previous comparisons with the Sunset and Stapleton radars (Warnock et al., 1986; Warnock et al., 1988), which are located in and near the mountains, respectively, we used identical values of all the model parameters and constants except one: the constant in the equation giving the distribution of wind shears. This parameter quantifies the shear environment in the range of scales important in the onset of turbulence flow; therefore, the evaluation of this parameter allows the Flatland shear environment at these scales to be contrasted with the mountainous environment.

## 2.5 Description of Campaign

This experimental campaign was conducted at the Flatland radar site from 6-15 June 1988. The radar and  $r_0$  measurements were made as continuously as possible throughout both the daytime and nighttime. The scintillometer and isoplanometer systems shared a single telescope; the scintillometer operated at night and the isoplanometer operated during the day and in twilight. Thermosonde balloon launches were usually made after noontime and before midnight local time. A typical schedule was to launch a few packages in the afternoon and a few after dark. The radar operated during clear and cloudy conditions, whereas the optical systems operated during clear sky conditions. The optical telescopes were located about forty meters northeast of the center of the radar antenna, and the thermosonde launch site was about sixty meters east of the antenna center.

## 3. PRELIMINARY RESULTS

As described in section 2.1 above we used the cosmic noise power received by the radar system to calibrate the observed signal-to-noise ratio to derive  $C^2_n$ . At the low ranges there are several practical problems with this procedure such as receiver recovery after the transmitted pulse. Clark et al. (1988) discussed this problem for the data taken with the Flatland system operating during this campaign. They found that the cosmic noise calibration may be used for the sixth range gate (4.85 km) and above. Thus, the radar measurements used in this paper begin at 4.85 km and continue until the signal-to-noise ratio becomes too small to measure accurately.

Measurements made by both the radar and scintillometer remote sensors are average values over both time and space. Five-minute data averages were used in this paper by both systems, and these profiles are relatively smooth. In contrast, each thermosonde in situ measurement is an average over four seconds which gives about a 20-meter height resolution. The four-second thermosonde data displays many very thin large peaks in  $C^2_n$ . Frequently, the measured  $C^2_n$  values fall to the observing noise level between peaks. Thus, to compare the thermosonde profiles with the others, we smoothed the thermosonde data. We used a Gaussian filter with  $\sigma = 0.5$  km and truncated the filter at  $\pm 5\sigma$ .

Figures 1 through 3 show height profiles of the  $C^2_n$  measurements from the radar, thermosonde, and scintillometer together with two model estimate profiles. All the radar

data used in this preliminary study were taken with the antenna pointed  $20^\circ$  toward the east. The thermosonde and model profiles have been smoothed with the same Gaussian filter. One model profile gives the total  $C^2$  including the humidity terms; this model, called model (radar), is compared to the radar data. The other model, called model (dry), omits the humidity terms; it is compared to the scintillometer and thermosonde profiles. Note that the dry and radar model profiles merge together at about ten km and are identical at higher altitudes.

Figure 1 shows the first example in this data set that has data from all three instruments. Recall that the thermosonde, scintillometer, and dry model profiles form one set of profiles, and that these three profiles are to be compared with each other; whereas the radar and radar model are a separate set of profiles. The agreement among the profiles in each set is very good to excellent. The radar data are on the model (radar) curve except for the lowest point at 4.85 km; at that height the model (radar) is smaller than radar measurement. The next example, shown in Figure 2, is a daytime example, so there are no scintillometer data. Figure 3 shows the next nighttime example. In both cases the model (radar) is smaller than the radar data for the lowest two to three range gates. The data from the other range gates fit the model (radar) well.

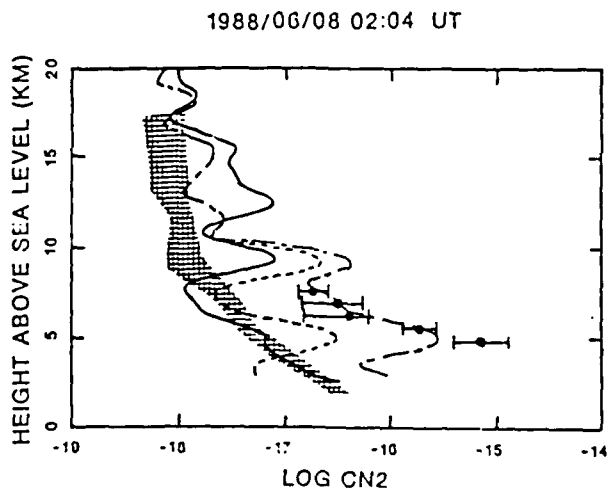


Fig. 1 Height profile of  $\text{Log } C^2$  for 02-03 hours, 8 June 1988 UT. Each large solid dot is the median of the radar data for the hour, and the horizontal bars give the extreme value of the radar measurements for the hour. The solid line is the thermosonde profile; the balloon was launched at 0204 UT. The hatched area gives the range of scintillometer measurements over the hour. The long-short dashed line is the model (radar) profile, and the dashed line is model (dry), which is compared with the thermosonde and scintillometer profiles.

Figure 2 is not a typical example of the thermosonde measurements made during the day. For flights later in the afternoon, the thermosonde data were much larger than the nighttime measurements. This day/night effect is not yet understood.

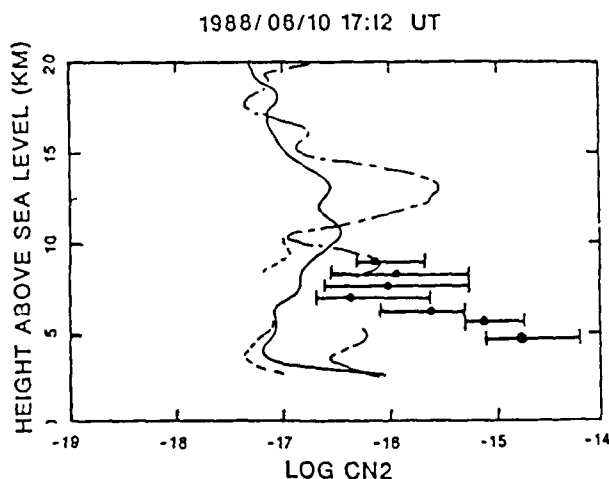


Fig. 2 Same as for Fig. 1 except for 18-19 hours, 10 June 1988 UT; the thermosonde balloon was launched at 17:12 UT. Because this was a daytime flight, there are no scintillometer data.

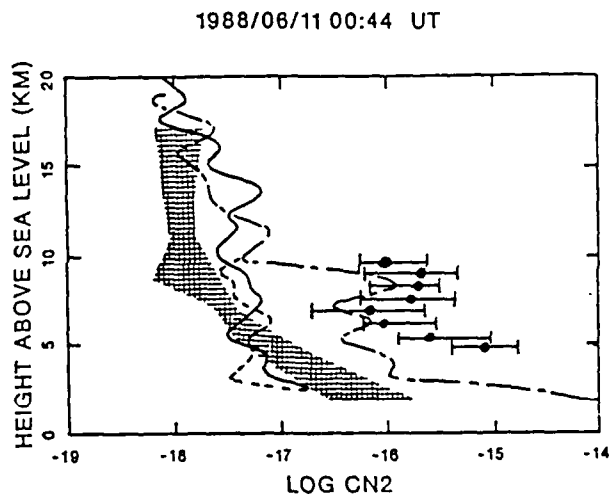


Fig. 3. Same as for Fig. 1 except for 00-01 hours, 11 June 1988, UT; the balloon was launched at 00:44 UT.

All observational methods used in this study make several fundamental assumptions to derive a  $C^2$  value from the raw data. The most important assumption is that the mixing is due to turbulent flow, and, further, that the turbulent flow is homogeneous and isotropic and that the observing scales are in the inertial subrange. Since the measurements and model estimates used in this preliminary study are generally very consistent, these simplifying assumptions and analysis in terms of the  $C^2$  structure parameter are useful. The relative importance of convective mixing, viscous damping at scales smaller than the inner scale, and anisotropic turbulent fluctuations in explaining the times of disagreement will require further research.

#### 4. SUMMARY AND CONCLUSIONS

An experimental campaign was conducted at the Flatland clear-air VHF radar site located near Champaign-Urbana, Illinois, in June 1988, to measure height profiles of the refractivity turbulence structure parameter  $C^2$  and related turbulent parameters. This Flatland site was chosen because it is located in very flat terrain far removed from mountains, so that orographic effects are minimized. Three different techniques were used to measure the height profiles of  $C^2$ . The 50 MHz pulse Doppler Flatland radar and a stellar scintillometer measured the profile remotely, and high resolution in situ measurements of  $C^2$  were obtained from over 20 thermosonde balloon flights. The balloon instruments also measured the standard thermodynamic and wind data with excellent height resolution.

Model estimates were calculated from the standard balloon data, and compared with the measurements. Because the radar measurements are sensitive to humidity and its gradient, whereas the thermosonde and scintillometer are not, two model profiles were calculated. One model profile included the humidity terms, called model (radar), and the other, called model (dry), did not.

During the nighttime, all the measurements and model profiles are generally consistent. There are two exceptions that occur systematically through the data set. One difference is that the model (radar) values of  $C^2$  near five kilometers are consistently lower than the values measured by the radar. Another difference is that the scintillometer measurements at about 14 km are always smaller than the thermosonde and model estimates, and are near the instrumental noise level.

In all the nighttime cases, identical values of all the model parameters and constants were used in the calculations. Furthermore, these values were identical to those used in previous studies using the Sunset and Stapleton radars except for one important parameter. This parameter is the constant in the distribution function of wind shears. Its value at Sunset and Stapleton was 50% greater than its value at Flatland. This suggests that the wind shears at scales of the fine structure are smaller over Flatland than over mountainous terrain.

#### 5. REFERENCES

- Brown, J.H., R.E. Good, P.M. Bench, G.E. Faucher, 1982: Sonde experiments for comparative measurements of optical turbulence, AFGL-TR-82-0079, AD-A118740, Air Force Geophysics Laboratory, Hanscom Air Force Base, MA.
- Clark, W.L., and D.A. Carter, 1980: Real-time scaling of atmospheric parameters from radars using the MST technique, Preprint volume, 19th Conference on Radar Meteorology, April 15-18, 1980; Miami Beach, FL; American Meteorol. Society, Boston, MA, 599-604.
- Clark, W.L., J.L. Green, and J.M. Warnock, 1988: Monitoring VHF radar system performance using cosmic noise, Fourth MST Radar Workshop, Nov. 29-Dec. 2, 1988, Kyoto, Japan; MAP Handbook, in press.
- Eaton, F.D., W.A. Peterson, J.R. Hines, and G. Fernandez, 1985: Isoplanatic angle direct measurements and associated atmospheric conditions, Appl. Opt., 24, 3264-3273.
- Eaton, F.D., W.A. Peterson, J.R. Hines, K.R. Peterman, R.E. Good, R.R. Beland, and J.H. Brown, 1988: Comparisons of VHF radar, optical, and temperature fluctuation measurement of  $C^2$ ,  $r_0$ , and  $\theta_0$ , Theor. Appl. Climatol., 39, 17-29.
- Good, R.E., B.J. Watkins, A.F. Quesada, J.H. Brown, and G.B. Lorient, 1982: Radar and optical measurements of  $C^2$ , Appl. Opt., 21, 3373-3376.
- Green, J.L., K.S. Gage, and T.E. VanZandt, 1979: Atmospheric measurements by VHF pulsed Doppler radar, IEEE Trans. Geosci. Elec., GE-17, 262-280.
- Green, J.L., J. Vernin, T.E. VanZandt, W.L. Clark, and J.M. Warnock, 1984: A comparison of optical and radar measurements of  $C^2$  height profiles, Preprint volume, 22nd Conference on Radar Meteorology, 10-13 Sept. 1984, Zurich, Switzerland, 470-475.
- Green, J.L., K.S. Gage, T.E. VanZandt, W.L. Clark, J.M. Warnock, and G.D. Nastrom, 1988: Observations of vertical velocity over Illinois by the Flatland Radar, Geophys. Res. Lett., 15, 269-272.
- Ochs, G.R., T.-I. Wang, and T. Merrem, 1977: Stellar scintillometer Model II for measurements of refractive-turbulence profiles, NOAA Tech. Memo ERL WPL-25.
- VanZandt, T.E., K.S. Gage, and J.M. Warnock, 1981: An improved model for the calculation of profiles of  $C^2$  and  $\epsilon$  in the free atmosphere from background profiles of wind, temperature, and humidity. Preprint volume, 20th Conference on Radar Meteorology, Nov. 30-Dec. 3, 1981; Boston, MA. American Meteorol. Society, Boston, MA, 129-135.
- Warnock, J.M., and T.E. VanZandt, 1985: A statistical model to estimate the refractivity turbulence structure constant  $C^2$  in the free atmosphere, NOAA Tech. Memo ERL NL-10, NOAA Environmental Research Laboratories, Boulder, CO, 175 pp.
- Warnock, J.M., T.E. VanZandt, and J.L. Green, 1985: A statistical model to estimate mean values of parameters of turbulence in the free atmosphere. Preprint volume, 7th Symposium on Turbulence and Diffusion, Nov. 12-15, 1985; Boulder, CO. American Meteorol. Society, Boston, MA, 156-159.
- Warnock, J.M., J.L. Green, and W.L. Clark, 1986: Studies of  $C^2$  and its variability measured by the Sunset clear-air radar. Preprint volume, 23rd Conference on Radar Meteorology, Sept. 22-26, 1986, Snowmass, CO. American Meteorol. Society, Boston, MA, 34-37.
- Warnock, J.M., N. Sengupta, and R.G. Strauch, 1988: Comparison between height profiles of  $C^2$  measured by the Stapleton UHF clear-air Doppler radar and model calculations, Preprint volume, 8th Symposium on Turbulence and Diffusion, Apr. 26-29, 1988, San Diego, CA. American Meteorol. Society, Boston, MA, 267-270.

## THE SPECTRUM OF VERTICAL VELOCITY FROM FLATLAND RADAR OBSERVATIONS

T. E. VanZandt<sup>1</sup>, G. D. Nastrom<sup>2</sup>, J. L. Green<sup>1</sup>, and K. S. Gage<sup>1</sup><sup>1</sup>Aeronomy Laboratory, NOAA/ERL, Boulder, Colorado<sup>2</sup>Department of Earth Sciences, St. Cloud State University, St. Cloud, Minnesota

## 1. INTRODUCTION

The clear-air Doppler radar technique (also called the wind-profiling or MST radar technique) has been applied to a wide range of meteorological problems since its development by Woodman and Guillén (1974) and Green et al. (1975). Nevertheless, research on some important problems has been frustrated by the location near mountains of most such radars. The resulting geophysical noise has been especially serious for studies of the vertical velocity  $w$ .

When the background wind was light Röttger (1981) and Ecklund et al. (1986) found that frequency spectra of  $w$  were flat at frequencies less than the buoyancy frequency and broke to a steep negative slope at higher frequencies. Very similar  $w$  spectra are observed in the ocean, which Garrett and Munk (1972, 1975) modelled as a spectrum of internal gravity waves. Thus, we can be confident that the light-wind spectra are due to gravity waves.

But when the background wind speed was large at stations near mountains, Ecklund et al. found that the spectral amplitude increased and the shape changed so as to become quite inconsistent with the light-wind spectra, as shown in Figure 1. They suggested that these changes might be due to mountain waves. Also, Nastrom et al. (1985) found that large-scale vertical velocities due to synoptic-scale motions could be extracted from the data when the wind blew toward the mountains from the plains, but not when the wind blew over the nearby Rocky Mountains in Colorado.

It appeared, therefore, that a clear-air Doppler radar located in flat terrain might be used to study vertical gravity wave motions and large-scale vertical motions. For this reason we have constructed the Flatland radar near Champaign-Urbana, Illinois. In this paper we show that the behavior of  $w$  over flat terrain is indeed quite different from that near mountains.

## 2. DATA AND METHODS

The Flatland radar is located about 8km west of Champaign-Urbana, Illinois, at 40.5°N, 88.4°W, 212m above sea level. It operates at a frequency of 49.8MHz. The antenna is a 60m × 60m array of coaxial-collinear dipoles, with a two-way, half-power to half-power beam-width of 3.2°. The data analyzed here were

taken using 750m pulse lengths and range gates centered from 1.4 to 19.4km, but useful data were usually obtained only from 2.2 to 16.4km, with often a region of missing echoes just below the tropopause. The Doppler spectra have 128 points with a velocity resolution of 5cm/s and an unaliased velocity range of ±3.2m/s. Further details, including examples of the data, are given in Green et al. (1988).

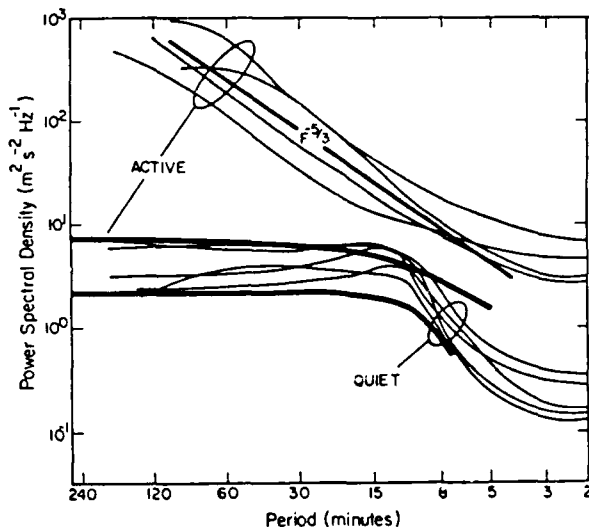


Fig. 1. Frequency spectra of  $w$  in the troposphere. The thin curves are from southern France (Ecklund et al., 1986) and the two thick curves are from Flatland. The spectra labeled QUIET and ACTIVE were obtained when the wind speed was  $\leq 5$  and  $\geq 20$ m/s, respectively.

The vertical velocity was measured about every 2 1/2min from 2 March 1987 until April 1988, with brief interruptions due to power failures, etc. and a break of about six weeks in the summer of 1987. Power spectra were derived from time series of two different lengths, 6h and 45h. If more than three successive observations were missing or eliminated by the quality control procedures described in Green et al. (1988), that is, if there was a gap greater than 10min, then the time series was rejected. The data in the accepted time series at each altitude were then linearly interpolated to uniform 153s intervals. The mean and a linear trend were removed and power spectra were derived by Fourier transform of the residuals.

Routine radiosonde profiles of horizontal wind and temperature for Peoria, Illinois, about 125 km northwest of the Flatland radar, were obtained from the National Climatic Data Center.

### 3. RESULTS: 6h SPECTRA

We computed 6h spectra from March through May centered on the nominal times of the routine radiosonde balloons, 0000 and 1200Z (1800 and 0600 90°W time). Because the number of individual 6h spectra is large, we are able to study the dependence of the spectra on altitude, wind speed, buoyancy frequency, etc.

In Figure 2 the spectra are stratified by altitude from 2.2 to 14.2 km. For each mean spectrum the number  $N$  of individual spectra that enter the average and the variance  $VAR$  in  $(\text{cm/s})^2$  are given in the table in the upper righthand corner. During this period the average tropopause altitude was about 12 km. There is no discernible altitude variation within the troposphere and the stratosphere, but at long periods the spectral energy density in the troposphere is about a factor of two larger than in the stratosphere.

These spectra closely resemble the QUIET spectra at ALPEX in Figure 1, even though the mean horizontal wind for the present spectra was about 15 m/s, and they are quite different from mean spectra at sites near mountains, such as Poker Flat (Bemra et al., 1985; Ecklund et al., 1986) and SOUSY (Kuo et al., 1985; Larsen et al., 1988).

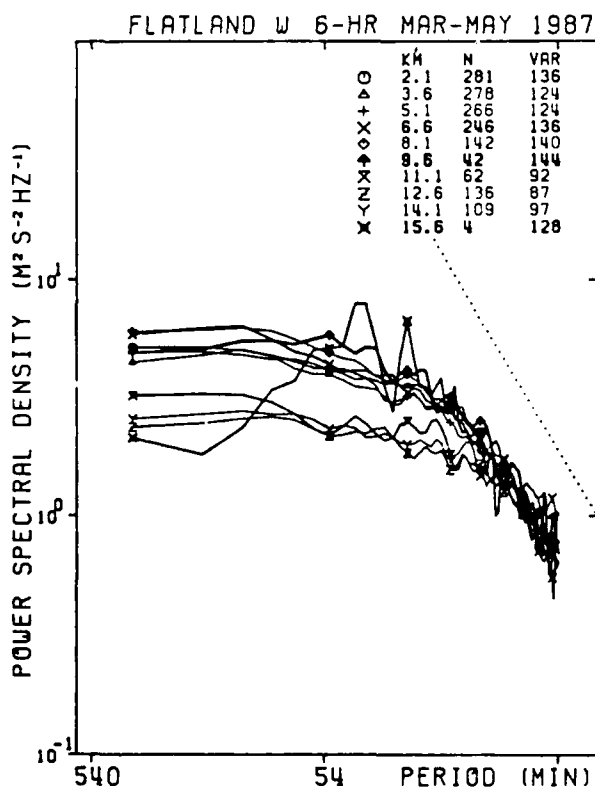


Fig. 2. Frequency spectra stratified by altitude. The mean spectrum at 15.6 km is noisy because it includes only 4 spectra.

We have also sorted the spectra at 3.7 and 5.2 km according to the buoyancy frequency  $N$  over the layer from 700 hPa to 500 hPa (about 3.5 to 5.5 km) at Peoria. There was not any detectable difference between the mean spectra corresponding to the upper and lower quartiles, with  $N = 13.1$  and  $9.6 \times 10^{-3}$  rad/s, respectively, a ratio of 1.4. This is surprising, since in Fig. 2 the ratio of 1.8 between the stratosphere and the troposphere causes very noticeable differences.

This behavior is considered in more detail in Figure 3, where the spectra at 3.7 km are plotted as a function of horizontal wind speed  $WS$  in five bins with boundaries at 0, 3.5, 5.5, 11, and 22 m/s. These boundaries were selected so that each bin contains at least 10 spectra and so that the boundaries lie near minima in the histograms of wind speeds. The spectra have been multiplied by  $WS^2$  to separate them vertically and divided by  $VAR$  to facilitate comparison with model Doppler-shifted spectra in the next section.

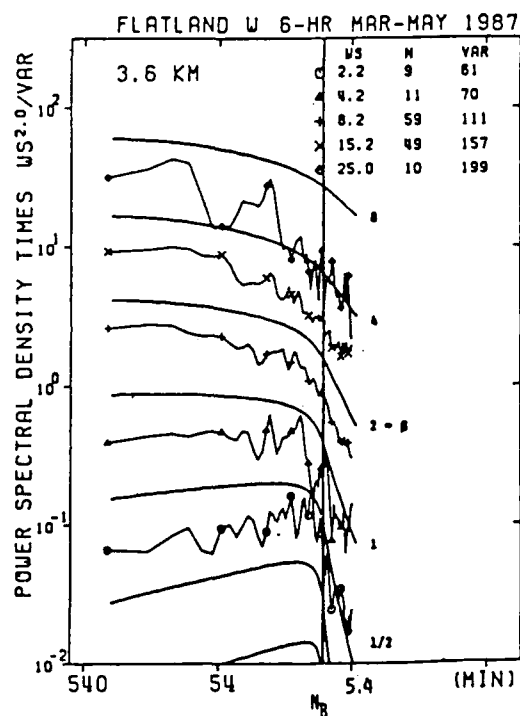


Fig. 3. Observed spectra and model Doppler-shifted spectra stratified by wind speed. The observed and model spectra have been multiplied by  $WS^2$  and  $B^2$ , respectively, and divided by the variance.

It is evident that the shape of the spectra changes systematically with increasing  $WS$ . As  $WS$  increases, the slope becomes more negative at periods longer than the buoyancy period  $1/N$  and less negative at shorter periods, so that the spectra become flatter. The spectra at other altitudes behave in much the same way. It will be shown in the next section that this behavior is consistent with Doppler-shifted spectra of gravity waves.

Figure 4 shows that VAR increases as a power of WS. This behavior will be discussed more quantitatively in the next section.

#### 4. COMPARISON WITH MODEL DOPPLER-SHIFTED GRAVITY WAVE SPECTRA

Models for Doppler-shifted atmospheric gravity wave spectra have been presented by Scheffler and Liu (1986) and by Fritts and VanZandt (1987). In this paper we have chosen to use the approach of Fritts and VanZandt, because we are more familiar with it. Their model has been programmed numerically in order

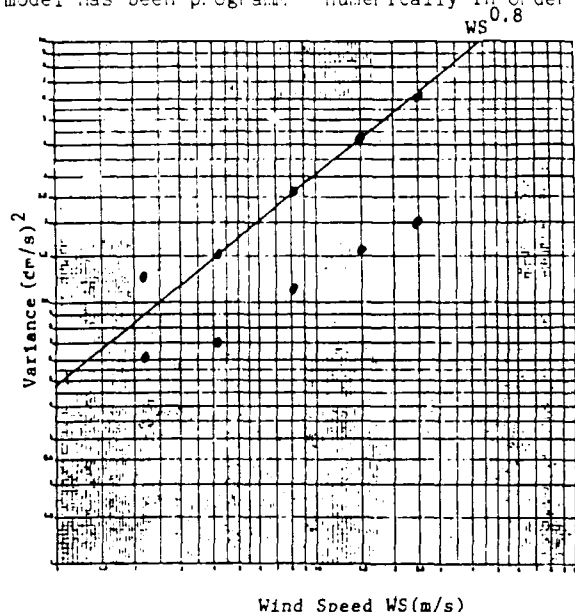


Fig. 4. Variance  $(\text{cm/s})^2$  versus wind speed WS (m/s). The lower set of points are the observed variances VAR. The upper set fitted by the straight line are the total variances estimated using the Doppler-shifting model.

to be able to investigate the effect of both their approximations to the physics of gravity waves and to the assumed intrinsic spectrum. We found that the physical approximations had little effect on the results. On the other hand, some of the approximations to the intrinsic spectrum are important.

Fritts and VanZandt used  $p = 2$  in order to obtain solutions in closed form. We find that in order for the calculated spectra to agree with the observed spectra,  $p$  must be nearer  $5/3$ , as is commonly observed.

We also considered two different extreme azimuthal distributions. First, we used the approximation of Fritts and VanZandt, with a fraction  $a_+$  of the wave energy propagating in the azimuth of the background wind vector and a fraction  $1 - a_+$  in the opposite direction. Alternatively, we assumed that a fraction  $a_+$  was uniformly distributed in the semicircle containing the wind vector and a fraction  $1 - a_+$  in the opposite semicircle. We found that if  $a_+ = 1/2$ , then either distribution can fit the observed spectra, but that if  $a_+$  is not near  $1/2$ , then the model spectra cannot fit the observed spectra.

The model Doppler-shifted spectra depend on the wind speed through the scaled background wind speed  $\beta = WS/c_*$ , where  $c_*$  is the characteristic horizontal phase speed, estimated to be  $\sim 5.5 \text{ m/s}$  in the troposphere (Fritts and Chou, 1987).

In Figure 3 the model Doppler-shifted spectra are shown by the curves labeled with  $\beta$ . In order to scale them in the same way as the observed spectra they have been multiplied by  $\beta^2$  and divided by the variance over the same frequency range as the observed spectra. It is evident that the shape of the model spectra changes in the same way as the observed spectra. The results at other heights are similar. From this we conclude that the observed spectra are Doppler-shifted gravity wave spectra.

It must be kept in mind that the model Doppler-shifted spectra all use the same intrinsic spectrum. In reality, the intrinsic spectrum must be a function of wind speed or actually a function of the entire velocity and  $N$  profile. The fact that the Doppler-shifted spectra fit the observed spectra at several altitudes and over a wide range of wind speeds shows that the intrinsic spectrum is not a strong function of altitude or wind speed. However, the intrinsic spectrum could vary somewhat at large wind speeds, since for large  $\beta$  the model spectra are rather insensitive to the shape of the intrinsic spectrum.

VAR for the observed spectra was plotted versus WS in Figure 4. However, VAR is only a fraction of the total variance in the gravity wave field, since part of the wave energy has been Doppler-shifted outside the observed frequency range, especially toward higher frequencies. The total variances estimated using the model are also plotted in Figure 4.

For  $WS > 3.5 \text{ m/s}$  the total variance varies approximately as  $WS^{0.8}$ , or, to compare variance with variance, as  $(WS^2)^{0.4}$ . This increase must be taken into account when comparing spectra taken at different wind speeds.

#### 5. RESULTS: LOW-FREQUENCY SPECTRUM

The mean of the 34 available individual spectra from the 45h time series at 5.2km is shown as a usual log-log graph in Figure 5a and as an area-preserving spectrum in Figure 5b, where the area under the spectrum is proportional to the contribution to the total energy. It is clear that most of the vertical energy lies near the buoyancy period and that a significant fraction of it appears to lie at periods shorter than the 5.1min Nyquist period.

For the 45h spectrum the mean WS is estimated to be about 10m/s, corresponding to  $\beta \sim 2$ . The model spectrum for  $\beta = 2$ , shown as the curve in the figures, fits the observed spectrum rather well for periods shorter than about 6h, as expected from the previous discussion, but it falls increasingly below the observed spectrum with increasing period. The difference between the observed and model spectra may be largely due to large-scale vertical motions. This possibility will be explored in future research.

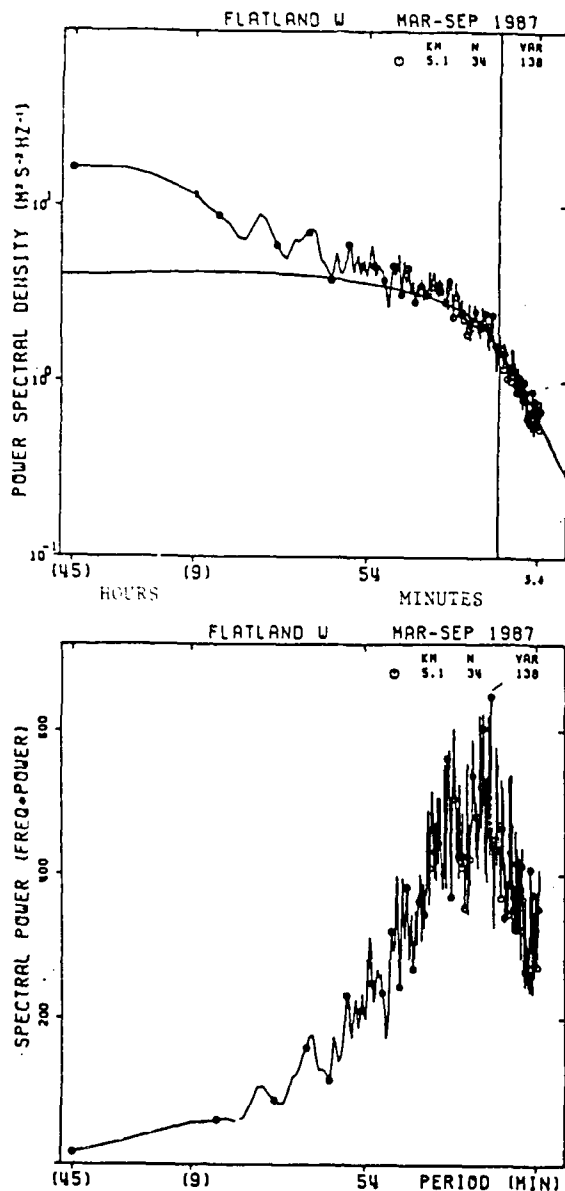


Fig. 5. Mean 45h spectrum. a) Plotted as a usual log-log graph. The curve is a model Doppler-shifted spectrum with  $\beta = 2$ . b) Plotted as an area-preserving graph. To express the ordinate in  $(\text{m/s})^2/\text{decade}$ , multiply by  $\ln 10/45 \times 3600$ .

## 6. CONCLUSIONS

We find that the high-frequency vertical velocity spectra are quite consistent with Doppler-shifted gravity-wave spectra. We suggest that the low-frequency spectra are dominated by large-scale vertical motions.

## 7. ACKNOWLEDGMENTS

We wish to thank W.L. Clark and C.H. Love for their assistance in preparing this manuscript.

## 8. REFERENCES

Bemra, R. S., P. K. Rastogi, and B. B. Balsley, 1986: A study of gravity-wave

spectra in the troposphere and stratosphere at 5-min to 5-day periods with the Poker Flat MST radar, *Handbook for MAP*, 20, 216-224.

Ecklund, W. L., K. S. Gage, G. D. Nastrom, and B. B. Balsley, 1986: A preliminary climatology of the spectrum of vertical velocity observed by clear-air Doppler radar, *J. Clim. Appl. Meteorol.*, 25, No. 7, 885-892.

Fritts, D. C., and H.-G. Chou, 1987: An investigation of the vertical wavenumber and frequency spectra of gravity wave motions in the lower stratosphere, *J. Atmos. Sci.*, 44, 3610-3624.

Fritts, D. C., and T. E. VanZandt, 1987: Effects of Doppler shifting on the frequency spectra of atmospheric gravity waves, *J. Geophys. Res.*, 92, 9723-9732.

Garrett, C., and W. Munk, 1972: Oceanic mixing by breaking internal waves, *Deep-Sea Res.*, 19, 823-832.

Garrett, C., and W. Munk, 1975: Space-time scales of internal waves: a progress report, *J. Geophys. Res.*, 80, 291-297.

Green, J. L., J. M. Warnock, R. H. Winkler, and T. E. VanZandt, 1975: Studies of winds in the upper troposphere with a sensitive VHF radar, *Geophys. Res. Lett.*, 2, 19-21.

Green, J. L., K. S. Gage, T. E. VanZandt, W. L. Clark, J. M. Warnock, and G. D. Nastrom, 1988: Observations of vertical velocity over Illinois by the Flatland radar, *Geophys. Res. Lett.*, 15, 269-272.

Kuo, F.-S., H.-W. Shen, I.-J. Fu, J.-K. Chao, J. Röttger, and C.-H. Liu, 1985: Altitude dependence of vertical velocity spectra observed by VHF radar, *Radio Sci.* 20, No. 6, 1349-1354.

Larsen, M. F., J. Röttger, and D. N. Holden, 1987: Direct measurements of vertical velocity power spectra with the SOUSY-VHF-radar wind profiler system, *J. Atmos. Sci.*, 44, 3442-3448.

Nastrom, G. D., W. L. Ecklund, and K. S. Gage, 1985: Direct measurement of large-scale vertical velocities using clear-air Doppler radars, *Monthly Weather Rev.*, 113, 708-718.

Röttger, J., 1981: Preprint volume, 20th Conference on Radar Meteorology, Boston, MA, Wind Variability in the stratosphere deduced from spaced antenna VHF radar measurements, American Meteorological Soc., Boston, MA, 22-37.

Scheffler, A. O., and C.-H. Liu, 1988: The effects of Doppler shift on the gravity wave spectra observed by MST radar, *J. Atmos. Terr. Phys.*, 48, 1225-1231.

Woodman, R. F., and A. Guillén, 1974: Radar observations of winds and turbulence in the stratosphere and mesosphere, *J. Atmos. Sci.*, 31, 493-505.